NUREG/IA-0208

International Agreement Report

Analysis of the VTI Test Data on the Behavior of the Heated Rod Temperatures in the Partially Uncovered VVER-440 Core Model Using RELAP5/MOD3.2.2 Gamma

Prepared by:
V.A. Vinogradov, and A.Y. Balykin

Russian Research Center "Kurchatov Institute"
Kurchatov Square 1
123182, Moscow, Russia

Office of Nuclear Regulatory Research
U.S. Nuclear Regulatory Commission
Washington, DC 20555-0001

July 2002

Prepared as part of
The Agreement on Research Participation and Technical Exchange
under the International Code Application and Maintenance Program (CAMP)

Published by
U.S. Nuclear Regulatory Commission

AVAILABILITY OF REFERENCE MATERIALS IN NRC PUBLICATIONS

NRC Reference Material

As of November 1999, you may electronically access NUREG-series publications and other NRC records at NRC's Public Electronic Reading Room at www.nrc.gov/NRC/ADAMS/index.html.
Publicly released records include, to name a few, NUREG-series publications; *Federal Register* notices; applicant, licensee, and vendor documents and correspondence; NRC correspondence and internal memoranda; bulletins and information notices; inspection and investigative reports; licensee event reports; and Commission papers and their attachments.

NRC publications in the NUREG series, NRC regulations, and *Title 10, Energy*, in the Code of *Federal Regulations* may also be purchased from one of these two sources.

1. The Superintendent of Documents
   U.S. Government Printing Office
   Mail Stop SSOP
   Washington, DC 20402–0001
   Internet: bookstore.gpo.gov
   Telephone: 202-512-1800
   Fax: 202-512-2250
2. The National Technical Information Service
   Springfield, VA 22161–0002
   www.ntis.gov
   1–800–553–6847 or, locally, 703–605–6000

A single copy of each NRC draft report for comment is available free, to the extent of supply, upon written request as follows:
Address: Office of the Chief Information Officer,
Reproduction and Distribution
Services Section
U.S. Nuclear Regulatory Commission
Washington, DC 20555-0001
E-mail: DISTRIBUTION@nrc.gov
Facsimile: 301–415–2289

Some publications in the NUREG series that are posted at NRC's Web site address www.nrc.gov/NRC/NUREGS/indexnum.html are updated periodically and may differ from the last printed version. Although references to material found on a Web site bear the date the material was accessed, the material available on the date cited may subsequently be removed from the site.

Non-NRC Reference Material

Documents available from public and special technical libraries include all open literature items, such as books, journal articles, and transactions, *Federal Register* notices, Federal and State legislation, and congressional reports. Such documents as theses, dissertations, foreign reports and translations, and non-NRC conference proceedings may be purchased from their sponsoring organization.

Copies of industry codes and standards used in a substantive manner in the NRC regulatory process are maintained at—

The NRC Technical Library
Two White Flint North
11545 Rockville Pike
Rockville, MD 20852–2738

These standards are available in the library for reference use by the public. Codes and standards are usually copyrighted and may be purchased from the originating organization or, if they are American National Standards, from—

American National Standards Institute
11 West 42nd Street
New York, NY 10036–8002
www.ansi.org
212–642–4900

Legally binding regulatory requirements are stated only in laws; NRC regulations; licenses, including technical specifications; or orders, not in NUREG-series publications. The views expressed in contractor-prepared publications in this series are not necessarily those of the NRC.

The NUREG series comprises (1) technical and administrative reports and books prepared by the staff (NUREG–XXXX) or agency contractors (NUREG/CR–XXXX), (2) proceedings of conferences (NUREG/CP–XXXX), (3) reports resulting from international agreements (NUREG/IA–XXXX), (4) brochures (NUREG/BR–XXXX), and (5) compilations of legal decisions and orders of the Commission and Atomic and Safety Licensing Boards and of Directors' decisions under Section 2.206 of NRC's regulations (NUREG–0750).

NUREG/IA-0208

International Agreement Report

Analysis of the VTI Test Data on the Behavior of the Heated Rod Temperatures in the Partially Uncovered VVER-440 Core Model Using RELAP5/MOD3.2.2 Gamma

Prepared by:
V.A. Vinogradov, and A.Y. Balykin

Russian Research Center "Kurchatov Institute"
Kurchatov Square 1
123182, Moscow, Russia

Office of Nuclear Regulatory Research
U.S. Nuclear Regulatory Commission
Washington, DC 20555-0001

July 2002

Prepared as part of
The Agreement on Research Participation and Technical Exchange
under the International Code Application and Maintenance Program (CAMP)

Published by
U.S. Nuclear Regulatory Commission

ABSTRACT

This report has been prepared as a part of the Agreement on Research Participation and Technical Exchange under the International Code Application and Maintenance Program.

VTI test data on the behavior of the heated rod temperatures in the partially uncovered VVER-440 core model were simulated with RELAP5/MOD3.2.2GAMMA to assess the code, especially its heat transfer models for modeling phenomena in the partially uncovered core under Small Break LOCA conditions. This problem addresses the phenomena of high importance to VVER-440 safety.

Series of the experiments have been carried out in the VVER-440 loop model at the VTI Test Facility which are directly related to this issue. Two tests conducted in the stationary conditions with the transition mode of a steam flow in the core channel were chosen for the assessment calculations with the code.

Experimental VVER-440 loop model includes the models of all the main elements of a reactor, loop's hot leg model and cold leg simulator, and also a steam generator simulator with an active heat removal. The fuel assembly model consists of 19 electrically heated rod simulators of 9.1 mm outer diameter and 2.5 m heated height. The rod simulators are composed in the rod bundle in a hexagonal array with a pitch equal 12.2 mm (P/D=1.34).

First a study of the effect of the hydraulic nodalization to the code results was performed using different number of hydraulic volumes for the core model. After the choice of proper nodalization and maximum user-specified time step, the base case calculations were done for the tests. The differences between the code predictions for the behavior of rod's wall temperatures and test data are described and analyzed.

Sensitivity studies were carried out to investigate the influence of an increase in the calculated coefficients of heat transfer from the heated rods to a steam flow on the axial distribution of rod's wall temperatures in the uncovered part of core model.

Table of Contents

LIST OF FIGURES

LIST OF TABLES

EXECUTIVE SUMMARY

VTI test data on the behavior of rod's cladding temperatures in the partially uncovered VVER-440 core model were simulated with RELAP5/MOD3.2.2GAMMA to assess the code. These calculations were performed to evaluate the code prediction capability in modeling heat transfer phenomena in the partially uncovered core under specific conditions of VVER-440 type reactor during Small Break LOCA.

Series of the tests have been carried out in the VVER-440 loop model at the VTI Test Facility which are directly related to this issue. Two tests were chosen for the code simulations of heat transfer phenomena occurring in the partially uncovered core during SB LOCA.

Experimental VVER-440 loop model includes the models of all the main elements of a reactor, loop's hot leg model and cold leg simulator, and also a steam generator simulator with an active heat removal. The fuel assembly model consists of 19 electrically heated rod simulators of 9.1 mm outer diameter and 2.5 m heated height. The rod simulators are composed in the rod bundle in a hexagonal array with a pitch equal 12.2 mm (P/D=1.34).

Special emphases were given to:

* Hydrodynamics and heat transfer processes in the partially uncovered core model during steam-condensate natural circulation in the primary coolant system with small specific heat fluxes and medium pressures, and also in condition of absence of counter-current flow of phases in the uncovered part of the core;
* Axial distributions of the heat transfer coefficients and rod's wall temperatures in the uncovered part of the fuel assembly model in the stationary conditions with the transition mode of a steam flow in the core channel.

First a study of the effect of the hydraulic nodalization to the code results was performed using different number of hydraulic volumes for the core model. After the choice of proper nodalization and maximum user-specified time step, the base case calculations were done for the tests. The differences between the code predictions for the behavior of rod's wall temperatures and test data are described and analyzed.

Sensitivity studies were carried out to investigate the influence of an increase in the calculated coefficients of heat transfer from the heated rods to a steam flow on the axial distribution of rod's wall temperatures in the uncovered part of core model.

Code results are presented as time–dependent curves. The results of comparison of the calculated and measured values of the determinative and determined parameters are a base for a conclusion about adequacy of the code simulation of the initial and boundary conditions, realizing in the test, and then about adequacy of the code simulation of a steady regime.

The adequacy of the code modeling of heat transfer phenomena in the uncovered part of the core model has been estimated by comparison of the core axial profiles of the calculated and measured rod's cladding temperatures at the end of a steady regime.

In this work some deficiencies of RELAP5/MOD3.2.2GAMMA in analyses of VTI test 7.12.15.4 and test 8.6.3.2 could be identified, and the following conclusions can be drawn:

• RELAP5/MOD3.2.2GAMMA and the base case methods of computer modeling of the experiments have provided adequate simulation of the initial and boundary conditions only for hydrodynamics, realized during the tests with steam-condensate natural circulation in the VVER-440 loop model. In these tests the transition mode of a steam flow is realized in the uncovered part of the FA model with corresponding Reynolds numbers $Re_g = Vg \cdot Dh / \nu_g \approx 1860 - 830$. This mode is realized between laminar and turbulent modes of a steam flow in the uncovered part of the FA channel.

• Shown is an insufficient code adequacy for the description of rod's wall temperatures behaviors in the uncovered part of the FA model. There are significant quantitative differences of the axial profiles of calculated and measured rod's wall temperatures in the uncovered part of the FA model in the base case calculations for these tests.

The code over predicts rod's wall temperatures in the uncovered part of the FA model at the initial time moment, and then during "steady regime". The calculated rod's wall temperatures are much higher (up to ~ 150 K) than measured ones at the FA outlet. This is the main problem of the code for the base case calculations for these tests.

• The sensitivity studies show, that the increase in calculated coefficients of heat transfer in the uncovered part of the FA model results in a reasonable adequacy of the code simulation of the initial and boundary conditions for both hydrodynamics and heat transfer process, realized in the uncovered part of the core model. Using fouling factor $K_{HW1}=3.0$ the code reasonably describes the axial distributions of the rod's wall temperatures in the uncovered part of the FA model for the initial steady states, and then during the steady regimes in considered tests.

NOMENCLATURE

W – power of the FA model, W, kW
qw – heat flux, W/ m^2 , kW/ m^2
q_w average – FA average heat flux, kW/ m^2
Pup – pressure at the upper plenum model outlet, bar
Lm – mixture level in the FA channel, m
TF – water temperature in the lower plenum model, K
TW – rod's cladding temperature, K
Ts – saturation temperature, K
Tg – vapor temperature, K
D – diameter, mm
Dh – hydraulic diameter of the channel, mm
De – heated equivalent diameter, mm
P – rod pitch, mm
Psg – spacer grid pitch, mm
ξ – local hydraulic resistance coefficient
G – mass flow rate at natural circulation in the loop, kg/s
G_L – liquid mass flow rate, kg/s
Gg – vapor mass flow rate, kg/s
V_L – liquid velocity, m/s
Vg – vapor velocity, m/s
Hw1 – coefficient of heat transfer from the rod to the coolant, W/ m^2 K
K_{Hw1} – fouling factor
t – time, s
exp – experimental value
cal – calculated value
vol – volume
sv – subvolume
sj – single junction
n – node
hs – heat structure

RRC KI – Russian Research Center "Kurchatov Institute"
VTI – Russian Thermal Technology Institute
VVER – Russian light water reactor
SB LOCA – small break loss of coolant accident
LP – lower plenum
UP – upper plenum
HL – hot leg
CL – cold leg
DC – downcomer
SG – steam generator
FA – fuel assembly
FE – fuel element
DAS – data acquisition system
NC – natural circulation
CCF – counter-current flow

1. INTRODUCTION

1.1.Objectives

The main goals of this work are:

- Analysis and estimation of the VTI test data on the behavior of the rod's cladding temperatures in the partially uncovered VVER-440 core model using RELAP5/MOD3.2.2GAMMA;
- Investigation thermal and hydraulic processes during steam-condensate natural circulation in the primary coolant system under SB LOCA conditions with small specific heat fluxes and medium pressures, and also in condition of absence of counter-current flow of phases in the uncovered part of the core;

- Assessment of RELAP5/MOD3.2.2GAMMA code, especially its models for modeling heat transfer phenomena in the uncovered part of the core model.

1.2. Background

To help ensure RELAP5 code can be used with confidence, Russian Research Center "Kurchatov Institute" has agreed to perform and document independent assessment of the code for a wide range of applications. These exercises are necessary to help identify and quantify any code shortcoming, in particular for the Russian types of reactors VVER and RBMK. This report has been prepared as a part of the Agreement on Research Participation and Technical Exchange under the International Code Application and Maintenance Program. Analysis of VTI tests with partially uncovered VVER-440 core model under SB LOCA conditions was performed using the latest version of code RELAP5/MOD3.2.2GAMMA.

1.3. Study Description

SB LOCA is one of the design basis accidents in VVER-440 power pressure water reactor. VVER-440 loop model is a semi-integral one loop model of VVER primary coolant system designed for investigations hydrodynamics and heat transfer in transients and SB LOCA conditions of a reactor. In this facility series of the tests with partially uncovered VVER-440 core model under SB LOCA conditions were performed during 1984-1989 [1, 2].

Phenomena of hydrodynamics and heat transfer in VVER-440 core under uncovering conditions are specific. So, it is necessary to estimate RELAP5/MOD3.2.2GAMMA code models adequacy for modeling these phenomena, because there are specific features in design of the core and fuel

assembly of VVER-440. These specific features are the rod location in a triangular grid in the bundle, geometry of the rod and fuel assembly elements, hydraulic diameters of the rod bundle's cells and number of the spacer grids. Temperature of the fuel rod's cladding directly depends on these factors.

VTI test 7.12.15.4 and test 8.6.3.2 with the partially uncovered core model were chosen to assess RELAP5/MOD3.2.2GAMMA. This code capability was investigated. Special emphases were given to: - thermal and hydraulic processes during steam-condensate natural circulation in the primary circuit with a mixture level in the partially uncovered core model and under conditions of small specific heat fluxes and medium pressures; - axial distributions of the coefficients of heat transfer from the heated rods to a steam flow and rod's cladding temperatures in the uncovered part of the core model under steady conditions with the transition mode of a steam flow in the core channel; - the influence of an increase in the calculated coefficients of heat transfer from the heated rods to a steam flow on the axial distribution of rod's cladding temperatures in the uncovered part of the fuel assembly model.

1.4. Report Organization: The following sections present and describe the steps that were taken to facilitate the code assessment. In Section 2 the VVER-440 Loop model at VTI Test Facility is described, and VTI tests 7.12.15.4 and 8.6.3.2 are described in Section 3. Descriptions of released code version and base case input deck for the test modeling are given in Section 4. Nodalization, including variation from base case, the base case analysis results for the tests, discussion of the calculated and measured values and conclusions are presented in Section 5. Sensitivity studies are given in Section 6. Run statistics are given in Section 7. In Section 8 summary of conclusions is presented. In the Appendix D one finds the base case input deck listing for VTI test 8.6.3.2.

2. DESCRIPTION OF VTI TEST FACILITY

2.1. Description of the VVER-440 loop model at VTI Test Facility

The VVER–440 loop model at VTI Test Facility is a semi-integral one loop model of VVER primary coolant system. It has been designed for modeling of boiling-condensing mode in the primary coolant system and heat transfer processes in the partially uncovered core at small residual heat power and medium pressure under SB LOCA conditions of a reactor. A principle scheme of the VVER-440 loop model is shown in Fig.2.1.

This model includes the models of all the main elements of a reactor: - lower plenum model (1), core model with fuel assembly model (2), upper plenum model (7). Also, it includes the hot leg model (8), steam generator simulator (9) with an active heat removal and downcomer simulator. The SG simulator consists of the two parts: the upper part is a steam condenser, and the bottom part is a water cooler, which only qualitatively simulate hydrodynamics and heat transfer processes under conditions of steam condensation in the steam generator.

The DC simulator at the bottom and the lower plenum model are connected by a lower water pipeline (11). The up-coming and down-coming circuit branches are linked in the upper part by a pipeline of the hot leg model. So, a natural circulation is formed in the model of VVER primary coolant system. An orifice installed in the lower water pipeline is used to measure a liquid mass flow rate at the core inlet during steam-condensate natural circulation in the loop.

A secondary coolant system connected to the steam condenser provides a wide range of pressure Pup in the upper plenum. A secondary coolant system connected to the water cooler provides a wide range of water temperature TF at the core inlet.

The mode parameters in the loop in the course of the series of the tests were varied in the following ranges:

- Pressure at the UP model outlet Pup : 23 – 73 bar;
- Specific heat flux in the FA model qw : 3.5 - 29 kW/m^2;
- Mass flux in the FA channel : 1 - 7 kg/(m^2 s).

Water pipeline (10) from SG simulator into expansion tank is to drain a water through the valve. It serves for formation of the initial conditions with a break in two-phase natural circulation in the loop and with a mixture level in the partially uncovered core model.

VTI Test Facility and DAS provide preparation and implementation of the planned experiments.

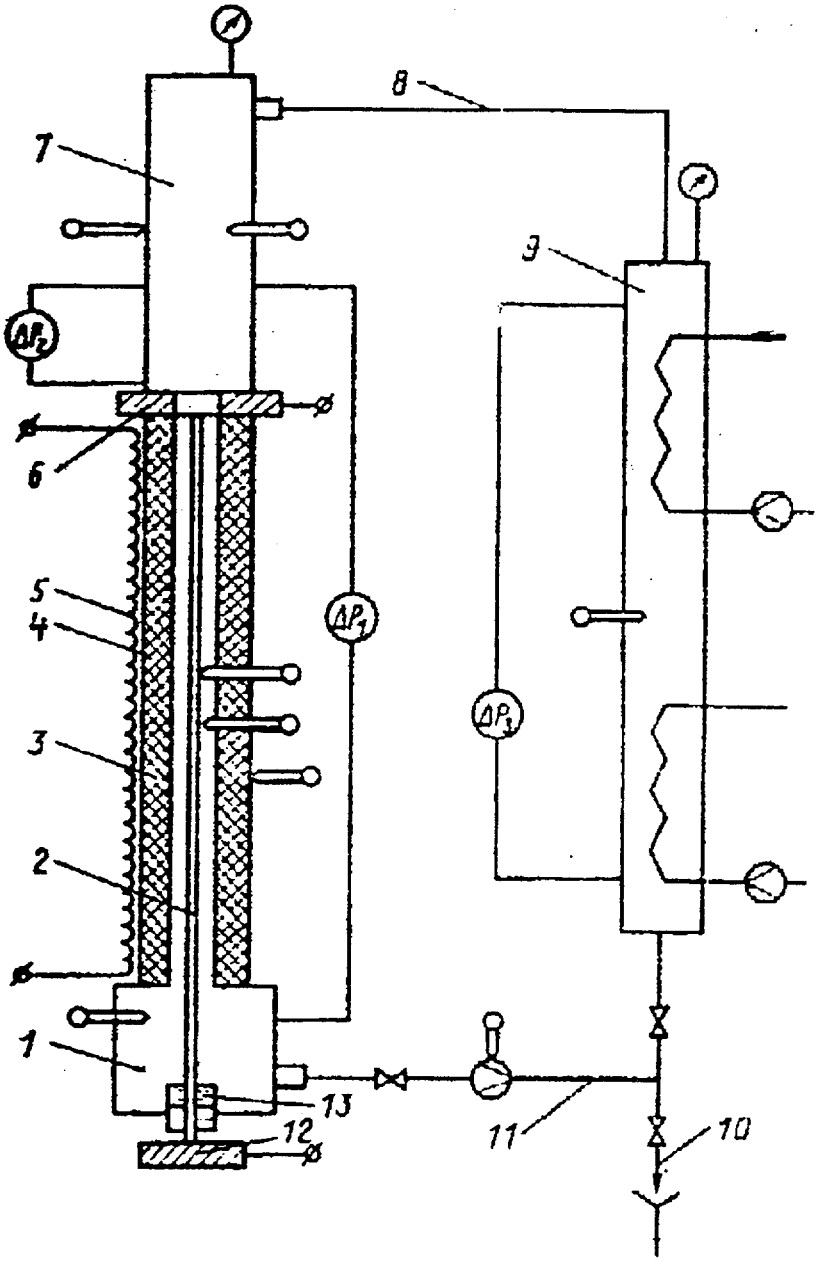

Fig.2.1 Scheme of the VVER-440 loop model and measurements on VTI Test Facility [2]:

1 – Lower plenum; 2 – FA model; 3 – Insulator bush;
4 – Pressure vessel; 5 – Protective electric heater; 6 – Upper conductor;
7 – Upper plenum; 8 – Hot leg model; 9 – SG simulator and DC simulator;
10 – Drainage pipeline; 11 – Lower water pipeline.

2.2. Main components characteristics

Core model with VVER-440 fuel assembly model. A sketch of the core model is presented in Fig.2.1. The core model consists of: - electrically heated VVER-440 fuel assembly model (2) enclosed by a pressure vessel (4) made of 12X18H10T stainless steel tube with internal electric and heat insulator bushes of talkochlorite (3), protective electric heater (5) located on the outer surface of the pressure vessel, upper conductor (6) and lower conductor (12) for supply of current to the rod simulators.

A power of the protective electric heater (5) located around the core pressure vessel (4) is to compensate heat losses from the outer surface of the core model to an ambient air.

A cross section of the core model with the fuel assembly model is shown in Fig.2.2 b.
Parameters of the core model with the fuel assembly model are presented in Table 2.1.

Table 2.1. Parameters of the core model with VVER-440 fuel assembly model

Heated length of the FA model	2500 mm
Number of rod simulators	19
Outer diameter of rod simulators	9.1 mm
Distance between rod simulators	12.2 mm
Size of FA channel hexahedron	56 mm
Channel cross section area	0.001478 m^2
Heat transfer surface area of the FA model	1.358 m^2
Hydraulic diameter of the FA channel	8.02 mm
Designed axial and radial power distribution	uniform
Distance between spacer grids	240 mm
Number of spacer grids	10

Fuel assembly model. A sketch of the model of the VVER-440 fuel assembly is presented in Fig.2.2. The FA model consists of 19 electrically heated rod simulators of 9.1 mm outer diameter and of 2500 mm heated length. The rod simulators are composed in the rod bundle in a hexagonal array with a pitch equal 12.2 mm (P/D=1.34). The fuel assembly model is equipped with 10 spacer grids, axially located at equal distances of 240 mm. All the spacer grids are of VVER-440 FA type. The local hydraulic resistance coefficient of the grid is ξ=0.27.

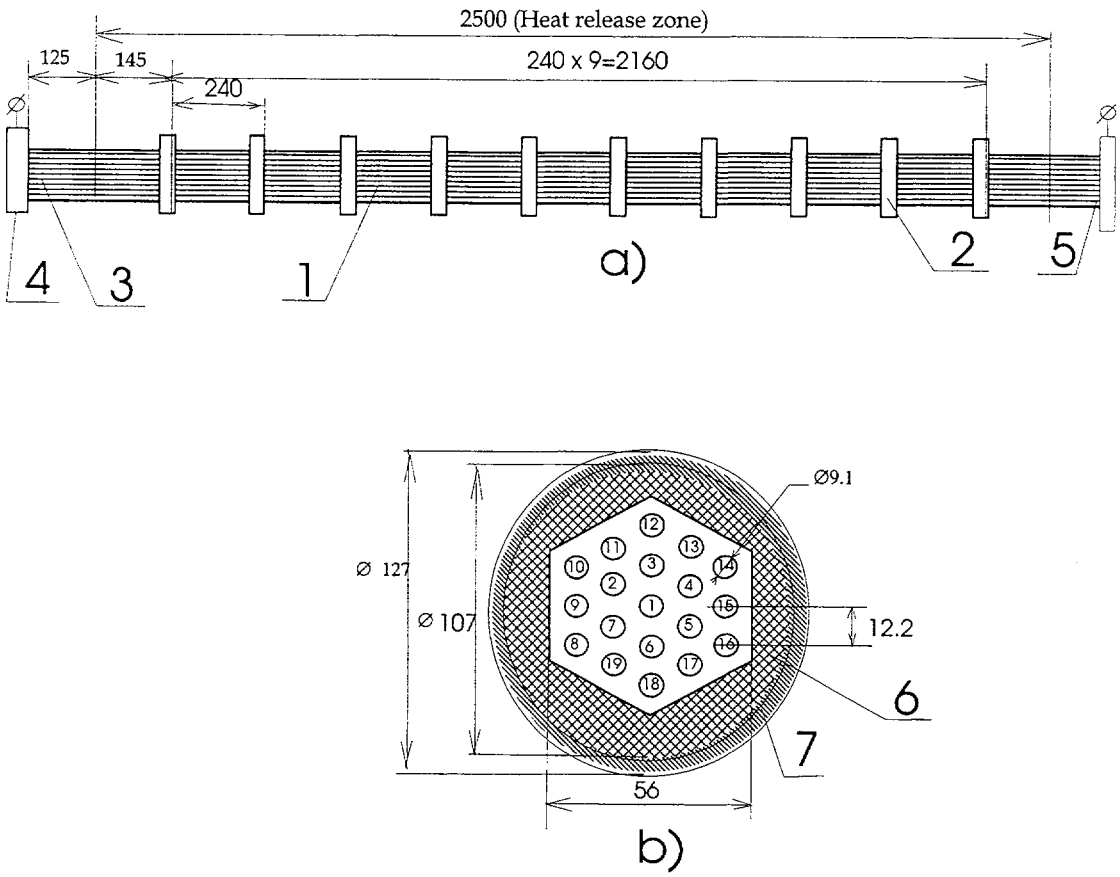

Fig.2.2. Model of the VVER-440 fuel assembly.

a) bundle of the rod simulators
b) cross section of the core model with the FA model

1. Steel cladding of the rod simulator
2. Spacer grid
3. Cooper wire of the upper conductor of the rod simulator
4. Upper conductor
5. Cooper pin of the lower conductor of the rod simulator
6. Insulator bush
7. Pressure vessel

Fuel rod simulators. The fuel rod simulators are electrically indirectly heated. The rod simulator consists of a stainless steel (12X18H10T) heater made of a rod with outer diameter of 3.3 mm and length of 2500 mm, of a magnesium oxide (MgO) electrical isolation, and a stainless steel (12X18H10T) cladding with wall thickness of 0.5 mm.

The present fuel rod simulators are designed to have the uniform axial and radial heat flux distributions. The fuel assembly model is heated by the alternating current passing through these stainless steel heaters. Therefore, the power distribution within the rod bundle is uniform only in the conditions of full FA covering with a boiling liquid.

51 cable thermocouples of 0.3 mm outer diameter are embedded in grooves inside the rod simulator's cladding at 32 elevations in the FA model.

Upper plenum model. The location of the Upper plenum model (7) in the VVER-440 loop model is shown in Fig.2.1. It is made of a stainless steel tube ∅ 108 x 8 (Dh==92 mm) with the height of 2.6 m. A power of the protective electric heater located around the upper plenum is to compensate heat losses from the outer surface of the upper plenum model to an ambient air.

Hot leg model. Hot leg model (8) shown in Fig.2.1 is a pipeline made of a stainless steel tube ∅ 60 x 8 (Dh=44 mm) with length of 3.0 m.

Lower water pipeline. The lower water pipeline (11) is made of a stainless steel tube ∅ 16 x 3 (Dh=10 mm) with length of 3.0 m.

2.3. Measurements and errors

Locations of the gauges in the Lower plenum model, Core model, Upper plenum model and Lower water pipeline are presented on a scheme of measurements in VVER-440 loop model, shown in Fig.2.1.

Measurements of core axial and radial distributions of the rod's cladding temperatures were made with 51 thermocouples installed in cladding of the rod simulators (in 6 rods) at 32 elevations in the FA model. A scheme of location of the thermocouples along the FA height is shown in Fig.2.3. The thermocouples are numbered as 0 – 50 on Fig.2.3.

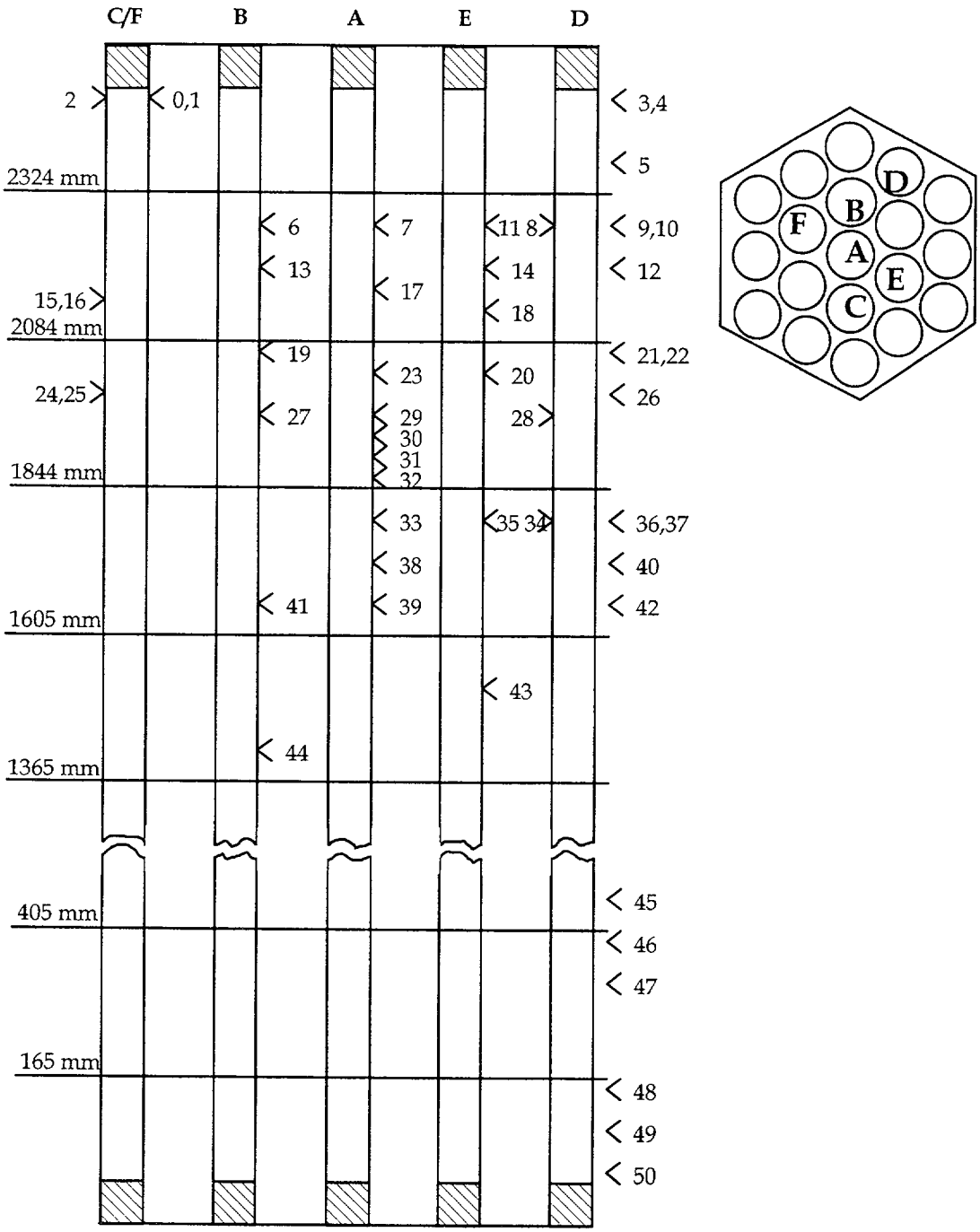

Fig.2.3. Scheme of location of the thermocouples along the FA model height [2].

Measurements of the rod's cladding temperatures along the height of the FA model at 32 elevations have provided also an axial distribution of the rod's cladding temperatures in the FA model and test data about a mixture level in the FA channel with accuracy of ± 25 mm.

An electric power W of the FA model was determined on the base of measurements of voltage drop U on the FA model and current.

List of the measured parameters, and their measurement errors are presented in Table 2.3.

Table 2.2. List of measured parameters used in calculations and measurement errors

Parameter	Measurement error
Electric power W of the FA model	± 2 %
Water mass flow rate G in the lower pipeline	± 3 %
Pressure Pup at the UP outlet	± 0.4 %
Coolant temperature TF	± 1.8 %
Rod simulator's cladding temperatures TW	± 1.4 %

3. DESCRIPTION OF THE TESTS

3.1. VVER specific phenomena investigated in the tests

Phenomena of hydrodynamics and heat transfer in VVER-440 core under uncovering conditions are specific. So, it is necessary to estimate RELAP5/MOD3.2.2GAMMA code models adequacy for modeling of these phenomena, because there are specific features in design of the core and fuel assembly of a reactor. These specific features are the rod location in a hexagonal array, geometry of the rod and FA elements, hydraulic diameters of the rod bundle's cells, and enlarged number of the spacer grids. Temperature of the fuel rod's cladding directly depends on these factors.

Comparison of the key parameter values for the FA model and corresponding values in VVER-440 reactor is presented in Table 3.1.

Processes of hydrodynamics and heat transfer in the partially uncovered core under SB LOCA conditions are very important for VVER-440 safety, since at these conditions there is rod temperature increase realization, which may lead to rod damage. For safety analysis it is very important to know the initial time moment and conditions of FA uncovering, behavior dynamics of

a mixture level, distributions of the velocities of a vapor and liquid in the FA channel, and also the distributions of the heat transfer coefficients, rod's cladding temperatures and vapor temperatures above the mixture level.

Table 3.1.Parameters of the core model with VVER-440 fuel assembly model and VVER-440 fuel assembly

Key parameter values	VTI experiment	VVER-440
Configuration of the rod assembly	Hexagonal	Hexagonal
Heated length of the rod assembly	2500 mm	2500 mm
Number of rods in the rod assembly	19	126
Outer diameter of rod	9.1 mm	9.1 mm
Distance between rods (rod pitch)	12.2 mm	12.2 mm
Distance between spacer grids	240 mm	240 mm
Shroud material	Talkochlorite	Zr-2.5%Nb
Cladding material	12X18H10T	Zr-1%Nb

3.2. Experiment performance technique

To investigate a heat transfer in the partially uncovered core model, VTI test 7.12.15.4 and test 8.6.3.2 were carried out in conditions of a break in two-phase natural circulation in the VVER-440 loop model, and with a coolant collapsed level in the middle of the core model height. These two tests were conducted with small specific heat fluxes qw1 and medium pressures, and also under conditions of absence of counter-current flow of a steam and its condensate in the core uncovered part.

In these tests the behaviors of the rod's cladding temperatures have been studied in the steady regimes with the following values of the main parameters:

- Power of the fuel assembly model W=16.8; 23.0 kW;
- Pressure in the UP model Pup=27.3; 70.1 bar;
- Mixture level in the FA channel Lm=1.87 m;
- Temperature of rod simulator's cladding TW $\leq$ 950 K.

The tests essentially differ by the conditions of their performance. These conditions cover wide range of VVER accidental conditions. In particular, the different heat fluxes, pressures, mass flow rates of a generated steam in the FA model were realized during these tests (see Table 3.1). At the same time the mixture level Lm (texp) in the FA channel was at the same position in both tests.

The steady regime was conducted as follows. The up-coming and down-coming branches of the loop got warm with a steam, and then were filled with a steam condensate which expelled an air from the loop. The loop was cut off from a source of a steam condensate, and the power-up attained value of FA power specified in the test.

To provide test conditions, it was performed preliminary heating of a water and pipeline metal up to required coolant temperature at the core model inlet under natural circulation. Coolant pressure was increased, and then coolant drainage from the lower pipeline to an expansion tank via the valve was started. Boiling NC regime was started under slightly greater pressure Pup than needed.

Full draining of the UP model was made after heating-up of pipeline metal in the upper parts of the VVER loop model up to saturation temperature. Coolant collapsed level in the Upper plenum model was controlled with differential manometer DP2. Then collapsed level was fallen down to the set value of the initial collapsed level in the FA channel. Thus there was set a partial uncovering in the core model using water drainage from the lower pipeline to an expansion tank through the valve. Coolant collapsed level was controlled with differential manometer DP3 in the SG simulator and with differential manometer DP1 in the core model.

Changing the flow rate and temperature of a secondary coolant fed to a steam condenser and to a water cooler, the regime of a break in two-phase natural circulation was established in the loop under required stationary conditions. Due to a balance between steam generation and steam condensation in the loop, a "steady regime" was realized at the stable values of pressure Pup (texp) in the upper plenum and of mixture level Lm (texp) in the FA channel, and at the stable rod's cladding temperatures TW (texp). This steady regime was realized at constant mass flow rate G and temperature TF of a subcooled water at the FA inlet, and at a constant electric power W (texp) of the FA model specified in the test.

To avoid steam condensation in the up-coming branch of the loop model, and, as a consequence, to avoid counter-current flow of a steam and its condensate in the uncovered part of the core model, the protective electric heaters located around the core pressure vessel and upper plenum were used.

To compensate heat losses from the outer surface of the core model to an ambient air, the power of each section of the protective electric heater located around the core pressure vessel was controlled

depending on a temperature differential of the coolant and the pressure vessel wall at the corresponding elevation in the core model. The power of each section of the protective electric heater located around the upper plenum was too controlled to compensate heat losses to an ambient air.

After establishment of the required initial conditions in the VVER-440 loop model (see Table 3.1) the test for investigation of a heat transfer in the partially uncovered core model was started. The steady regime was conducted during ~ 1 hour.

3.3. Initial and boundary conditions

3.2.1. Boundary conditions at the outer surfaces of the VVER-440 loop model. Heat losses

As noted above, to avoid a steam condensation in the up-coming branch of the loop model, and, as a consequence, to avoid counter-current flow of a steam and its condensate in the uncovered part of the core model, the protective electric heaters located around the core pressure vessel and upper plenum were used.

In this case heat losses and their distribution along the up-coming branch of the loop model may weakly influence on the rate of steam cooling and its condensation, hence, on the mass flow rate of a condensate, flowing into the SG model and into the inlet of the core model. Therefore, a real distribution of heat losses on the length of the hot leg model and down-coming branch of the loop model can not essentially influence on the code results for the behavior of rod's cladding temperature in the uncovered FA part.

3.2.2. Initial and boundary conditions inside of the primary coolant circulation circuit

A temperature regime of the heated rod in the uncovered part of the FA model is directly coupled with two-phase mixture level dynamics in the core under steam-condensate natural circulation in the primary coolant system. In this case a mixture level determines also a vapor mass flow rate in the uncovered part of the FA model. Therefore, adequate test data about the mixture level in the FA channel are required to calculate the rod's cladding temperatures.

The FA model consists of 19 fuel rod simulators with just the same design, in which the identical heater's elements are made of stainless steel rods with the same outer diameter of 3.3 mm. Therefore, during water boiling in the full wetted FA model and under nearly uniform distribution

of the rod simulator's cladding temperatures, the specific volumetric power qv and heat flux qw distributions in the parallel rod heaters are too uniform on radius and height of the FA model.

But, under condition of the partially uncovering of the FA model, axial and radial distributions of the rod simulators temperatures become essentially non-uniform. Under electric heating of the rod simulator's heaters, the local power at the various elevations in the FA model is determined by the electric resistance of the heater element, which essentially increases with temperature increase of the cladding and with temperature raising of the heaters in the fuel rod simulators. The influence of the electric resistance variation of the heater element with temperature on the radial and axial power distributions in the FA model may be taken into account using the distribution of measured rod's cladding temperatures and reference data [3] about specific electric resistance of 12X18H10T stainless steel at various temperatures.

During the test coolant temperature along the loop varied in a certain range, so variations of heat conductivity and specific heat capacity of the talkochlorite insulator, and stainless steel tubes and rods in the core model were noticeable. Therefore, the temperature dependencies of these parameters were used for the code calculations.

The initial and boundary conditions for modeling the steady regime are as follows:

- DC model and Lower plenum model have been filled up with a liquid under defined temperature TF (t0exp) and with a mixture level Lm (t0exp) in the Core model, and corresponding collapsed level in the DC model;
- the other parts of the loop model located above the mixture level: Upper plenum model, Hot leg model, SG simulator have been filled up with a superheated steam at the specified pressure Pup (t0exp);
- the water mass flow rate at the core inlet is determined by a driving head under condition of steam-condensate natural circulation in the loop model at the specified FA model power W (t0exp);
- FA axial and radial distributions of rod's cladding temperatures TW (x) are determined in a steady regime at the specified conditions with constant in time FA model power W (t0exp) in the test.

The time interval for cladding temperature stabilization in the fuel rod simulators was smaller than 1 hour. When the protective electric heaters were used, this time interval was enough for a complete temperature stabilization of the talkchlorite insulator and core pressure vessel having essentially greater thermal inertia than ones of the fuel rod simulators.

Non-steady heating of the talkchlorite insulator, of the core model pressure vessel may be calculated, if specific densities, heat capacities and thermal conductivity coefficients of the stainless steel and talkchlorite are known [3, 4].

3.4. Experimental Data used

This report presents test data on the behaviors of the rod's cladding temperatures TW (texp) along the FA model height and pressure Pup (texp) at the upper plenum outlet at constant in time FA power W (texp).

The initial values of the determinative parameters for test 7.12.15.4 and test 8.6.3.2 in steady regimes are presented in Table 3.1. Original data plots from test 7.12.15.4 and test 8.6.3.2 are presented in Figures A-1 and A-2, accordingly, in the Appendix A. Complete set of experimental data obtained in the VVER–440 loop model at VTI Test Facility is in [1, 2].

Table 3.2. Initial values of determinative parameters for test 7.12.15.4 and test 8.6.3.2 in steady regimes

Test code	FA power W (t0exp), kW	FA average heat flux qw kW/m^2	Pressure at the UP outlet Pup (t0exp), bar	Mixture level Lm(t0exp), m	NC mass flow rate, G(t0exp), kg/s	Mass flux in the FA channel kg/m^2 s
7.12.15.4	16.8	12.4	27.3	1. 87	5.1 -3	3.46
8.6.3.2	23.0	17.0	70.1	1.87	6.5 -3	4.40

Experimental axial distributions of the rod's cladding temperature in steady regimes for test 7.12.15.4 and test 8.6.3.2 were used for comparisons with the code results.

An experimental axial distribution of the rod's cladding temperature for test 7.12.15.4 is presented in Fig.A-1, and an axial distribution of the rod's cladding temperature for test 8.6.3.2 is presented in Fig.A-2. As seen, there are three characteristic areas in the axial distribution of the rod's cladding temperature:

- Area 1 where the rod's cladding temperature increases on the length of an economizer section of the FA model;
- Area 2 where the rod's cladding temperature is fixed and close to saturation temperature at the specified pressure in the FA channel;

- Area 3 where the rod's cladding temperature sharply increases on the height of the FA uncovered part.

The position of a boundary line between 1 and 2 areas is determined by the beginning of boiling on the surfaces of the rod simulators. The position of a boundary line between 2 and 3 areas is determined by dry out of a liquid film on the surfaces of the rod simulators. In this case the following assumption is used. A real mixture level is that level in the FA channel, at which a sharp increase of void fraction and local dryout of the rod's surface take place. And then a sharp decrease of the coefficient Hw1 (x) of heat transfer from outer surfaces of the rods to a coolant, and a local increase of the rod's cladding temperature TW (x) above saturation temperature take place, also. The mixture level in the FA channel is determined in basic by the coolant mass inventory in the loop, specific heat flux qw1 (x) on the outer surfaces of the rods, mass flow rate G and temperature TF of a liquid at the core inlet, and also pressure in the core model.

An experimental axial power distribution of the rod simulator's heater was calculated taking into account the influence of an electric resistance variation of 12X18H10T stainless steel with temperature on the power distribution in the partially uncovered FA model in a "steady regime". An experimental axial power distribution of the rod simulator's heater for test 7.12.15.4 is presented in Fig.3.1, and an axial power distribution of the rod simulator's heater for test 8.6.3.2 is presented in Fig.3.2.

For modeling the experimental initial and boundary conditions also it is necessary to know the real position of a mixture level in the FA channel. Therefore, the mixture level Lm (t0exp) in the FA channel is presented in Table 3.2, too. The mixture level Lm (t0exp) in the FA channel and its behavior Lm (texp) have been found out by a special analysis of the test data about rod's cladding temperatures TW (texp) and an axial distribution of the cladding temperatures TW (x) (see Fig. A-1 and Fig.A-2).

As seen, the same mixture levels in the FA channel, equal ~ 1.87 m were realized in these tests; but different values of the vapor mass flow rate Gg and vapor velocity Vg were realized in the uncovered part of the FA owing to the given different values of FA power, mass flow rate G and water temperature TF at the core inlet, and also pressure in the core model. The maximum temperature of the rod cladding was near 940 K which was measured in the uppermost part of the FA model.

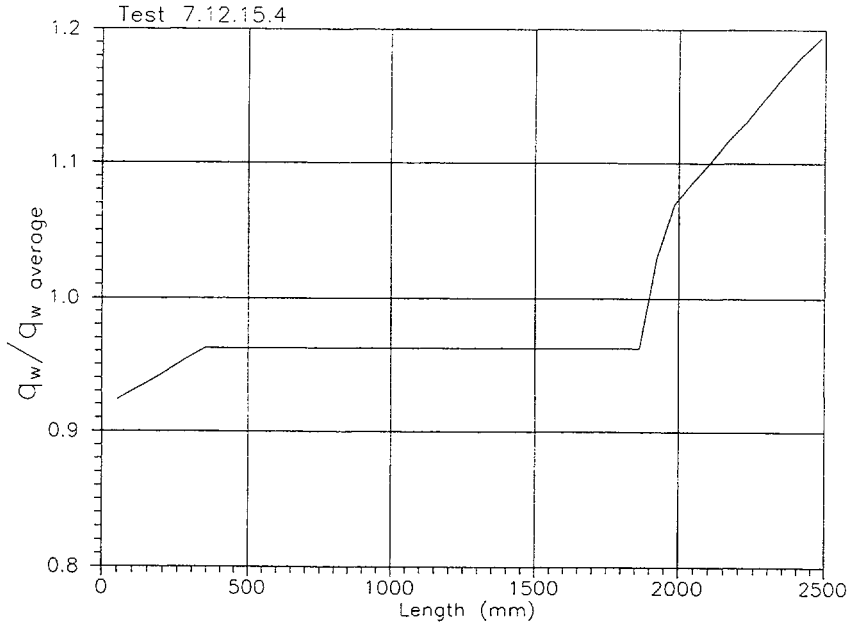

Fig.3.1. Experimental axial power distribution of the rod simulator's heater for test 7.12.15.4.

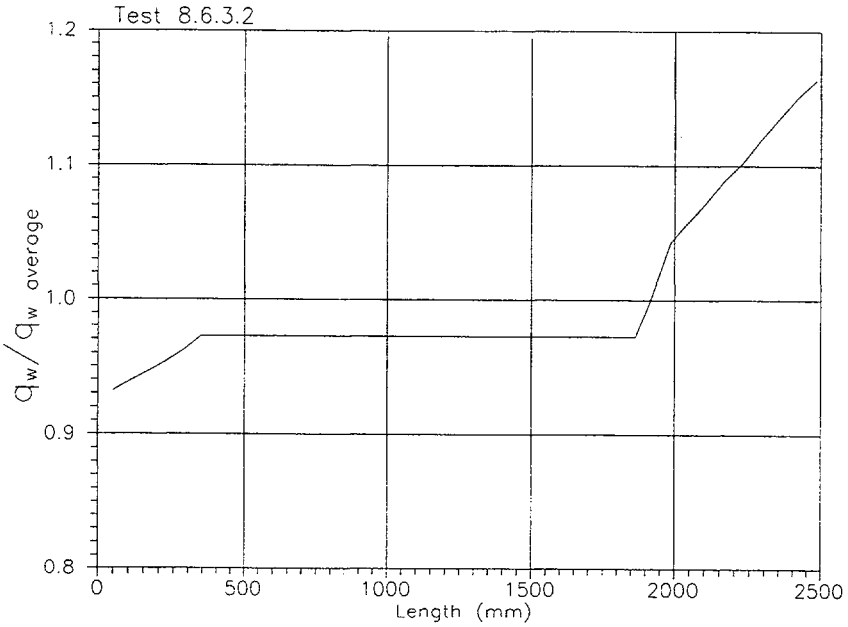

Fig.3.2. Experimental axial power distribution of the rod simulator's heater for test 8.6.3.2.

Analyzing the axial profiles of the rod's cladding temperatures it is possible to identify their almost linear character on the height of the FA uncovered part (see Fig.A-1, A-2). At the same time, it is visible, that near above a mixture level the temperature gradient on the FA height is a little bit higher than far from it.

Comparing the rod's cladding temperatures measured at the same levels, but on different rods in the bundle it was found out [1, 2], that the central rod and the rods located in the middle row in the bundle are in, practically, equal temperature conditions. Therefore, test data about cladding temperatures of the central rod and of the rods in the middle row marked as A, B, C, E and F in a cross section of the bundle (see Fig.2.3) were used for the comparisons with the code results.

4. DESCRIPTION OF RELAP5 MODEL AND BASE CASE INPUT DECK FOR THE TESTS

4.1. Code description

The code used for this work was RELAP5/MOD3.2.2GAMMA [4, 5] with no further updates. This code was used for the nodalization study and the base case calculations. The code has been installed on the IBM PC AT computer with processor Pentium 2 – 450 MHz. Windows 95 was used as an operating system.

4.2. RELAP5 model and Input Deck development

Figure 4.1 shows the nodalization to simulate the VVER-440 loop model and the test with RELAP5/MOD3.2.2. The code modeling of the test followed the specific calculation procedure used for simulation of the experimental initial and boundary conditions.

The RELAP5 model consists of all the components of the primary and secondary circuits of the VVER-440 loop model, in total of 12 RELAP5 components with 131 hydrodynamic Volumes, 129 Junctions and 167 Heat Structures with 611 mesh points. A complete listing of the base case input set for test 8.6.3.2 is listed in the Appendix E.

Nodalization scheme for VVER440 loop model includes the following components of the primary circuit: - Lower Plenum model (v. 5, sj. 6), Core model (v. 7, sj. 8), Upper Plenum model (v. 9, sj. 10), Hot Leg model (v. 11, sj. 12), SG simulator with a steam condenser (sv. 1401 – sv.1406) and Cold Leg simulator with a water cooler (v. 1415 – 1420), and Lower Water Pipe (sv. 1601 – 1616, sj.17).

A "pipe" hydrodynamic component Core Model 7 (sv. 701 - sv. 742), representing the test FA channel's fluid volumes, is connected to Lower Plenum model 5 at the bottom and to Upper Plenum model 9 at the top by the Single Junctions (SJ 6, SJ 8).
Volumes from 701 to 740 represent the part of the core channel with the heated rod bundle. Here the core node pitch equal a quarter spacer grid pitch (1/4 Psg = 60 mm) was chosen.

A "pipe" hydrodynamic components Upper Plenum 9 (sv. 901- sv. 915), representing the test UP fluid volumes, is connected to Core Model at the bottom and to Hot Leg at the top by the Single Junctions (SJ 8, SJ 10).

A "pipe" hydrodynamic component Hot Leg (sv. 1101 - sv. 1118), representing the test HL fluid volumes, is connected to SG simulator by Single Junction (SJ 12).

A "pipe" hydrodynamic component Lower Water Pipe 16 (sv. 1601 - sv. 1616) represents the test Lower Water Pipeline's fluid volumes with initial water temperature TF (t0exp).
Heat structure scheme used to describe power distribution of the heated rod bundle and circuit heat losses in an environment is shown in Figure 4.1.Taking into account our experience of the code simulation of the Standard Problem INSCSP-V4 [7], when modeling the core model with the FA model a fine nodalization was chosen for hydrodynamic components and heat structures along the FA height. This nodalization was connected to the pitch between spacer grids. When calculating hydrodynamics and heat exchange in the FA channel, such a nodalization scheme makes it possible to account the influence of all the spacer grids located with the pitch of 240 mm in the FA heated region.

A fine nodalization with 40 nodes for hydrodynamic components and heat structures along the FA height is used to have accurate calculations for the initial mixture level location Lm (t0 cal) and its behavior during transient, and also for the experimental axial power distribution of the rod simulator's heater and axial distribution of rod's wall temperatures for the test.

The rod simulator's heaters were modeled with "heat structure" components with internal heat sources to be uniformly distributed on the heater radius and non-uniformly distributed on the heater height (see Fig.3.1 and Fig.3.2).

Boundary conditions on the rod simulator's outer surfaces were set with Right Boundary Condition Cards with boundary condition type W3 (I)=110 ("Vertical bundle without crossflow" with P/D =1.34). Heat transfer hydraulic diameter (i.e., heated equivalent diameter) De=10.9 mm is used for the core channel with the heated FA model.

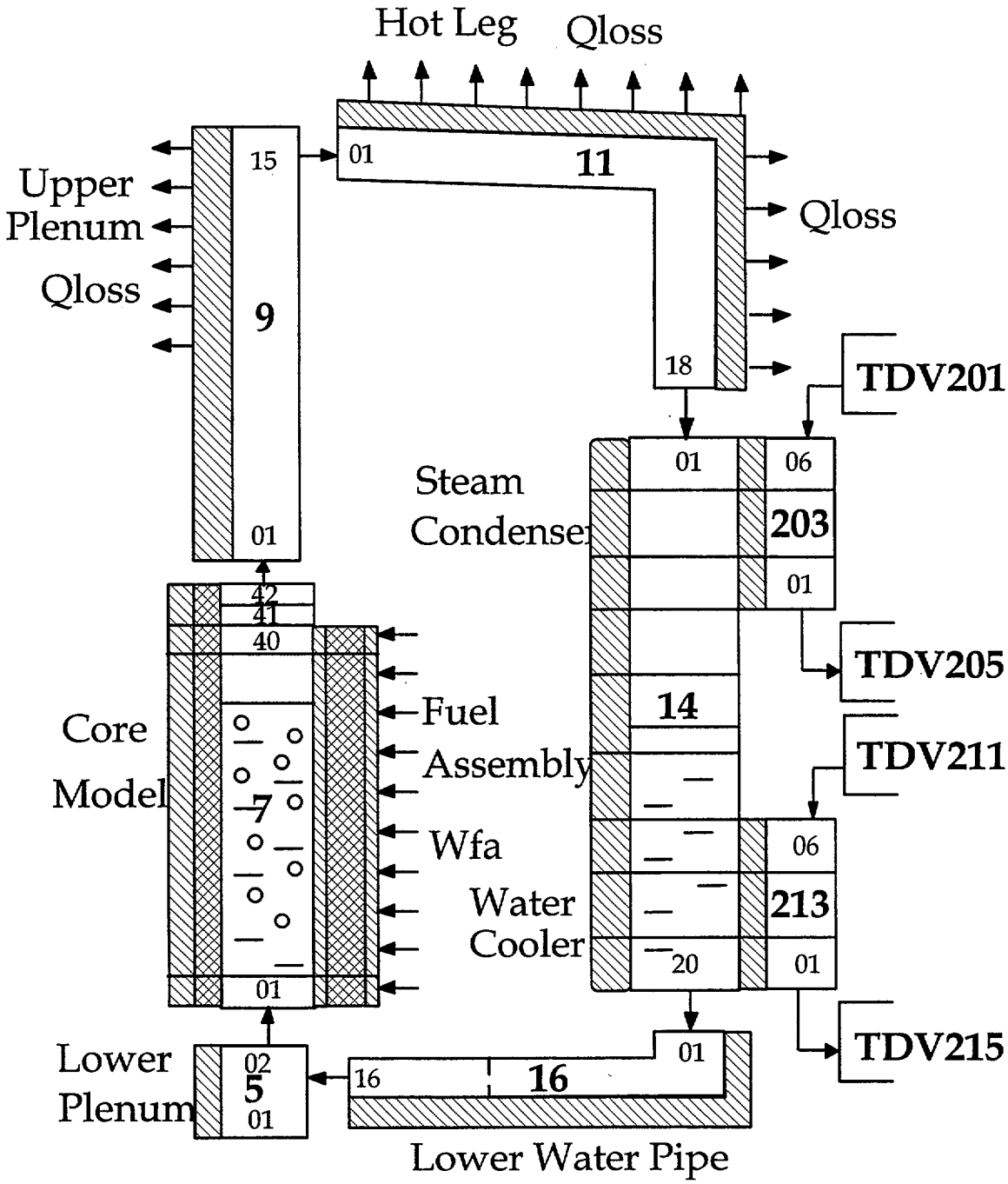

Fig.4.1. Base case nodalization scheme of VVER-440 loop model at VTI Test Facility.

To account the heat exchange processes to be impact by the grids, "Additional Right Boundary Cards" were used. Local hydraulic resistance ξ=0.27 is to simulate 10 spacer grids arranged with the pitch of 240 mm in the heated region.

Channel walls of the Core model, UP, HL, SG and Lower Water Pipeline were also modeled with "heat structure" components in order to simulate heat accumulation in the metal and external heat losses, if ones needed.

4.3. Method of computer modeling of the experiments

This computer model makes it possible to simulate directly the experiment. When computer modeling the experiment the problem is setting up the adequate thermal and hydraulic characteristics of the components in the primary and secondary circuits.

Mixture level determines the power portion for a steam generation in the covered part of the FA model and, accordingly, mass flow rate Gg (texp) of a saturated steam at the inlet of the FA uncovered part. Also, the mixture level determines the power portion in the FA uncovered part. The power portion in the FA uncovered part determines heat-up and distributions of the steam flow's temperatures and rod simulator's temperatures along the height of the FA uncovered part.

Thus, to calculate the distribution of rod's wall temperatures along the core height it is necessary to have accurate data about the initial mixture level Lm (t0exp) and its behavior Lm (texp) during the test.

In the uncovered part of the FA model it is possible local power excess over a heat transfer from the rod surface to a steam flow. As a result, local rod's wall temperature will increase with some rate dTW/dt, which depends on mentioned above power excess and on heat capacity of the rod simulator part. In other case, local cooling of the rod simulator part is possible. Hereof, the rate of change of rod's wall temperature during local heating or local cooling with the certain local power and known heat capacity is one of the main determined parameters of a heat transfer in the uncovered part of the FA model. This rate dTW/dt and absolute value of rod's wall temperature TW characterize a heat transfer in the uncovered part of the core model.

Local value of the rod's wall temperature is determined by local temperature of a steam flow and by the local temperature difference between a steam and rod's wall. This difference is determined by a local heat flux qw and by a heat transfer coefficient Hw1.

Temperature distribution in a steam flow along the core height depends on the steam mass flow rate and also on intensity of a heat exchange between the steam flow and the surfaces of the rods and talkochlorite insulator. Also, it depends on intensity of an interphase heat exchange of a superheated steam and condensate under counter-current flow, which may be formed in the Upper Plenum and Core model when the protective electric heaters are not used.

Heat flux qw2 (t) from a steam to the insulator and its stabilization time, and also temperature regime of the inner wall of insulator TWi (t) are determined by intensity of the heat transfer:

- between coolant and talkochlorite insulator;
- between outer surface of the core model pressure vessel and an ambient air when the protective electric heaters are not used.

Heat flux qw2 (t) and its stabilization time also depend on the thermal conductivity coefficients and relatively large heat capacities of the considered massive parts of the core model.

Thus, quality of the code modeling for rod temperature behavior in the uncovered part of the FA model depends on both accurate simulation of hydrodynamic processes in the loop model and accurate simulation of processes of a heat transfer from the rod simulators to the coolant flow and, further, in an environment.

Therefore, to simulate a heat transfer in the partially uncovered FA model in a "steady regime", it is necessary to provide close coincidence of the calculated and experimental values of pressure Pup (tcal) and Pup (texp), mixture level location Lm (tcal) and Lm (texp) in the FA channel, coolant temperature at the core inlet TF (tcal) and TF (texp), and of a steam generation rate in the FA channel Gg and liquid mass flow rate G at the core inlet.

Also, it is important to take into account the influence of an interphase heat transfer on complex processes in the uncovered part of the core model, if CCF takes place in the up-coming branch of the loop during the test when the protective electric heaters have not been used [7, 8].

The following determinative parameters (which initial values and behavior are defined in the experiment) have to be adequate provided during the code simulation using specified boundary conditions:

- behavior of heat release power in the FA model W (texp);
- initial value of pressure at the upper plenum model outlet Pup (t0exp);
- initial value of coolant temperature at the FA model inlet;

- initial distribution of void fraction on the length of the NC circuit and also on the height of the FA channel;
- initial distributions of temperatures of vapor and liquid on the length of the NC circuit;
- initial distributions of averaged on wall thickness wall's temperatures of pipelines, core pressure vessel and others, which determine accumulated heat in the circuit elements;
- initial distributions of temperatures of the rod simulators and inside parts of the core model with talkochlorite bushes;
- pressure and temperature of a secondary coolant at the inlet of a steam condenser;
- mass flow rate of a secondary coolant at the inlet of a steam condenser;
- pressure and temperature of a secondary coolant at the inlet of a water cooler;
- mass flow rate of a secondary coolant at the inlet of a water cooler;
- power of heat losses from the outer surfaces of the loop to an ambient air. In our case the heat losses are compensated by particular power of the protective electric heaters.

All the mentioned above parameters govern further behaviors of the following determined parameters:
- pressure at the upper plenum model outlet Pup (tcal);
- coolant temperature at the FA model inlet TF (tcal);
- mixture level in the FA channel Lm (tcal);
- mass flow rate of a coolant at the core model inlet G (tcal) under NC conditions;
- mass flow rate of a steam condensate G_L out (tcal), flowing down from circuit elements to the core model outlet (in our case it is absent when the protective electric heaters are used);
- flow rate of a steam condensate G (tcal), flowing down from circuit elements to the SG simulator and then to the core model inlet;
- distribution of steam flow rate Gg (tcal) on the height of the uncovered part of the FA model;
- distribution of steam velocity Vg (tcal) on the height of the uncovered part of the FA model;
- distribution of steam temperature Tg (tcal) on the height of the uncovered part of the FA model;
- distribution of temperatures of the outer surfaces of the rod simulators TW (tcal) on the FA height; rates dTW/dt;
- distribution of coefficient Hw1 (tcal) of heat transfer from the outer surfaces of rod simulators to the coolant on the FA height;
- distribution of coefficient Hw2 (tcal) of heat transfer from a coolant flow to the talkochlorite insulator on the core height;

- distribution of specific heat flux qw1 (tcal) from the outer surfaces of the rod simulators to the coolant on the FA height;
- distribution of specific heat flux qw2 (tcal) from a coolant flow to the talkochlorite insulator on the FA height;
- distribution of specific heat flux qw_{loss} (tcal) from the outer surface of the core pressure vessel to an ambient air (heat losses are absent when the protective electric heaters are used).

During definition of the assessment problem the main attention has been paid on evaluation of RELAP5/MOD3.2.2GAMMA adequacy to simulate separate phenomena/processes of heat transfer in the uncovered part of the core model. Simulations of hydrodynamic phenomena in the main loop components, presumably, have been considered as auxiliary tasks. Solution of these tasks was necessary to provide the required initial and boundary conditions in the partially uncovered core model.

Such approach is stipulated by the fact, that when modeling the interdependent hydrodynamic and thermal processes in the loop, essential shortcomings are possible during code simulation of such hydrodynamic parameters as the mixture level, void fraction distribution, distributions of mass flow rates and velocities of the phases, and interphase heat exchange along the height of the uncovered part of the FA model. In our opinion a special analysis of the code adequacy for simulation of mentioned hydrodynamic parameters in the loop need to be additionally implemented in a separate Standard Problem.

Therefore, to diminish possible effects of these shortcomings on the calculation results for axial distributions of the heat transfer coefficients Hw1 (tcal) and rod's wall temperatures TW (tcal), a special method has been developed for computer modeling the initial and boundary conditions in the partially uncovered core model for each separate test.

When modeling an experiment using RELAP5/MOD3.2.2GAMMA the definition of a certain steady state with known boundary conditions at the initial moment of time t0cal is required. Starting with this point and using a certain transition procedure, it is possible to achieve such a steady state, that one most adequate describes a steady state in the loop and core model at the initial time moment t0exp in the experiment.

It should be taken into account that code simulation of auxiliary tasks concerning of the transient hydrodynamic processes in the loop components and in the loop as a whole can lead to essential inaccuracies of the calculated parameters. So, in our method of computer modeling of the test there

is an opportunity to adjust a mixture level in the FA channel by selection of the suitable liquid mass inventory M_L in the loop and initial pressure Pup (t0cal).

The mixture level Lm (tcal) = Lm (t0exp) in the FA channel and its behavior Lm (tcal) are determined by a special analysis of the calculation results and test data about the behaviors of rod's wall temperatures TW (t) and their axial distribution, and also temperature change rates dTW/dt.

To avoid a steam condensation in the up-coming branch of the loop and, as a consequence, to avoid counter-current flow of a steam and its condensate in the uncovered part of the core model, the effect of the protective electric heaters, located around the core model and upper plenum, has been simulated using zero heat losses from the particular heat structures in an environment.

After establishment of the required initial conditions in the loop (see Table 3.1) the code simulation of a heat transfer in the partially uncovered core model in a "steady regime" was started. Stabilization of the calculated determinative and determined regime parameters was achieved during the particular interval of time (up to ~1 hour) which was used for a complete stabilization of the regime parameters under test conditions too.

The results of comparisons of the calculated and measured values of the determinative and determined parameters are a base for a conclusion about adequacy of the code simulation of the initial and boundary conditions, realizing in the test, and then about adequacy of the code simulation of a "steady regime".

When calculating and assessing suitability of RELAP5/MOD3.2.2GAMMA and its modeling units for description of the separate phenomena and complex processes, it is conventional to use the options recommended by the code developers for actuating the code models under analogous conditions. The general modeling approaches recommended in the RELAP5 manuals [5, 6] should continue to be used.

The following assumptions were made:

- Volume Vertical Stratification, Water Packing, Abrupt Area Change, Umbrella Model were process models activated for the corresponding circuit components;

- Process models such as an additional model of counter-current flow limitation (CCFL Model), model of critical mass flow rate (Choked Model) and Reflood Model were not to be used in the corresponding loop components.

When modeling transient in the core channel with the FA model, it was chosen a maximum time step dtmax =0.025 s.

To describe interphase friction in the coolant in the FA channel, an option designating to a rod bundle (with flag b=1) is applied. Semi-implicit scheme of numerical integration specified with the tt=3 option is used to calculate conjugate hydrodynamics and heat transfer/conduction processes. To activate convective boundary conditions for non-standard geometry when modeling a vertical bundle, the rod pitch-to-diameter ratio was input.

In the base case calculations for the tests, at use of the code models for description of a heat transfer in the FA model, it was pre-assigned Fouling factor K_{HW1}=1.0 to define the coefficients of heat transfer Hw1 (tcal) in the uncovered FA part which are recommended by the code developers.
To help development of an adequate nodalization scheme of the VVER-440 loop model and the computer methods of simulation of the initial and boundary conditions for each separate test, preliminary analyses of these tests were fulfilled using the code.

5. RESULTS OF THE CODE ASSESSMENT

5.1. Nodalization, including variations from base case

Before choosing a final model, the effect of different nodalizations to the results of RELAP5/MOD3.2.2GAMMA calculations was investigated for VTI test 7.12.15.4. Of interest was the influence of number of hydraulic volumes and heat structures chosen. The different nodalizations were studied using 20 and 40 volumes for the core channel (hydrodynamic component 7) with the heated FA model by fixing the number of fine mesh nodes in the heat conduction elements. Here the core node pitch was chosen equal a half or a quarter spacer grid pitch (1/2 Psg =·120 mm or 1/4 Psg = 60 mm).

As quality of the code modeling for rod's wall temperature behavior in the partially uncovered FA depends on accurate simulation of a mixture level in the core channel, it is necessary to provide close coincidence of Lm (tcal) calculated and Lm (texp) experimental values of the mixture level.

Higher number of volumes results in more accurate code simulation of the mixture level in the core channel. And, also, higher number of the volumes results in smaller error (± 30 mm), when the real mixture level Lm (t1cal) = Lm (t0exp) and its behavior Lm (tcal) are determined by a special analysis of the calculation results for TW (tcal) and test data about rod's wall temperatures TW (texp). Measurements of the TW (texp) temperatures along the height of the FA model with 51

thermocouples on 32 elevations have provided the temperature axial distribution in the FA model and test data about a mixture level in the FA channel with accuracy of ± 25 mm.

Therefore, when modeling the core model with the FA model, a fine nodalization was chosen for hydrodynamic components and heat structures along the FA height. A fine nodalization was connected to the pitch between spacer grids. When calculating hydrodynamics and heat exchange in the FA channel, this nodalization scheme makes it possible to account the influence of all the spacer grids located with the pitch of 240 mm in the FA heated region.

Nodalization with 40 nodes for hydrodynamic components and heat structures along the FA height results in more accurate calculations for the initial mixture level Lm (t0cal) and its behavior during the transient, and also for the experimental axial power distribution of the rod simulator's heater and axial distribution of rod's wall temperature during the test.

After the choice of proper nodalization and maximum user-specified time step dtmax, base case calculations were done for the tests. All the calculations to be presented latter in this report were performed by selecting the nodalization with 40 volumes for the core channel with the heated bundle as the base case (see Fig. 4.1).

5.2. Base case results for test 7.12.15.4, comparisons to VTI test data and conclusions

In this test the behaviors of the rod's cladding temperatures have been studied in a "steady regime" with the following values of the main parameters:

- Power of the fuel assembly model W=16.8 kW;
- Pressure in the UP model Pup=27.3 bar;
- Mixture level in the FA channel Lm=1.87 m;

During this "steady regime" a heat transfer in the core uncovered part takes place too under stationary conditions with the constant in time specific heat fluxes qw1(tcal), heat transfer coefficients Hw1(tcal) and rod's wall temperatures TW (tcal).

The base case calculations were performed for VTI test 7.12.15.4 using maximum user-specified time step dt max = 0.025 s and fouling factor K_{HW1}=1.0 to define the coefficients Hw1 (tcal) of heat transfer from the rods to a steam flow in the uncovered FA part which are recommended by the code developers [5, 6].

During simulation of the test with RELAP5/MOD3.2.2GAMMA we have defined the initial and boundary conditions of a steady state at the time moment t0cal taking into account the results of our preliminary code calculations for the test.

Starting from this steady state and using a procedure of the transition method, we have run the transition to such a steady state in the loop at the time t1cal which is adequate to the experimental "initial steady state" in the loop at the time moment t0exp. Code simulation of the transition was realized during the time interval from t0cal = 0 s to t1cal = 3000 s to set up the initial and boundary conditions and to achieve the needed "initial steady state" in the loop at the time t1cal=3000s. Then further code simulation for a "steady regime" was realized during the time interval from t1cal = 3000 s to t2cal = 4000 s to illustrate a complete stabilization of the calculated values for the regime parameters during the particular time interval which corresponds to the test interval from the initial time t0exp=0 s to the end of the test at t1exp=1000 s.

Within this time interval (Dtexp=1000 s) the calculation results for the "steady regime" and test data for VTI test 7.12.15.4 are presented as time–dependent curves on Figures B-1÷B-13 in the Appendix B. The curves serve for comparisons of the base case calculation results with test data to demonstrate the code suitability. Also, the calculated histories of determinative and determined parameters are shown in the figures to examine hydrodynamic interactions between adjacent components in the loop.

As in the test, during code modeling of the test the needed values of the mass flow rate G (tcal) and primary water temperature TF (tcal) at the inlet of the FA channel, and also pressure Pup (tcal) in the Upper Plenum were attained by change of the mass flow rate and temperature of a secondary coolant at the inlet of a Steam Condenser, and also by change of the mass flow rate and temperature of a secondary coolant at the inlet of a Water Cooler.

Due to a balance between steam generation in the Core model and steam condensation in the loop as a whole, in the code calculations a "steady regime" was realized too at the stable values of pressure Pup (tcal) in the Upper Plenum and mixture level Lm (tcal) in the FA channel, and at stable rod's wall temperatures TW (tcal). This "steady regime" was realized also at constant values of the mass flow rate G (tcal) and temperature TF (tcal) of a subcooled water at the FA inlet, and at constant electric power W (tcal) of the FA model.

The results of code simulation of the initial and boundary conditions for the test 7.12.15.4 are presented on Figures B-1÷B-6.

Comparisons of the calculation results and test data about the main regime parameters Pup(t) and G(t) at the FA inlet for the "initial steady state" are presented in Figures B-1 and B-3, respectively. In these figures one can see the calculated values of mentioned parameters are close to the experimental ones or they lie within the range of measurement accuracy.

The assumption is accepted, that an evidence of a good accuracy of modeling the water temperature TF (t1cal) at the inlet of FA channel is a coincidence of the axial profile of calculated rod's wall temperature TW (t1cal) with the distribution of the measured rod's cladding temperatures on the height of the economizer section in the bottom part of the FA model (see Fig.5.1).

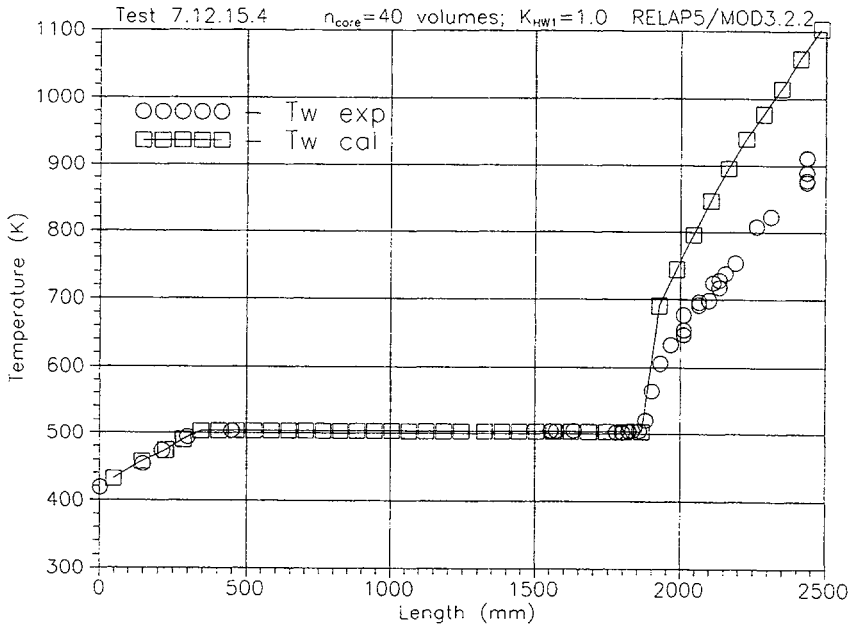

Fig.5.1. Comparison of the axial profile of calculated rod's wall temperature TW (t1cal) and axial distribution of the measured rod's cladding temperatures TW (t0exp) for the initial time moment for test 7.12.15.4 at FA power W=16.8 kW and pressure Pup= 27.3 bar.

A comparison of the axial distributions of experimental qw (t0exp) and calculated qw1 (t1cal) specific heat fluxes from the outer surface of the rod simulator to a coolant for the initial time moment t1cal is shown in Fig. B-4. As seen, there is a good agreement between the calculated and experimental axial profiles of the specific heat flux in the FA model at the initial time.

The mixture level Lm (t1cal) = Lm (t0exp) in the FA channel and its behavior Lm (tcal) are

determined by a special analysis of the calculation results TW (tcal) and comparison of the axial profile of the calculated rod's wall temperature TW (t1cal) and axial distribution of the measured rod's cladding temperatures TW (t0exp) at the initial time moment (see Fig.5.1). The assumption is used, that a real mixture level is that level in the FA channel, at which a sharp increase of void fraction takes place in the upper part of the FA channel (see Fig.B-11). And then the sharp decrease in calculated coefficient Hw1 (x) of heat transfer from the outer surface of the rod to a coolant (see Fig. B-8) and, consequently, a local increase of the rod's cladding temperature TW (x) above saturation temperature take place, too. As seen in Fig.5.1, the calculated value Lm (t1cal) for a mixture level is nearly equal the initial mixture level Lm (t0exp) = 1.87 m in the test.

Thus, the code results for the ***"initial steady state"*** are in good agreements with the test data about the main regime parameters: pressure Pup (t0exp), water temperature TF (t0exp), mass flow rate G (t0exp), mixture level Lm (t0exp) and heat flux qw (t0exp) in the core model. It provides the needed mass flow rate Gg (t1cal) of a generated steam flowing into the uncovered part of the core model under test conditions.

Behavior of the calculated TW (tcal) rod's wall temperature in the upper, middle and bottom parts of the FA model during a "steady regime" are presented in Fig.B-5. There is a significant quantitative difference between the axial profile of the calculated rod's wall temperature TW (t1cal) and axial distribution of the measured temperatures TW (t0exp) in the uncovered part of the FA model (see Fig.5.1). RELAP5/MOD3.2.2GAMMA over predicts rod's wall temperatures in the uncovered part of the heated FA model at the initial time moment. As seen, in the ***"initial steady state"*** the calculated TW (t1cal) rod's wall temperature is much higher (up to ~ 150 K) than measured one at the FA outlet. This is the main problem of the code for the base case calculations of the ***"initial steady state"*** .

It is a base for a conclusion about adequacy of the code simulation of the initial and boundary conditions only for hydrodynamics, realized in the experiment. At the same time, the code gives inadequate simulation of the heat transfer coefficients and axial distribution of rod's wall temperatures TW(t1cal) in the uncovered part of the FA model for the "initial steady state".

The adequacy of the code for analysis of heat transfer phenomena in the uncovered part of the core model has been estimated by comparison of the axial profile of the calculated rod's wall temperature TW (t2cal) and axial distribution of the measured rod's cladding temperatures TW (t1exp) at the end of a "steady regime" at the time moment t1exp=1000 s (see Fig. B-6).

Comparisons of the measured and calculated histories of the parameters Pup (tcal) and G (tcal) illustrate a good coincidence of these curves during a "steady regime" in Figures B-1 and B-3, respectively, in the Appendix B. The accuracy is shown for the regime parameters coincidence in the calculation and experiment at analogous time moments (at the calculation time t2cal and experimental time t1exp). The coincidence of the behaviors of the calculated and measured parameters during a "steady regime" is shown too.

As seen in Fig.B-6, in a ***" steady regime"*** the calculated TW (t2cal) rod's wall temperature is much higher (up to ~ 150 K) than measured one at the FA outlet. This is the main problem of the code for the base case calculations of the ***"steady regime"*** for test 7.12.15.4.

To found out the physical reasons for these essential discrepancies between code predictions and test data, the histories of the calculated coefficients Hw1 (tcal) of heat transfer in the uncovered part of the FA model are presented in Fig.B-7. An axial distribution of the calculated coefficients Hwl (t2cal) of heat transfer from the outer surfaces of the rods to a coolant in the upper part of the FA model is shown in Fig.5.2. Also, additional code results are shown too in Figures B-9÷B-13 in the Appendix B.

The main reason for the deviations between the experiment and calculations may be too low coefficients Hw1 (t2cal) ≈ 58–78 $W/m^2 \cdot K$ of heat transfer from the outer surfaces of the rod simulators to a coolant which are calculated for the uncovered part of the FA model (see Fig.5.2). It is a base for a conclusion about adequacy of the code modeling only for hydrodynamics, realized during a ***"steady regime"*** in the test. At the same time, the code gives inadequate simulation of the axial distributions of the heat transfer coefficients Hw1(t2cal) and rod's wall temperatures in the uncovered part of the FA model at the end of a "steady regime".

As seen in Figures B-9 and B-11, the calculated void fractions of a superheated vapor in the uncovered part of the core model are equal 1.0. It is the evidence of absence of counter-current flow in the uncovered part of the FA model. Therefore, these results give also the indications that the code models for modeling counter-current flow limitation (CCFL) and interphase heat transfer are not to be used for the uncovered part of the core model.

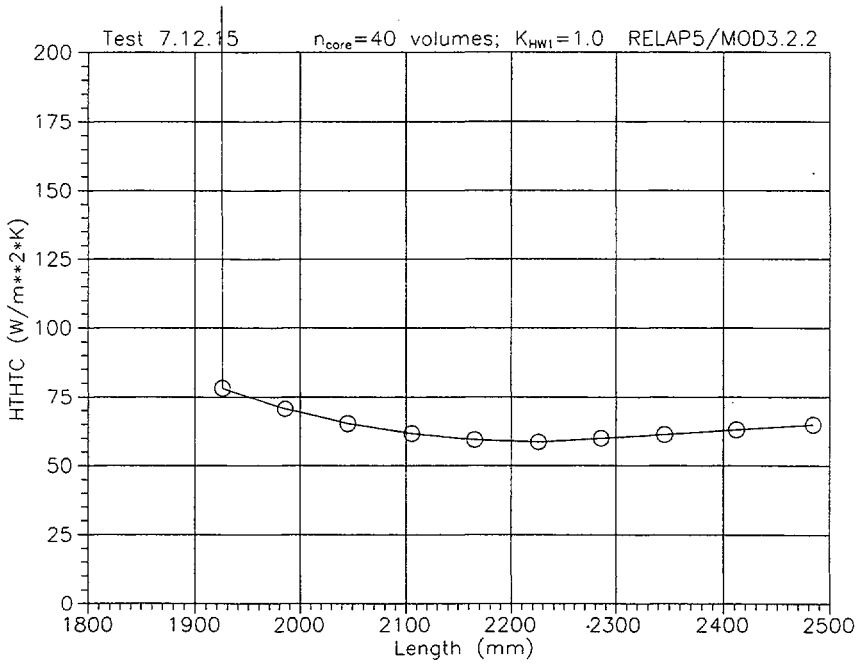

Fig.5.2. Axial distribution of the calculated coefficients Hw1 (t2cal) of heat transfer from the rods to a coolant in the upper part of the FA model for experiment 7.12.15.4.

Calculated Vg (tcal) vapor velocities histories in the upper part of the FA channel are shown in Fig. B-10. As seen, during a "steady regime" the vapor velocities Vg (tcal) at different elevations increase along the uncovered part of the FA model and the maximum value of vapor velocity is equal 0.52 m/s at the outlet of the FA model. The calculated axial distribution of the vapor velocities Vg (x) in the FA channel is shown in Fig.B-12.

In this test the transition mode of a steam flow (this mode is realized between laminar and turbulent modes of a steam flow) is realized along the height of the uncovered part of the FA model with corresponding Reynolds numbers $Re_g = Vg \cdot Dh / \nu_g \approx 1650 - 830$. An axial distribution of the calculated vapor temperatures Tg (x) in the uncovered part of the FA channel is shown in Fig.B-13.

Sensitivity studies are needed to determine the main reason for these deviations between the test data and code results.

Conclusions for VTI test 7.12.15.4

• RELAP5/MOD3.2.2GAMMA and the base case method of computer modeling of the VTI test 7.12.15.4 have provided adequate simulations of the initial and boundary conditions only for hydrodynamics, realized in a steady regime with steam-condensate natural circulation in the VVER-440 loop model. In this test the transition mode of a steam flow is realized along the height of the uncovered part of the FA model with corresponding Reynolds numbers $Re_g = Vg \cdot Dh / \nu_g \approx 1650 - 830$.

• The results for the "initial steady state" are in good agreements with the test data about the main regime parameters: pressure Pup (t0exp), water temperature TF (t0exp), mass flow rate G (t0exp), mixture level Lm (t0exp) and heat flux qw (t0exp) in the core model. It provides the needed mass flow rate Gg (t0exp) of a generated steam flowing into the uncovered part of the core model under the test conditions.

• At the same time, RELAP5/MOD3.2.2GAMMA gives inadequate simulation of the heat transfer coefficients Hw1 (t1cal) and axial distribution of the rod's wall temperatures in the uncovered part of the FA model for the "initial steady state". There is a significant quantitative difference of the axial profile of the calculated rod's wall temperature TW (t1cal) and axial distribution of the measured rod's cladding temperatures TW (t0exp) in the uncovered part of the FA model. The code over predicts rod's wall temperatures in the uncovered part of the FA model at the initial time moment and then during a "steady regime". The calculated TW (t1cal) rod's wall temperature is much higher (up to ~ 150 K) than measured one at the FA outlet. This is the main problem of the code for the base case calculations for the test 7.12.15.4.

• The main reason for these deviations between experiment and calculations may be too low calculated coefficients Hw1 (t1cal) ≈ 58–78 $W/m^2 \cdot K$ of heat transfer from the outer surfaces of the rod simulators to a coolant in the uncovered part of the FA model. It is a base for a conclusion about adequacy of the code simulation of the test conditions only for hydrodynamics, realized during the test. At the same time, the code gives inadequate simulation of the heat transfer coefficients Hw1 (t1cal) and behavior of rod's wall temperatures in the uncovered part of the FA model during the "steady regime".

• Sensitivity studies are needed to determine the main reason for these deviations between the code results and test data.

5.3. Base case results for test 8.6.3.2, comparisons to VTI test data and conclusions

In this test the behaviors of the rod's cladding temperatures have been studied in a "steady regime" with the following values of the main parameters:

- Power of the fuel assembly model W=23 kW;
- Pressure in the UP model Pup=70.1 bar;
- Mixture level in the FA channel Lm=1.87 m;

During this "steady regime" the regime of heat transfer in the core uncovered part is also stationary with the constant in time specific heat fluxes qw1 (tcal), coefficients of heat transfer Hw1(tcal) and rod's wall temperatures TW (tcal).

The base case calculations were performed for VTI test 8.6.3.2 using nodalization with 40 volumes for the Core model and maximum user-specified time step dt max = 0.025 s, and also using fouling factor K_{HW1}=1.0 to define the coefficients Hw1 (tcal) of heat transfer in the uncovered FA part which are recommended by the code developers [5, 6].

Taking into account the results of our preliminary code calculations for the test 8.6.3.2 we have defined the initial and boundary conditions of a steady state at the time moment t0cal.

Code simulation of the transition procedure was realized during the time interval from t0cal = 0 s to t1cal = 3000 s to set up the initial and boundary conditions and to achieve the needed "initial steady state" in the loop at the time moment t1cal=3000s. Then further code simulation for a "steady regime" was realized during the time interval from t1cal = 3000 s to t2cal = 4000 s to illustrate a complete stabilization of the calculated regime parameters during the particular time interval which corresponds to the test interval from the initial moment t0exp=0 s to the end of the test at t1exp=1000 s. Within this time interval the calculation results for the "steady regime" and test data for VTI test 8.6.3.2 are presented as time–dependent curves on Figures C-1÷C-13 in the Appendix C.

The results of code simulation of the initial and boundary conditions for the test 8.6.3.2 are presented on Figures C-1÷C-6. Comparisons of the calculation results and test data about the main regime parameters Pup (t) and G (t) at the FA inlet for the "initial steady state" are presented in Figures C-1 and C-3, accordingly. In these figures one can see the calculated parameters are close to the experimental ones or they lie within the range of measurement accuracy.

The evidence of a good accuracy of modeling the water temperature TF (t1cal) at the inlet of FA channel is a coincidence of the axial profile of calculated rod's wall temperature TW (t1cal) with the distribution of measured rod's cladding temperatures on the height of the economizer section in the bottom part of the FA model (see Fig.5.3).

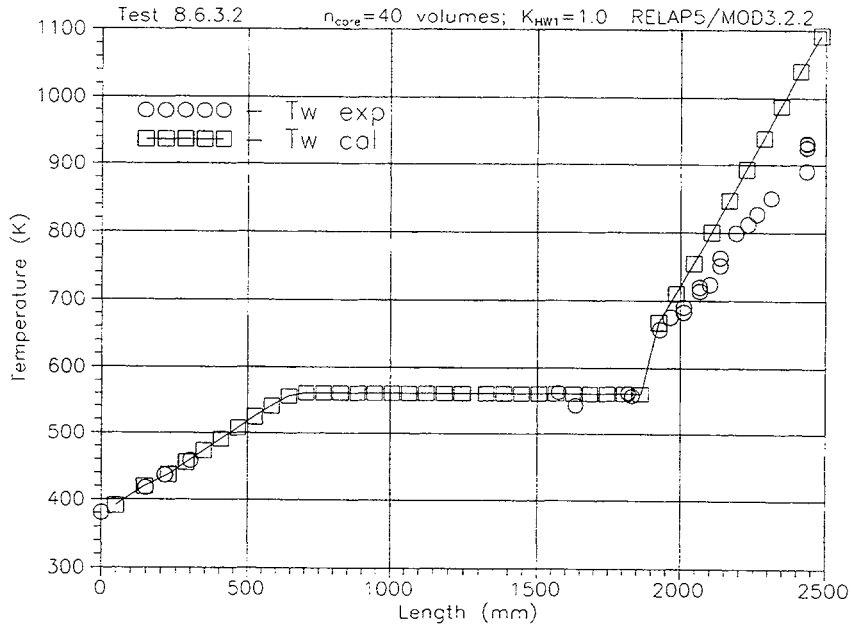

Fig.5.3. Comparison of the axial profile of calculated rod's wall temperature TW (t1cal) and axial distribution of measured rod's cladding temperatures TW (t0exp) for the initial time moment for test 8.6.3.2 at the FA power W=23 kW and pressure Pup= 70.1 bar.

A comparison of the axial distributions of experimental qw (t0exp) and calculated qw1 (t1cal) specific heat fluxes from the outer surface of the rod simulator to a coolant for the initial time moment t1cal is shown in Fig. C-4. As seen, there is a good agreement between the calculated and experimental axial profiles of the specific heat flux in the FA model at the initial time moment.

The mixture level Lm (t1cal) = Lm (t0exp) in the FA channel is determined by a comparison of the axial profile of calculated rod's wall temperature TW (t1cal) and axial distribution of the measured rod's cladding temperatures TW (t0exp) at the initial time. As seen in Fig.5.3, the calculated value Lm (t1cal) for a mixture level is nearly equal the initial mixture level Lm (t0exp) = 1.87 m in the test.

Thus, the code results for the "initial steady state" are in good agreements with test data about the main regime parameters: pressure Pup (t0exp), water temperature TF (t0exp), mass flow rate G (t0exp), mixture level Lm (t0exp) and heat flux qw (t0exp) in the core model. It provides the needed mass flow rate Gg (t1cal) of a generated steam flowing into the uncovered part of the core model under test conditions.

Behavior of the calculated TW (tcal) rod's wall temperature in the upper, middle and bottom parts of the FA model during a "steady regime" are presented in Fig.C-5. There is a significant quantitative difference between axial profile of the calculated rod's wall temperature TW (t1cal) and axial distribution of the measured temperatures TW (t0exp) in the uncovered part of the FA model (see Fig.5.3). The code over predicts rod's wall temperatures in the uncovered part of the heated FA model at the initial time moment. As seen, in the ***"initial steady state"*** the calculated TW (t1cal) rod's wall temperature is much higher (up to ~ 150 K) than measured one at the FA outlet. This is the main problem of the code for the base case calculations for the ***"initial steady state"*** for the test 8.6.3.2.

It is a base for a conclusion about adequacy of the code simulation of the initial and boundary conditions only for hydrodynamics, realized in the experiment. At the same time, the code gives inadequate simulation of the heat transfer coefficients and axial distribution of the rod's wall temperatures in the uncovered part of the FA model for the "initial steady state".

The adequacy of the code for analysis of heat transfer phenomena in the uncovered part of core model has been estimated by a comparison of the axial profile of the calculated rod's wall temperature TW (t2cal) in the FA model and axial distribution of the measured rod's cladding temperatures TW (t1exp) at the end of a "steady regime" at the time t1exp=1000 s (see Fig. C-6).

Comparisons of the measured and calculated histories of the regime parameters Pup (tcal) and G (tcal) illustrate good coincidence of these curves during a "steady regime" in Figures C-1 and C-3, accordingly.

As seen in Fig.C-6, at the end of a "steady regime" the calculated TW (t2cal) rod's wall temperature is much higher (up to ~ 150 K) than measured one at the FA outlet. This is the main problem of the code for the base case calculations for the ***"steady regime"*** for test 8.6.3.2.

To found out the physical reasons for these essential discrepancies between code predictions and test data, the histories of the calculated coefficients of heat transfer Hw1 (tcal) in the uncovered part of the FA model are presented in Fig.C-7. A core axial profile of the calculated coefficients

Hw1(t2cal) of heat transfer from the rods to a coolant is shown in Fig.C-8. Also, additional code results are shown too in the Figures C-8 ÷C-13 in the Appendix C.

An axial distribution of the calculated coefficients Hwl (t2cal) of heat transfer from the outer surfaces of the rods to a coolant in the upper part of the FA model is shown in Fig.5.4.

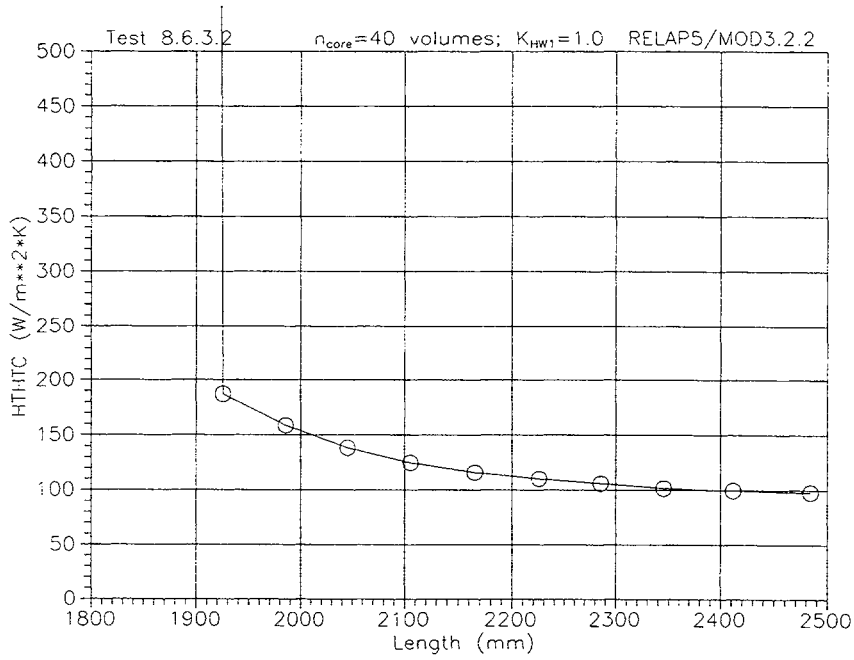

Fig.5.4. Axial distribution of the calculated coefficients Hw1 (t2cal) of heat transfer from the rods to a coolant in the upper part of the FA model for experiment 8.6.3.2.

The main reason for the deviations between the experiment and code results may be too low coefficients Hw1 (t2cal) ≈ 180–98 W/m^2·K of heat transfer from the outer surfaces of the rod simulators to a coolant which are calculated for the uncovered part of the FA model (see Fig.5.4). It is a base for a conclusion about adequacy of the code simulation of a "steady regime" only for hydrodynamics, realized in the test. At the same time, the code gives inadequate simulation of the axial distributions of the heat transfer coefficients Hw1(t2cal) and rod's wall temperatures in the uncovered part of the FA model for a "steady regime".

As seen in the Figures C-9 and C-11, the calculated void fractions of a superheated vapor in the uncovered part of the core model are equal 1.0. It is the evidence of absence of counter-current flow

in the uncovered part of the FA model. Therefore, these results give also the indications that the code models for modeling counter-current flow limitation (CCFL) and interphase heat transfer are not to be used for the uncovered part of the core model.

Calculated Vg (tcal) vapor velocities histories in the upper part of the FA channel are shown in Figures C-10. As seen, during a "steady regime" the vapor velocities Vg (tcal) at different elevations increase along the uncovered part of the FA model and the maximum value of vapor velocity is equal 0.26 m/s at the outlet of the FA model. The calculated axial distribution of the vapor velocities Vg (x) in the FA channel is shown in Fig.C-12. In this test the transition mode of a steam flow is realized along the height of the uncovered part of the FA model with corresponding Reynolds numbers $Re_g = Vg \cdot Dh / \nu_g \approx 1860 - 1060$.

An axial distribution of the calculated vapor temperatures Tg (x) in the uncovered part of the FA channel for the test 8.6.3.2 is shown in Fig.C-13.

Sensitivity studies are needed to determine the main reason for these deviations between test data and code results.

Conclusions for VTI test 8.6.3.2

• RELAP5/MOD3.2.2GAMMA and the base case method of computer modeling of the VTI test 8.6.3.2 have provided adequate simulations of the initial and boundary conditions only for hydrodynamics, realized in a steady regime with steam-condensate natural circulation in the VVER-440 loop model. In this test the transition mode of a steam flow is realized along the height of the uncovered part of the FA model with corresponding Reynolds numbers $Re_g = Vg \cdot Dh / \nu_g \approx 1860 - 1060$.

• The code results for the "initial steady state" are in good agreements with the test data about the main regime parameters: pressure Pup (t0exp), water temperature TF (t0exp), mass flow rate G (t0exp), mixture level Lm (t0exp) and heat flux qw (t0exp) in the core model. It provides the needed mass flow rate Gg (t0exp) of a generated steam flowing into the uncovered part of the core model under the test conditions.

• At the same time, RELAP5/MOD3.2.2GAMMA gives inadequate simulation of the heat transfer coefficients Hw1 (t1cal) and axial distribution of the rod's wall temperatures TW(t1cal) in the uncovered part of the FA model for the "initial steady state". There is a significant quantitative difference of the axial profile of the calculated rod's wall temperature TW (t1cal) and axial

distribution of the measured rod's cladding temperatures TW (t0exp) in the uncovered part of the FA model. The code over predicts rod's wall temperatures in the uncovered part of the FA model at the initial time moment and then during the "steady regime". The calculated TW (t1cal) rod's wall temperature is much higher (up to ~ 150 K) than measured one at the FA outlet. This is the main problem of the code for the base case calculations for the test 8.6.3.2.

• The main reason for these deviations between experiment and calculations may be too low Hw1 (t1cal) ≈ 180–98 $W/m^2 \cdot K$ coefficients of heat transfer from the outer surfaces of the rod simulators to a coolant in the uncovered part of the FA model.

It is a base for a conclusion about adequacy of the code simulation of the test conditions only for hydrodynamics, realized during the test. At the same time, the code gives inadequate simulation of the heat transfer coefficients Hw1 (t1cal) and behavior of rod's wall temperatures in the uncovered part of the FA model during the "steady regime".

• Sensitivity studies are needed to determine the main reason for these deviations between the code results and test data.

6. SENSITIVITY STUDIES

This assessment work has shown, that RELAP5/MOD3.2.2GAMMA and methods of computer modeling VTI test 7.12.15.4 and test 8.6.3.2 have provided the adequate simulations of the initial and boundary conditions only for hydrodynamics, realized in these tests under steam-condensate natural circulation in the loop.

There are significant quantitative differences of the axial profile of the calculated rod's wall temperature TW (t1cal) and axial distribution of the measured rod's cladding temperatures TW (t0exp) in the uncovered part of the FA model in the base case calculations for these tests.

The code over predicts rod's wall temperatures in the uncovered part of the FA model at the initial time moment, and then during the "steady regime". The calculated TW (t1cal) rod's wall temperatures are much higher (up to ~ 150 K) than measured ones at the FA outlet. This is the main problem of the code for the base case calculations for these tests.

The main reason for these deviations between experiments and calculations may be under estimation for Hw1(tcal) coefficients of heat transfer from the rod simulators to a steam in the uncovered part of the FA model in the stationary conditions with the transition mode of a steam flow in the channel.

Therefore, the sensitivity calculations were carried out to investigate the influence of an increase in the calculated Hw1 (tcal) coefficients of heat transfer from the rods to a steam flow on the axial distribution of the rod's wall temperatures in the uncovered part of the core model.

The main goal of the sensitivity studies is an attempt to reduce large differences between code predictions for the axial profile of the rod's wall temperature TW (t1cal) and axial distribution of the measured rod's cladding temperatures TW (t0exp) in the uncovered part of the FA model at the initial time moment t0exp, and then during a "steady regime".

The sensitivity calculations were performed for VTI test 7.12.15.4 using nodalization with 40 volumes for the Core model and maximum user-specified time step dt max = 0.025 s, and also using fouling factor K_{HW1}=3.0 to define the increased coefficients Hw1 (tcal) of a heat transfer in the uncovered FA part. The results of the code simulation for the test *7.12.15.4* are presented on the Figures D-1÷D-9 in the Appendix D.

As seen, the results of the sensitivity study for the "initial steady state" and then for a "steady regime" are in good agreements with the test data about the main regime parameters: pressure Pup (t0exp), mass flow rate G (t0exp), heat flux qw (t0exp) and mixture level Lm (t0exp) in the core model (see Figures D-1, D-3, D-4, D-6, accordingly). Also, it provides the needed mass flow rate Gg (t0exp) of a generated steam flowing into the uncovered part of the core model under the test conditions.

Using fouling factor K_{HW1}=3.0 the code reasonably describes the behaviors of the rod's wall temperatures in the uncovered part of the FA model during the "steady regime" (see Fig.D-5, Fig.6.1)). Comparison of the base case (with K_{HW1}=1.0) and sensitivity case (with K_{HW1}=3.0) calculated axial profiles of rod's wall temperatures TW (t1cal) with the measured distribution of the rod's cladding temperatures for the initial time moment is shown in the Figure 6.1. In the case with K_{HW1}=3.0 there is a good agreement between axial profile of the calculated rod's wall temperature TW (t1cal) and axial distribution of the measured temperatures TW (t0exp) in the uncovered part of the FA model.

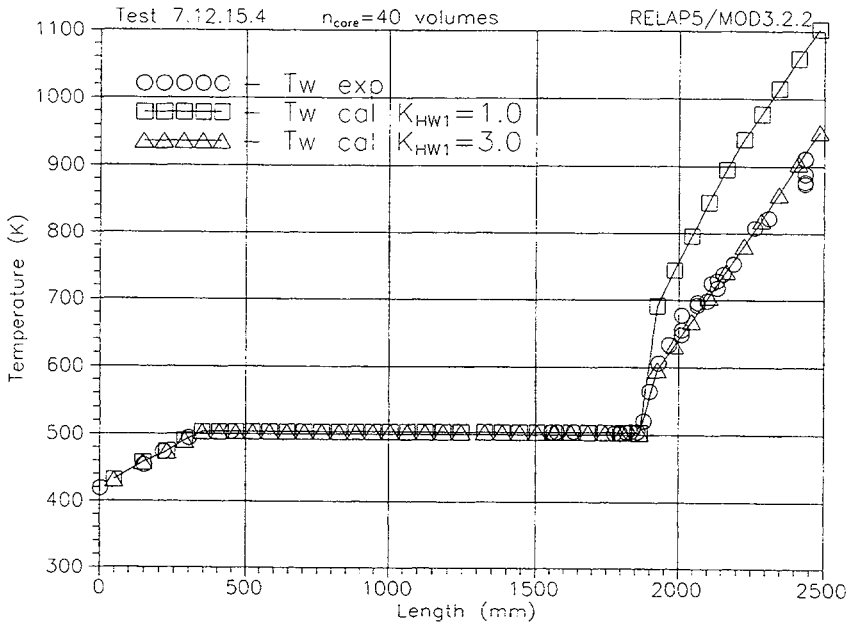

Fig.6.1. Comparison of the base case (K_{HW1}=1.0) and sensitivity case (K_{HW1}=3.0) calculated axial profiles of rod's wall temperatures TW (t1cal) with the measured distribution of the rod's cladding temperatures for the initial steady state in the test 7.12.15.4.

Thus, using fouling factor K_{HW1}=3.0 the code gives a completely adequate simulation of the initial and boundary conditions and then of a steady regime for both the hydrodynamics and heat transfer process, realized in the uncovered part of the core model during VTI test 7.12.15.4.

The sensitivity calculations were performed for VTI test 8.6.3.2 using nodalization with 40 volumes for the Core model and maximum user-specified time step dt max = 0.025 s, and also using fouling factor K_{HW1}=3.0 to define the increased coefficients of heat transfer Hw1 (tcal) in the uncovered FA part. The results of the code simulation for the test *8.6.3.2* are presented on the Figures D-10÷D-18 in the Appendix D. As seen, the results of the sensitivity study for the "initial steady state" and the "steady regime" are in good agreements with the test data about the main regime parameters.

The results of sensitivity study and test data for VTI test 8.6.3.2 are presented as time–dependent curves within the time interval 1000 s for the "steady regime" on the Figures D-10÷D-18 in the Appendix D.

Using fouling factor K_{HW1}=3.0 the code reasonably describes the behaviors of the rod's wall temperatures in the uncovered part of the FA model during a "steady regime" (see Fig.D-14, Fig.6.2). Comparison of the base case (with K_{HW1}=1.0) and sensitivity case (with K_{HW1}=3.0) calculated axial profiles of rod's wall temperatures TW (t1cal) with the measured distribution of the rod's cladding temperatures for the initial time moment is shown in the Figure 6.2.

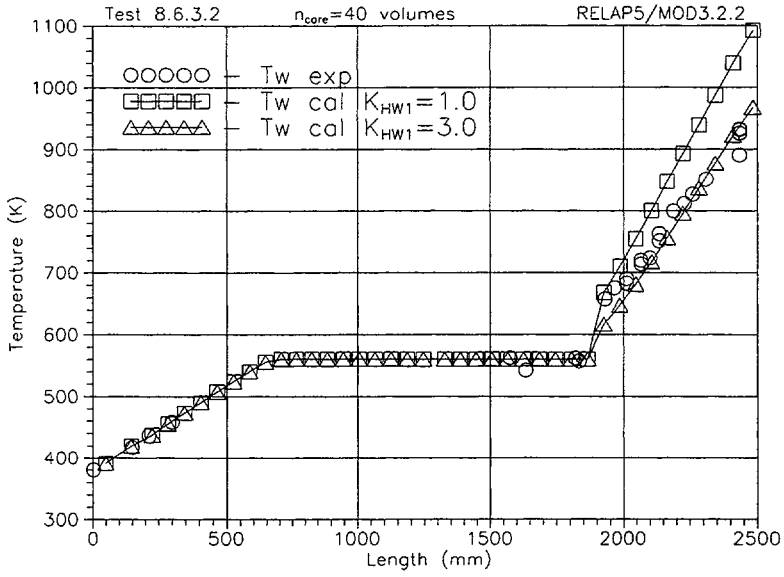

Fig.6.2. Comparison of the base case (K_{HW1}=1.0) and sensitivity case (K_{HW1}=3.0) calculated axial profiles of the rod's wall temperatures TW (t1cal) with the measured distribution of rod's cladding temperatures for the initial steady state in the test 8.6.3.2.

As seen, using fouling factor K_{HW1}=3.0 the code reasonably describes the axial distribution of the rod's wall temperatures TW(t1cal) in the uncovered part of the FA model for the "initial steady state".

Thus, using fouling factor K_{HW1}=3.0 the code gives a completely adequate simulation of the initial and boundary conditions and then of a steady regime for both the hydrodynamics and heat transfer process, realized in the uncovered part of the core mode during VTI test 8.6.3.2.

For example, the effect of the increase in the heat transfer coefficients (using K_{HW1}=3.0) and of the implementation the real axial profile of the rod simulator temperatures in the Restart input deck on

the histories of the calculated rod's wall temperatures in the uncovered part of the FA model is shown in the Figure 6.3. In the case with K_{HW1}=3.0 these histories of the rod's wall temperatures TW (tcal) are given in the Figure 6.3 within the time interval from t0cal = 0 s up to t1cal = 3000 s, the last corresponds to t0exp.

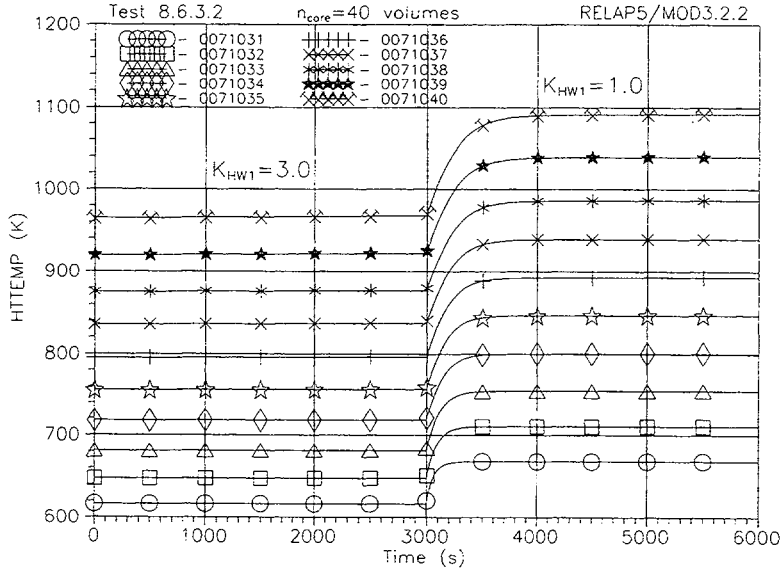

Fig. 6.3. The effect of the increase in the heat transfer coefficients Hw1 (tcal) and of the implementation real axial profile of the rod simulators in the Restart input deck on the histories of the calculated rod's wall temperatures TW (tcal) in the FA uncovered part.

The code results for the "initial steady state" at the time t1cal=3000 s are in good agreements with the test data about the regime parameters.

Then restarting from this completely adequate "initial steady state" at tcal = 3000 s and using fouling factor K_{HW1}=1.0 which is pre-assigned for the base case calculations, we have run the transition to such a steady state in the loop at the time moment tcal=6000 s, which has to be adequate to the experimental " steady state" at the beginning of the test. Code simulation of this transient with K_{HW1}=1.0 was realized during the time interval from tcal = 3000 s up to tcal = 6000 s to illustrate a complete stabilization of the calculated values for the regime parameters during the particular time interval.

The effect of the decrease in the heat transfer coefficients (with K_{HW1}=1.0) and of the implementation a real axial profile of the rod simulator temperatures in the Restart input deck on the histories of the calculated rod's wall temperatures in the uncovered part of the FA model is shown in Fig. 6.3, too. In the case with K_{HW1}=1.0 the histories of the rod's wall temperatures TW (tcal) are given in the Figure 6.3 within the time interval from tcal = 3000 s up to tcal = 6000 s.

As seen, restarting from needed "initial steady state", the rod simulator temperatures in the uncovered FA part begin to increase with the high rate after tcal=3000 s during the code simulation of the consequent regime with K_{HW1}=1.0, which is recommended by the code developers for the base case calculation. As a consequence, a significant quantitative difference of the calculated and measured axial temperature profiles in the uncovered FA model was achieved again at the end of the transition to a "steady state" at tcal = 6000 s, which corresponds to the beginning of a "steady regime" in the test. This fact shows that initial temperature conditions in the FA model weakly influence on the code simulation of the heat transfer process in the partially uncovered core in considered "steady regime".

The sensitivity studies show that the main reason for the deviations between experiment and calculations is the under estimation for the coefficients of heat transfer from the rod simulators to a steam in the uncovered part of the FA model under conditions of the transition mode of a steam flow in the channel.

Comparison of the base case (K_{HW1}=1.0) and sensitivity case (K_{HW1}=3.0) calculated axial distributions of the heat transfer coefficients Hw1 (t1cal) in the uncovered part of the FA model for the test *7.12.15.4* is shown in Fig.6.4.

Comparison of the base case (K_{HW1}=1.0) and sensitivity case (K_{HW1}=3.0) calculated axial distributions of the heat transfer coefficients Hw1 (t1cal) in the uncovered part of the FA model for the test *8.6.3.2* is shown in Fig.6.5.

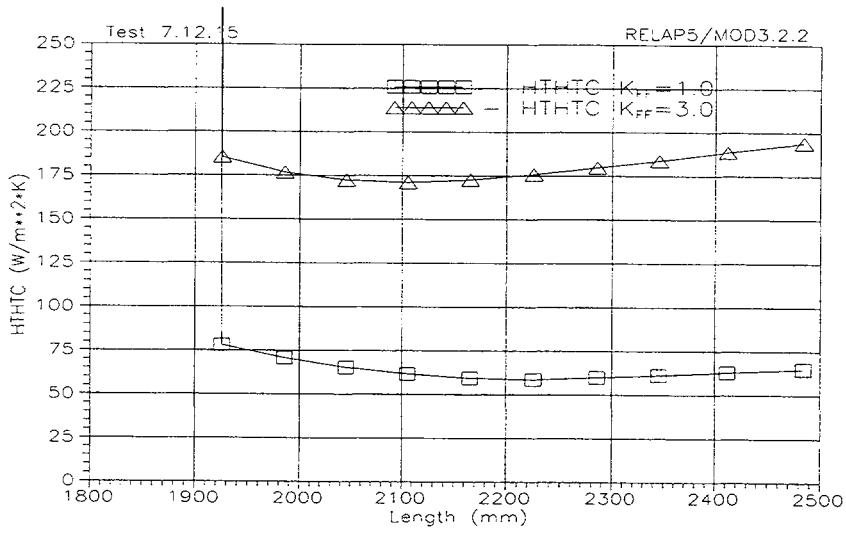

Fig.6.4. Comparison of the base case (K_{HW1}=1.0) and sensitivity case (K_{HW1}=3.0) calculated axial distributions of the heat transfer coefficients Hw1 (t1cal) in the uncovered part of the FA model for the test 7.12.15.4.

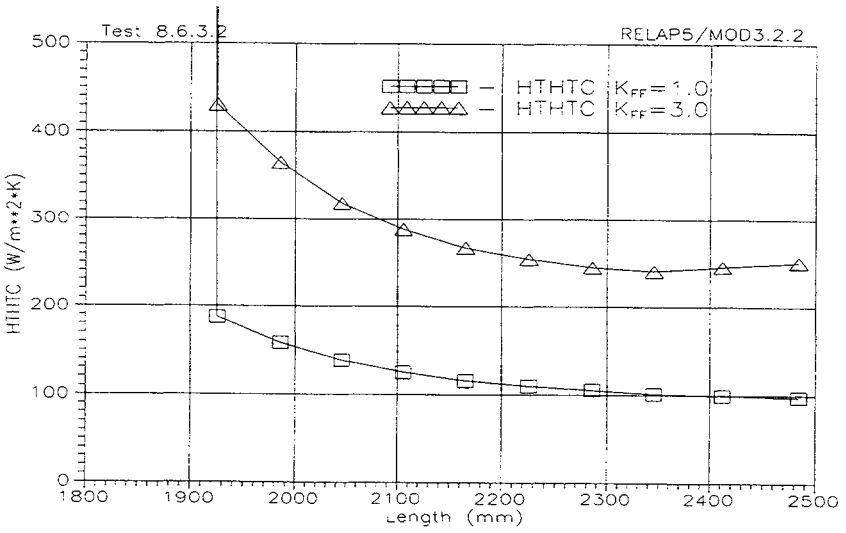

Fig.6.5. Comparison of the base case (K_{HW1}=1.0) and sensitivity case (K_{HW1}=3.0) calculated axial distributions of the heat transfer coefficients Hw1 (t1cal) in the uncovered part of the FA model for the test 8.6.3.2.

Conclusions for the sensitivity studies

• The sensitivity studies show, that the increase (with K_{HW1}=3.0) in calculated coefficients of heat transfer Hw1 (tcal) in the uncovered part of the FA model results in a reasonable adequacy of the code simulation of the initial and boundary conditions for both the hydrodynamics and heat transfer process, realized in the uncovered part of the core model. Using fouling factor K_{HW1}=3.0 and the implementation of a real (experimental) temperature profile for the FA model in the Restart input deck allow to reduce large differences between RELAP5/MOD3.2.2GAMMA predictions and test data for the axial temperature profile in the FA model for the initial time moment.

• However starting from this needed "initial steady state", the rod simulator temperatures in the uncovered FA part begin to increase with the high rate during code simulation of the consequent "steady regime" with K_{HW1}=1.0 which is recommended by the code developers. As a consequence, a significant quantitative difference of the calculated and measured axial temperature profiles in the uncovered FA model was achieved again at the end of the transient.

• Thus, the sensitivity studies show that the main reason for the deviations between experiments and calculations is the under estimation for coefficients of heat transfer from the rod simulators to a steam in the uncovered part of the FA model under conditions of the transition mode of a steam flow in the channel. Therefore, sensitivity calculations for the tests were performed using fouling factor K_{HW1}=3.0 to define the increase in coefficients of heat transfer in the uncovered FA part.

• Using fouling factor K_{HW1}=3.0 the code gives an adequate simulation of the initial and boundary conditions for both the hydrodynamics and heat transfer process, realized in the uncovered part of the core model. With K_{HW1}=3.0 the code reasonably describes an axial distribution of the rod's wall temperatures in the uncovered part of the FA model for the "initial steady state", and then during the "steady regime" under considered conditions.

7. RUN STATISTICS

The simulation model for 8.6.3.2 test includes:

131 volumes, 129 junctions, 167 heat structures with 611 mesh points.

There were the following resources been used for the calculation:

Run time – CPU = 1305.91 s;

Step number – DT = 40096;

Volume number – C = 131.

Calculation results of **grind time** (program efficiency factor)

$$\textit{Grind time} = \frac{\text{CPU} \cdot 10^3}{\text{C} \cdot \text{DT}} = 0.2486$$

For the calculations, it was used a computer IBM PC AT with processor INTEL Pentium 2 - 450. Windows-95 was used as an operating system. CPU-time and the integration step variations are presented in Figures 7.1 and 7.2, respectively.

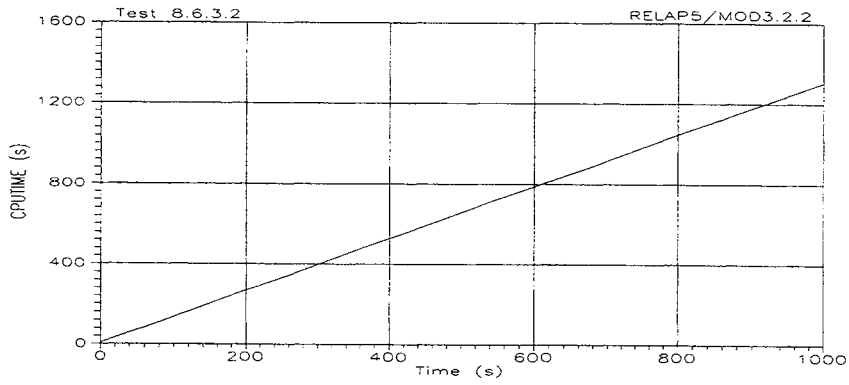

Fig.7.1. Execution times (CPU TIME) of the main variant computation for test 8.6.3.2.

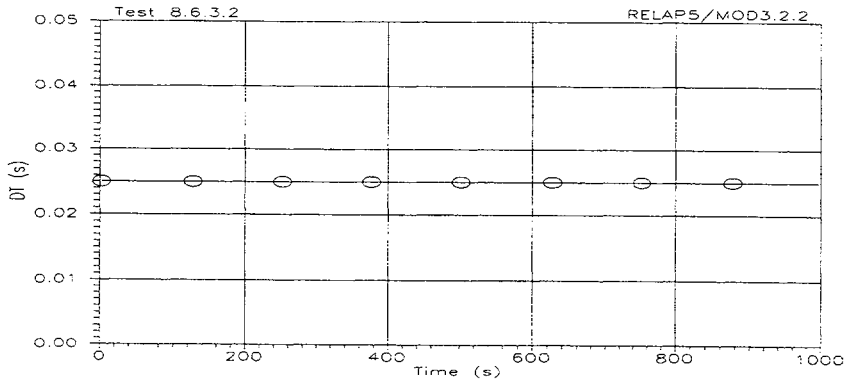

Fig.7.2. Integration step (DT) variations at the main variant computation for test 8.6.3.2.

8. SUMMARY OF CONCLUSIONS

• RELAP5/MOD3.2.2GAMMA and the base case methods of computer modeling of the experiments have provided adequate simulations of the initial and boundary conditions only for hydrodynamics, realized during the tests in steady regimes with steam-condensate natural circulation in the VVER-440 loop model. In these tests the transition mode of a steam flow is realized in the uncovered part of the FA model with corresponding Reynolds numbers $Re_g = Vg \cdot Dh / \nu_g \approx 1860 - 830$.

• Shown is an insufficient code adequacy for the description of the rod's wall temperatures behaviors in the uncovered part of the FA model. There are significant quantitative differences of the axial profiles of the calculated and measured rod's wall temperatures in the uncovered part of the FA model in the base case calculations for these tests.

The code over predicts rod's wall temperatures in the uncovered part of the FA model at the initial time moment, and then during "steady regimes". The calculated rod's wall temperatures are much higher (up to ~ 150 K) than measured ones at the FA outlet. This is the main problem of the code for the base case calculations for these tests.

• The sensitivity studies have shown that the main reason for the deviations between experiments and calculations is the under estimation for the coefficients of heat transfer from the rod simulators to a steam in the uncovered part of the FA model under conditions of the transition mode of a steam flow in the channel.

• The increase in calculated coefficients of heat transfer in the uncovered part of the FA model results in a reasonable adequacy of the code simulation of the initial and boundary conditions for both the hydrodynamics and heat transfer process, realized in the uncovered part of the core model. Using fouling factor $K_{HW1}=3.0$ the code reasonably describes the axial distributions of the rod's wall temperatures in the uncovered part of the FA model for the initial steady states, and then during the steady regimes in considered tests.

REFERENCES

1. Gordon B.G., Pomelnikov V.N. Study of Heat Transfer at Small LOCAs. Thermophysical Aspects of VVER Safety. Proceedings of the International Symposium "Thermophysics-90", Volume 1, p. 255-262.

2. Gordon B.G., Pomelnikov V.N. Study of Heat Transfer in the VVER Fuel Assembly at low mass flow. Journal "Atomic Energy" , volume 68, April 1990, p. 288-291.

3. V.G.Sorokin, A.V.Volosnikova, S.A.Vyatkin. Types of steels and alloys. M. Mashinostroenie, 1989 (In Russian).

4. Electrotechnical hand book. M.-L., GEI, 1962 (In Russian).

5. RELAP5/MOD3 Code Manual. Volume 4: Models and Correlations. INEL-95/0174, NUREG/CR-5535. 1995.

6. RELAP5/MOD3 Code Manual. Volume 2: User's Guide and Input Requirements INEL-95/0174, NUREG/CR-5535. 1995.

7. V.A.Vinogradov, A.Y. Balykin. Computer code validation for transient analysis of VVER and RBMK reactors: Standard Problem INSCSP-V4 Analysis "Investigation of heat transfer for partly uncovered VVER-1000 core at the test facility KS (RRC KI), International Nuclear Center of Russia Minatom, Moscow, Russia , 2001, 167 p.

8. V.A.Vinogradov, A.Y. Balykin. Analyses of KS-1 Experimental Data on the Behavior of the Heated Rod Temperatures in the Partially Uncovered VVER Core Model Using RELAP5/MOD3.2. International Agreement Report NUREG-IA-0169, November 1999.

Appendix A

Original Data Plots from the Tests

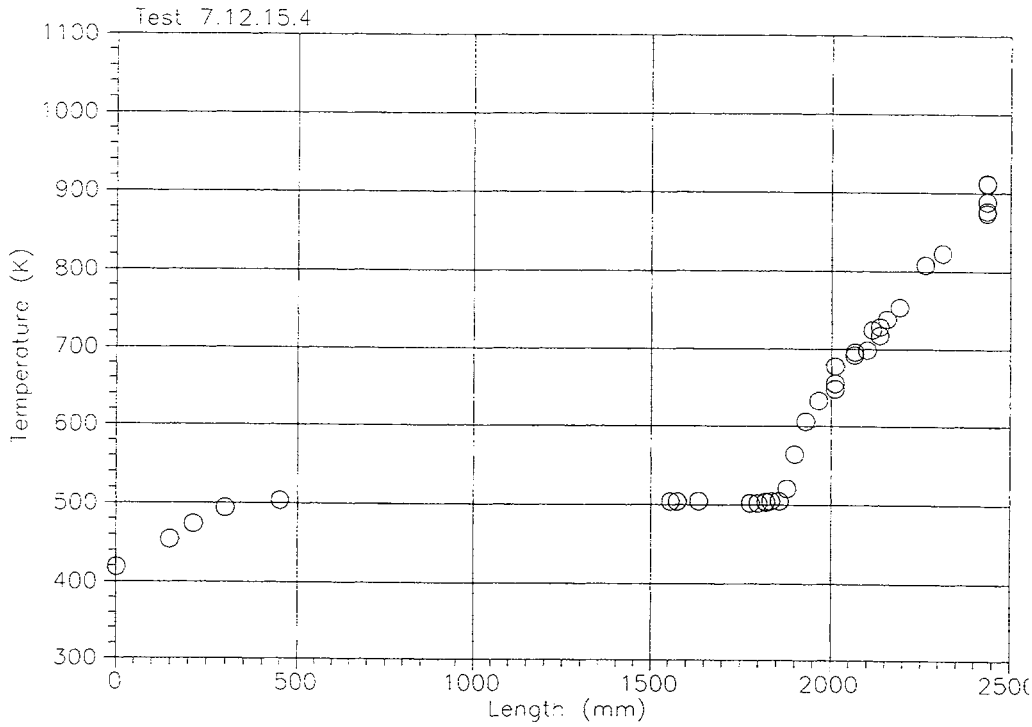

Fig.A-1. Experimental core axial distribution of rod's wall temperatures for test 7.12.15.4.

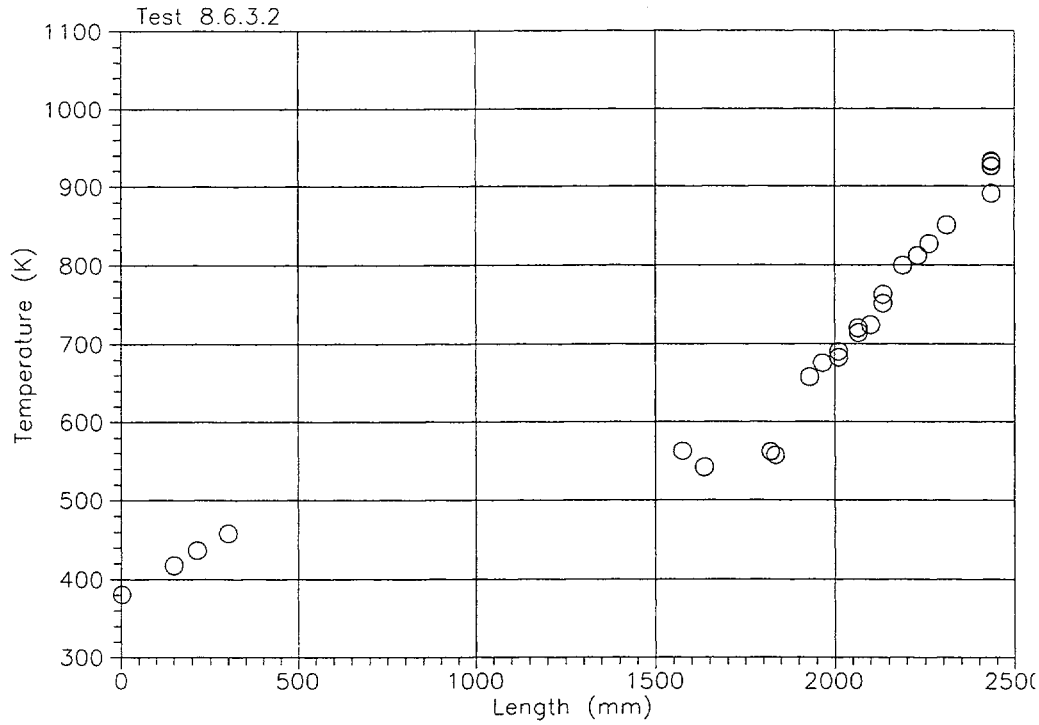

Fig.A-2. Experimental core axial distribution of rod's wall temperatures for test 8.6.3.2.

Appendix B

Base Case Results for Test 7.12.15.4

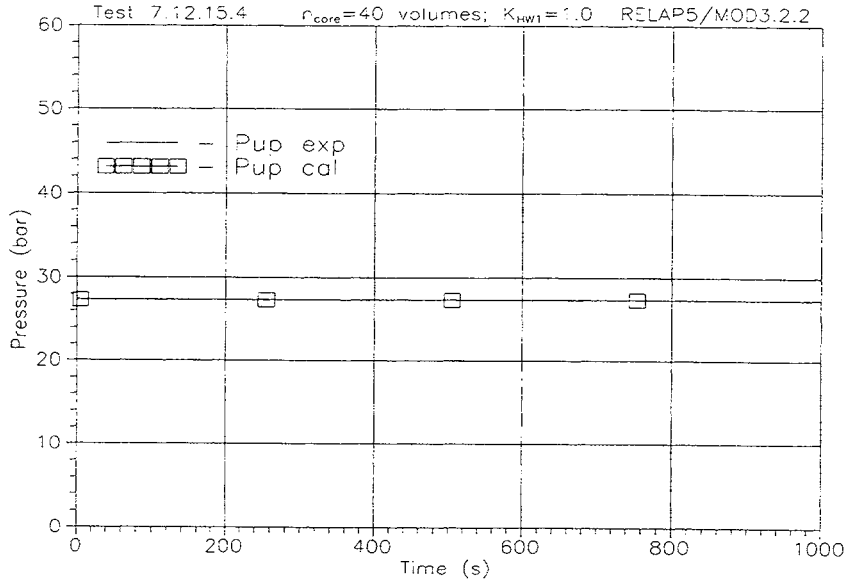

Fig.B-1. Comparison of the calculated P_{UP} (tcal) and measured P_{UP} (texp) pressure histories in the upper plenum model in experiment 7.12.15.4

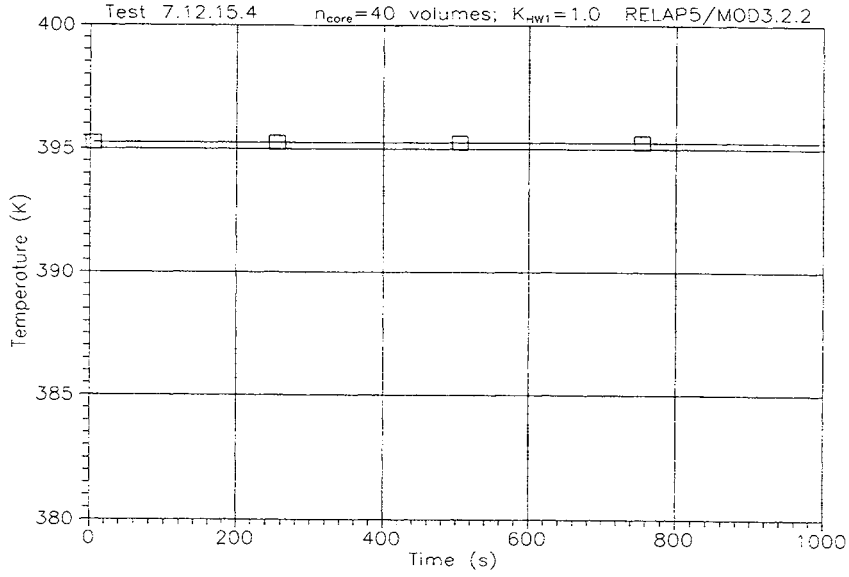

Fig.B-2. Calculated TF (tcal) water temperature history at the inlet of FA channel in experiment 7.12.15.4.

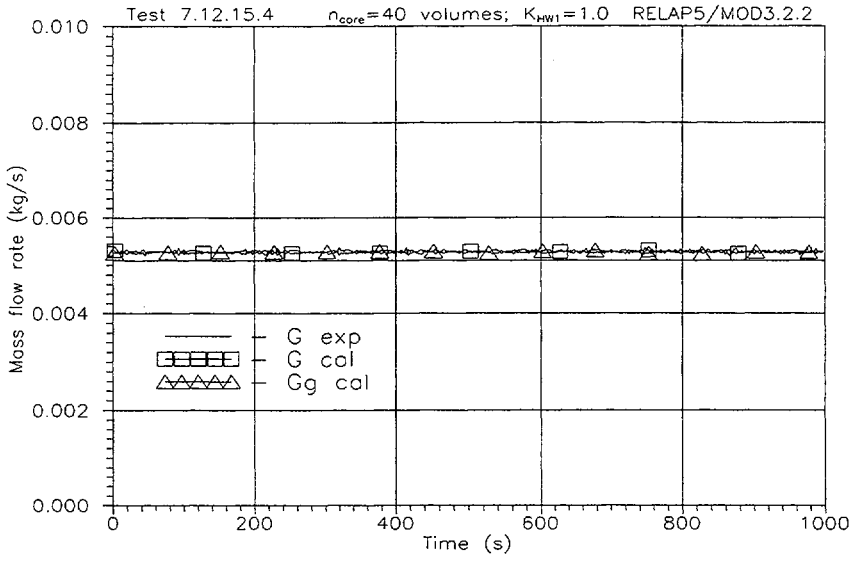

Fig.B-3. Comparison of the calculated G_L (tcal), Gg (tcal) and measured G (texp) mass flow rate histories at the inlet of FA channel in experiment 7.12.15.4.

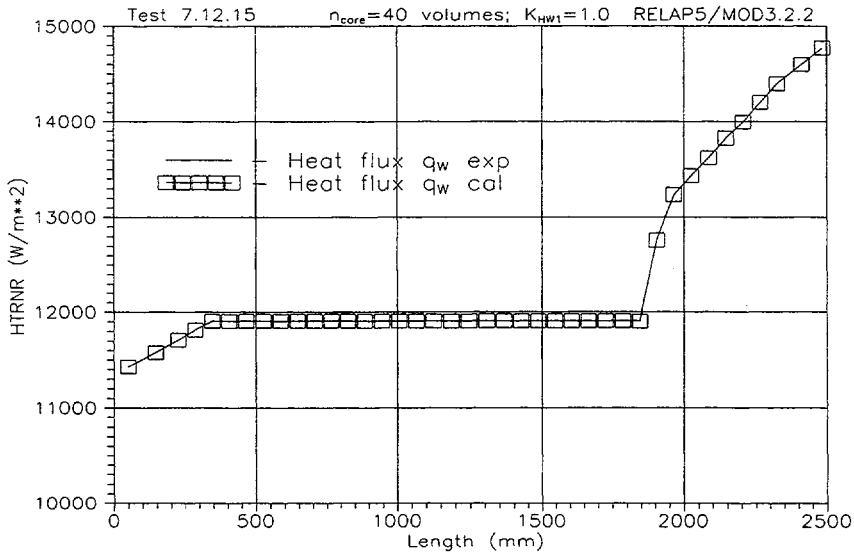

Fig.B-4. Comparison of the distributions of experimental qw (t0exp) and calculated qw (t1cal) specific heat fluxes from the outer surfaces of the rod simulators to a coolant on the FA height for the initial time moment in experiment 7.12.15.4.

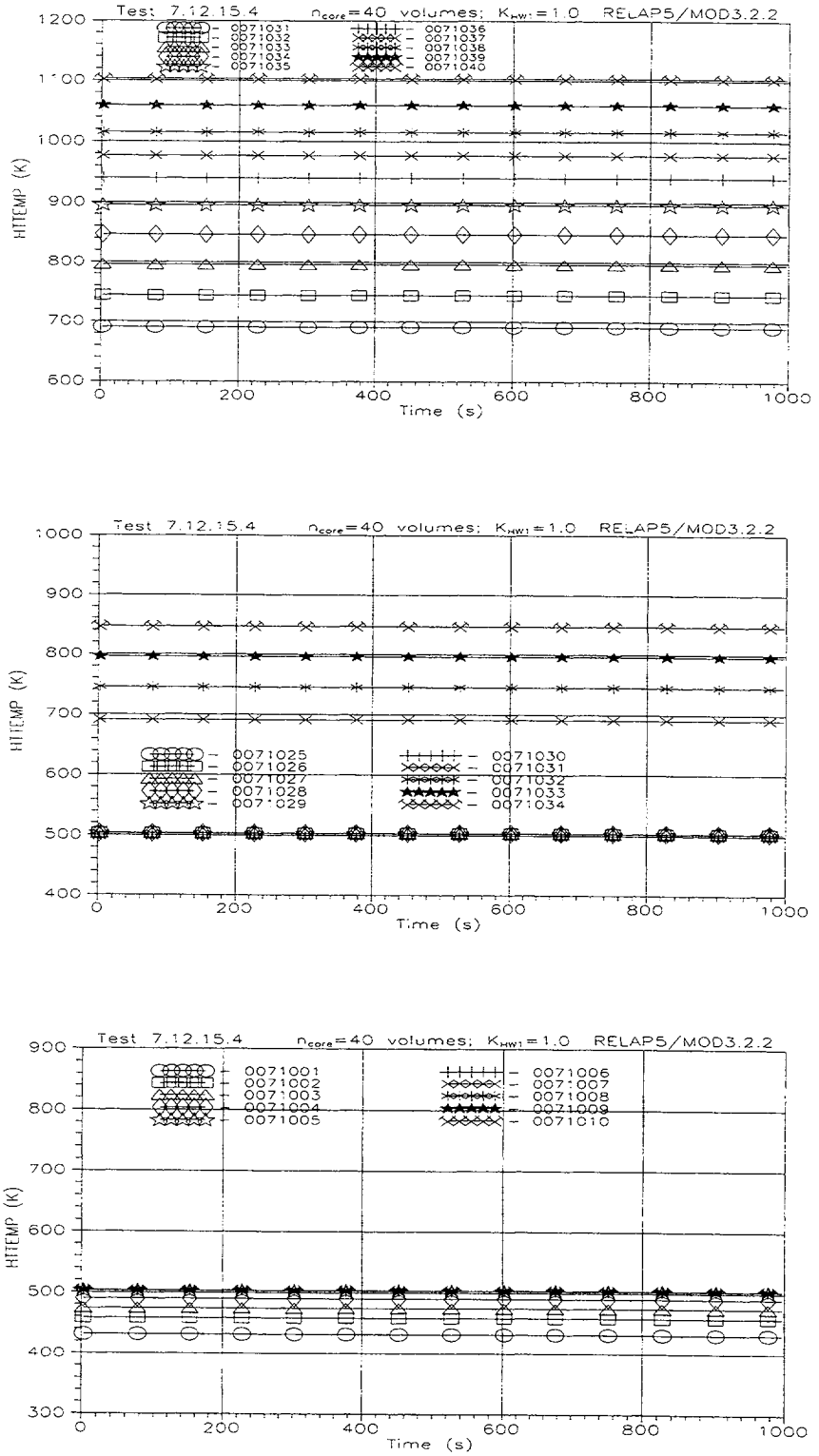

Fig.B-5. Calculated TW (tcal) rod's wall temperatures histories in the upper, middle and bottom parts of the FA model in experiment 7.12.15.4.

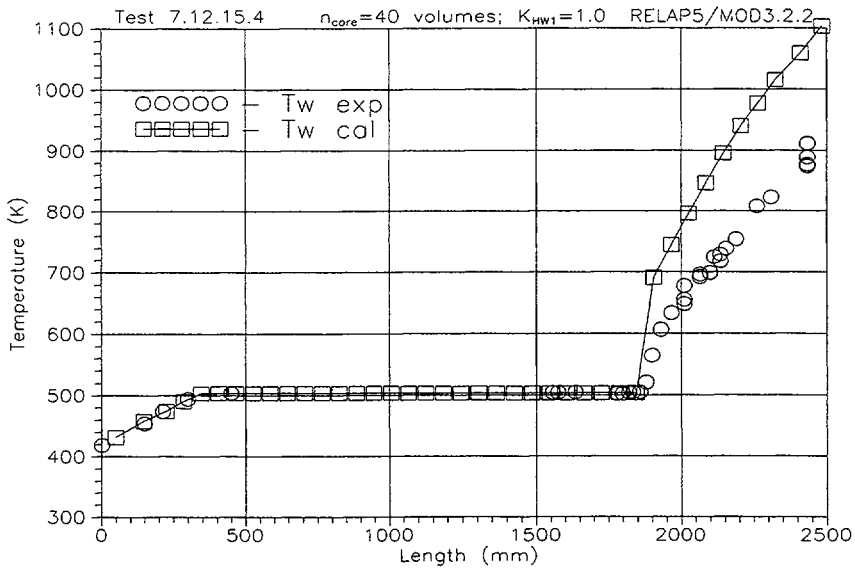

Fig.B-6. Comparison of the axial profile of calculated rod's wall temperature Tw (t2cal) in the FA model and axial distribution of measured rod's cladding temperatures for test 7.12.15.4.

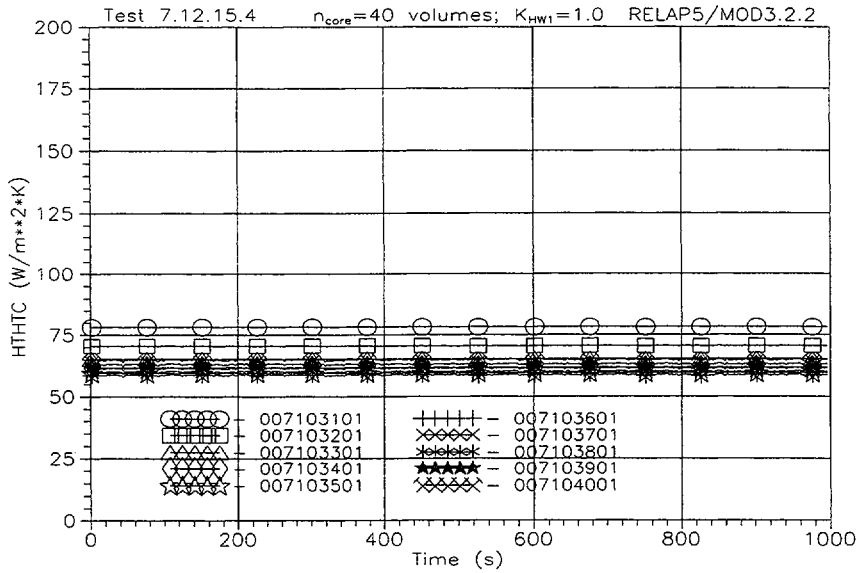

Fig.B-7. Histories of the calculated coefficients Hw1(tcal) of heat transfer from the rods to a vapor in the uncovered part of the FA model in experiment 7.12.15.4.

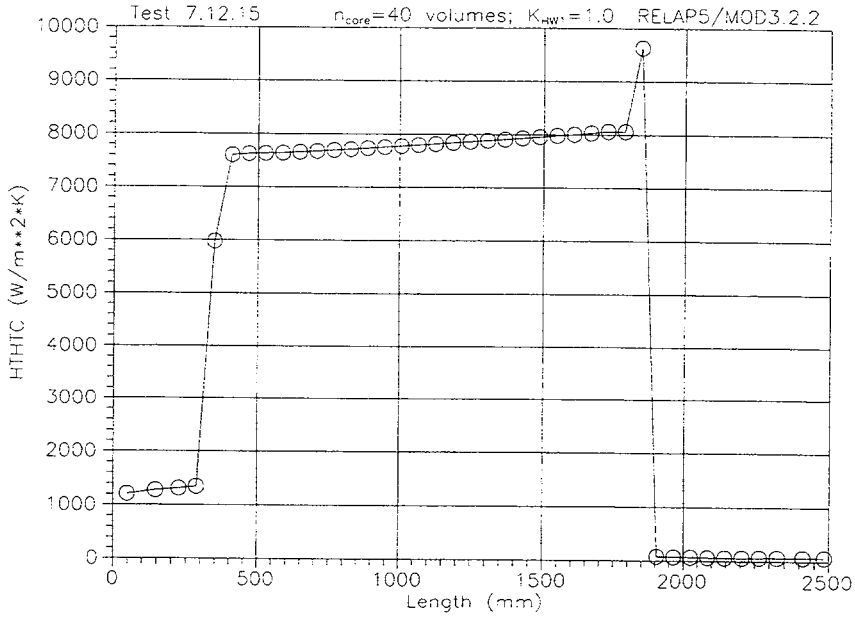

Fig.B-8. Axial distribution of the calculated coefficients Hw1(t2cal) of heat transfer from the rods to a coolant for experiment 7.12.15.4.

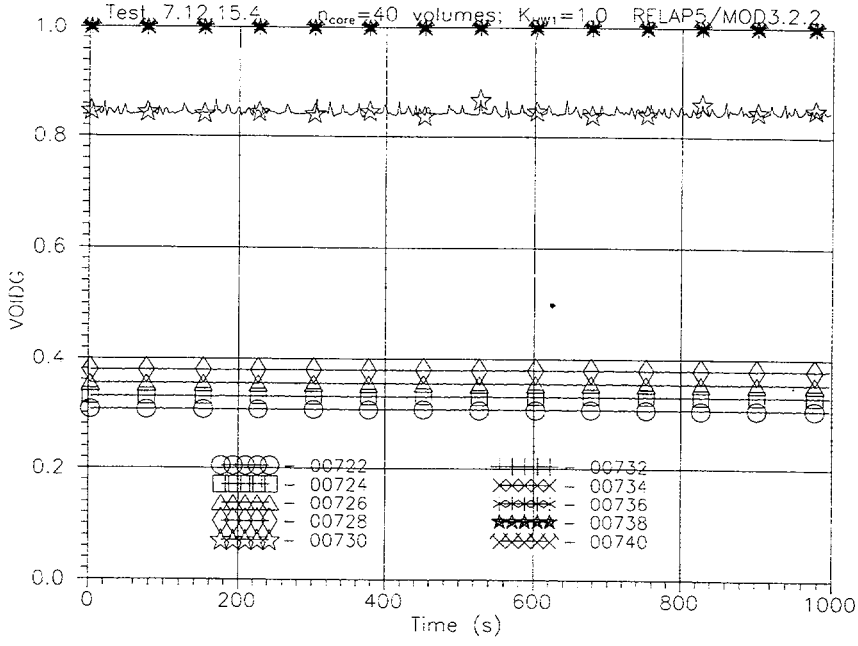

Fig.B-9. Calculated void fractions histories in the upper part of FA channel in experiment 7.12.15.4.

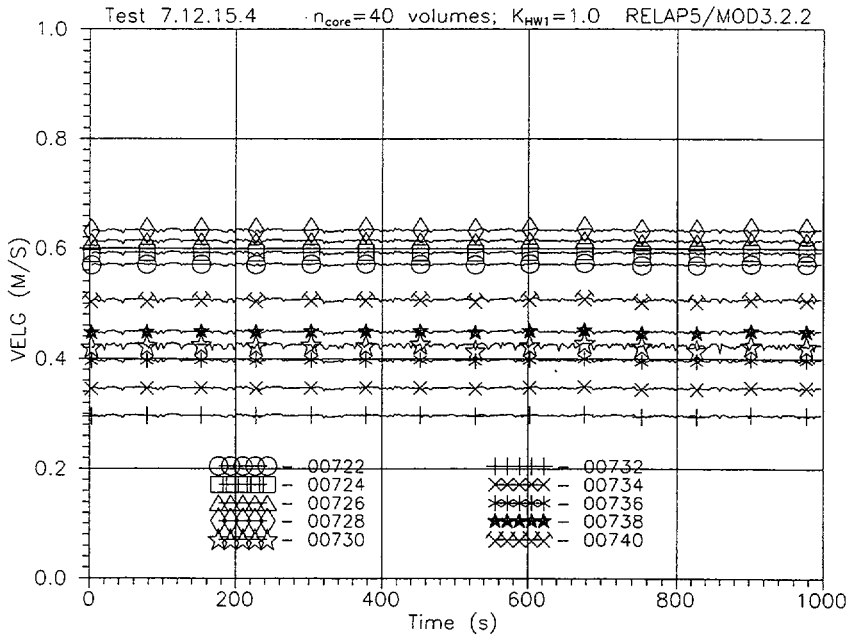

Fig.B-10. Calculated Vg (tcal) vapor velocities histories in the upper part of FA channel in experiment 7.12.15.4.

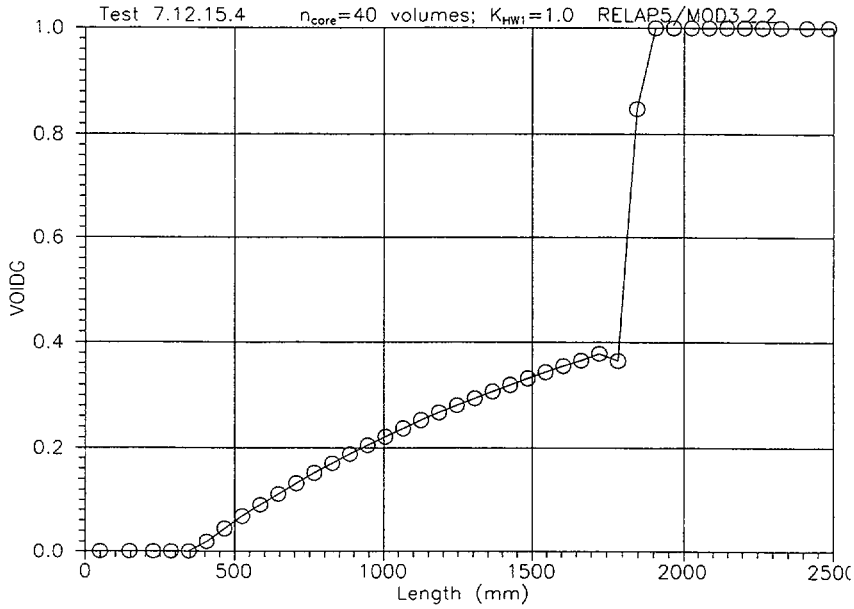

Fig.B-11. Calculated axial distribution of the void fractions in the FA channel in experiment 7.12.15.4.

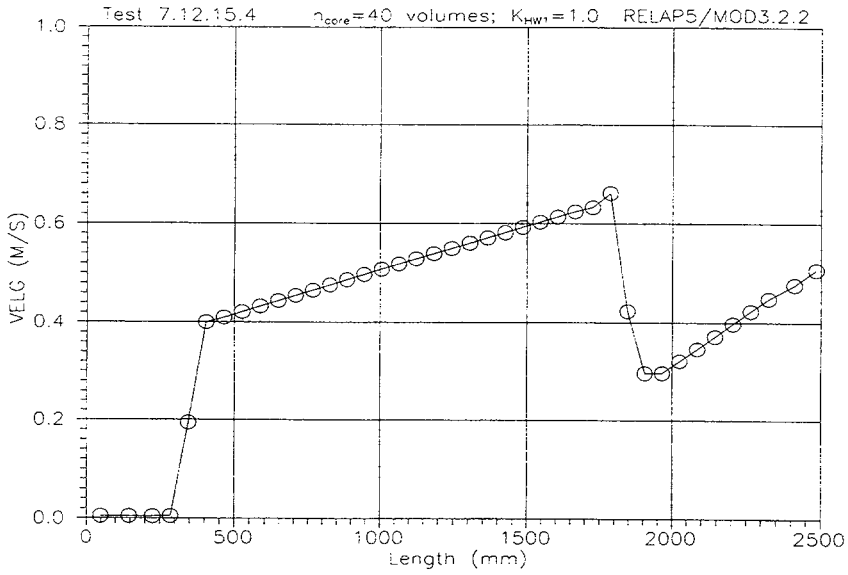

Fig.B-12. Calculated axial distribution of the vapor velocities in the FA channel at pressure Pup=27.3 bar and FA power W=16.8 kW in experiment 7.12.15.4.

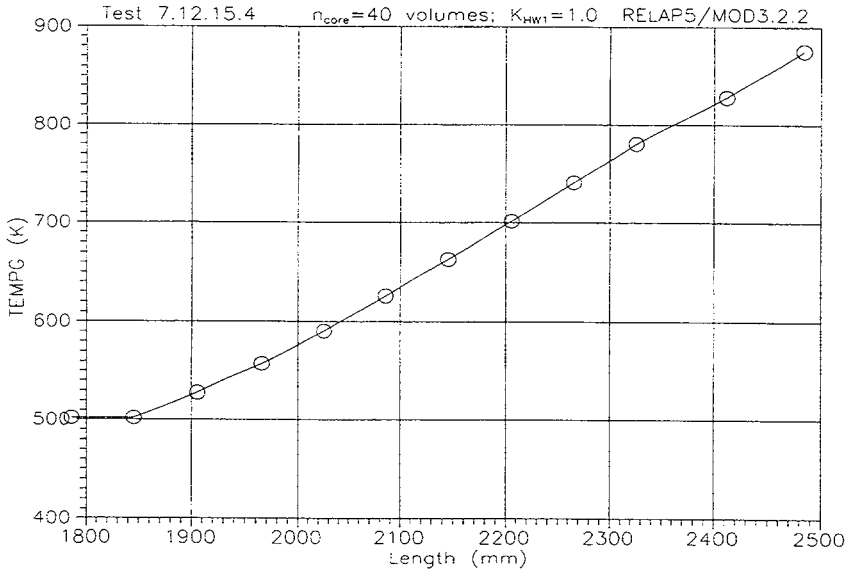

Fig.B-13. Axial distribution of the calculated vapor temperatures Tg (x) in the uncovered part of FA channel for the test 7.12.15.4.

Appendix C

Base Case Results for Test 8.6.3.2

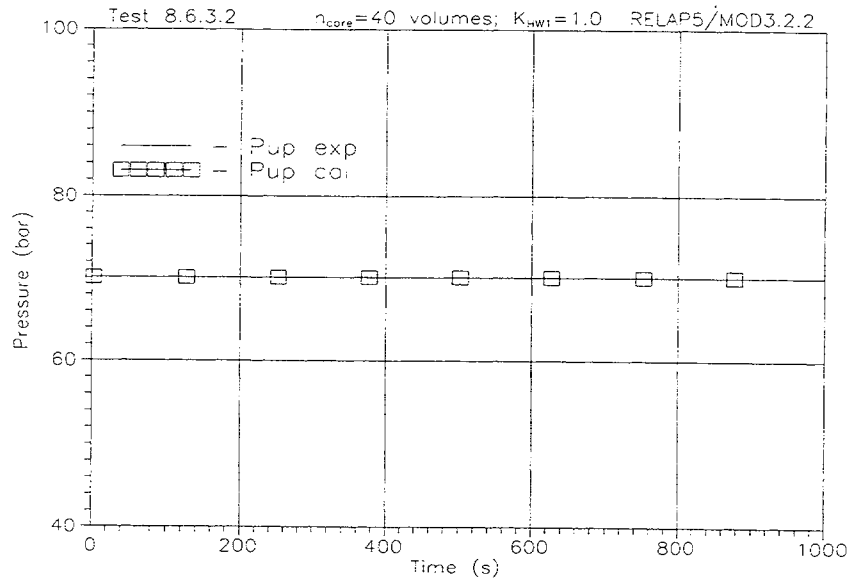

Fig.C-1. Comparison of the calculated P_{UP} (tcal) and measured P_{UP} (texp) pressure histories in the upper plenum model in experiment 8.6.3.2.

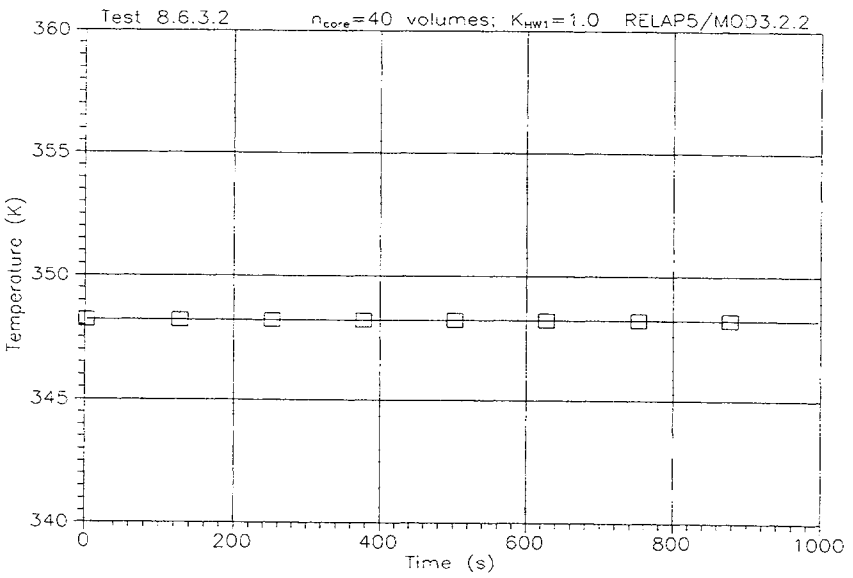

Fig.C-2. Calculated TF(tcal) water temperature history at the inlet of FA channel in experiment 8.6.3.2.

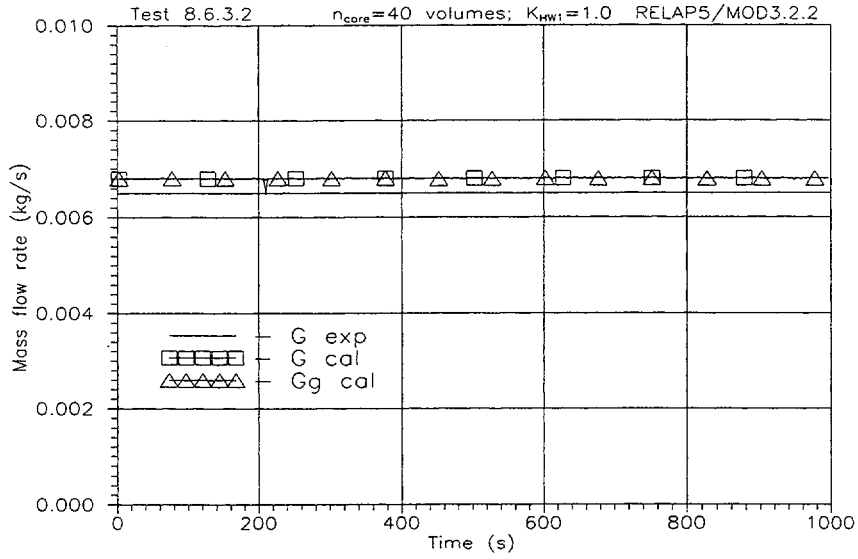

Fig.C-3. Comparison of the calculated G_L (tcal) , Gg (tcal) and measured G (texp) mass flow rate histories at the inlet of FA channel in experiment 8.6.3.2.

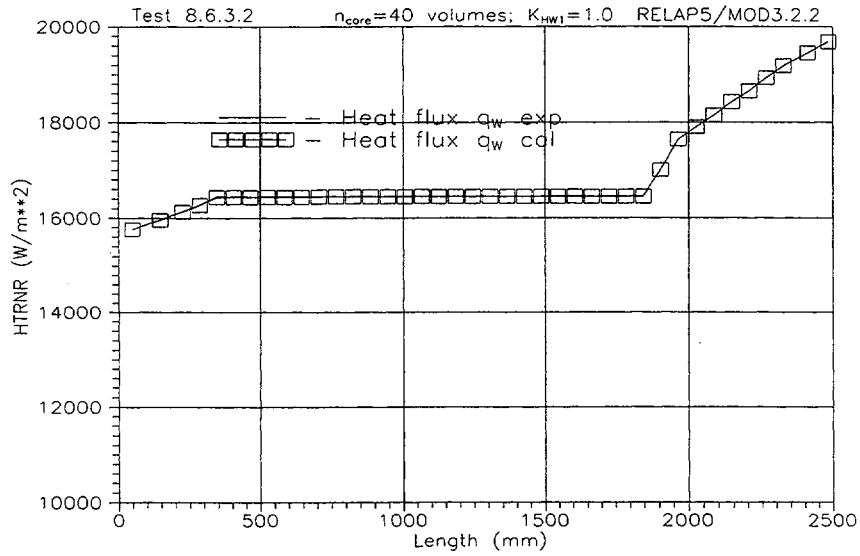

Fig.C-4. Comparison of the distributions of experimental qw (t0exp) and calculated qw (t1cal) specific heat fluxes from the outer surfaces of the rod simulators to a coolant on the FA height for the initial time moment in experiment 8.6.3.2.

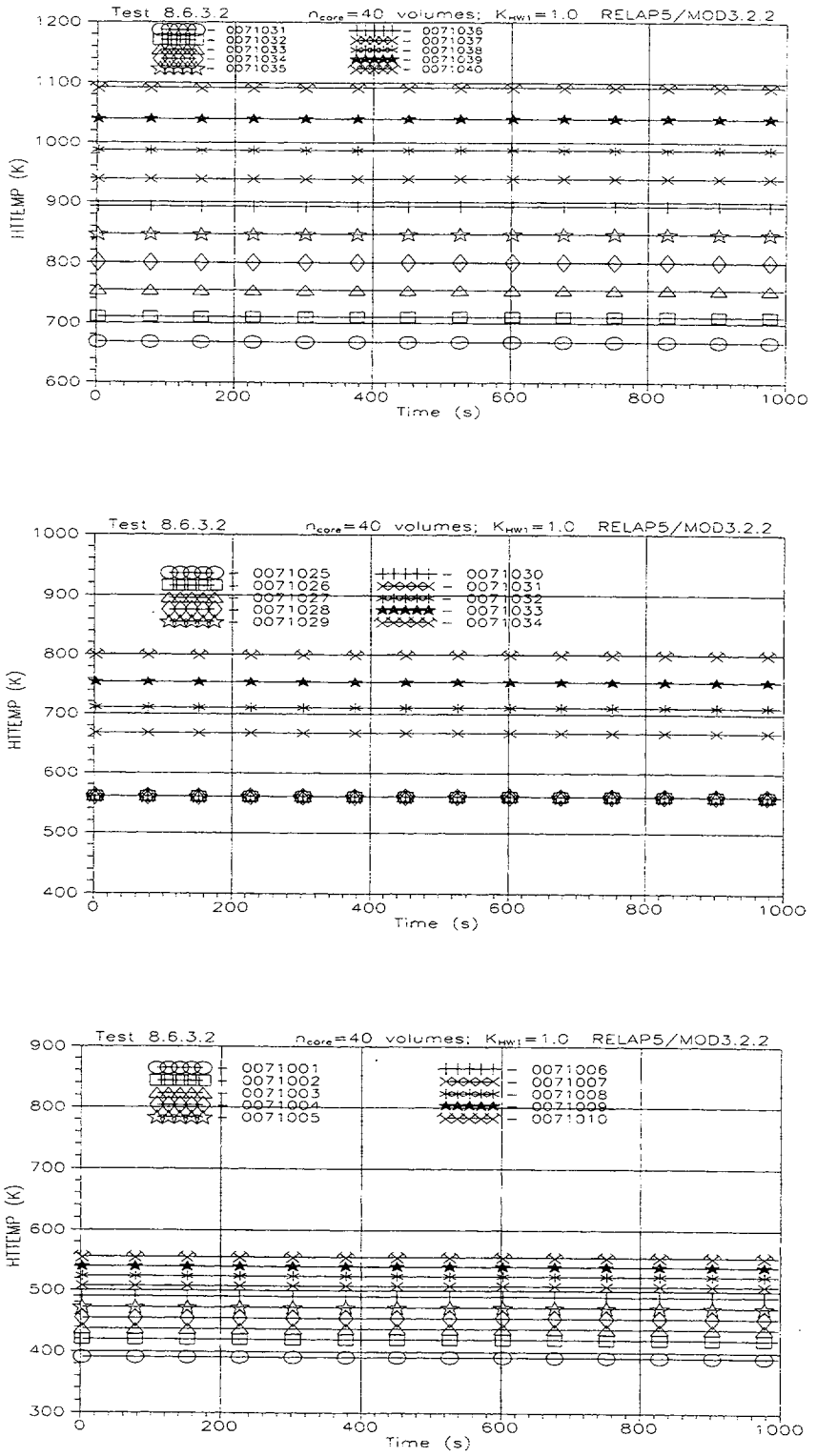

Fig.C-5. Calculated TW (tcal) rod's wall temperatures histories in the upper, middle and bottom parts of the FA model in experiment 8.6.3.2.

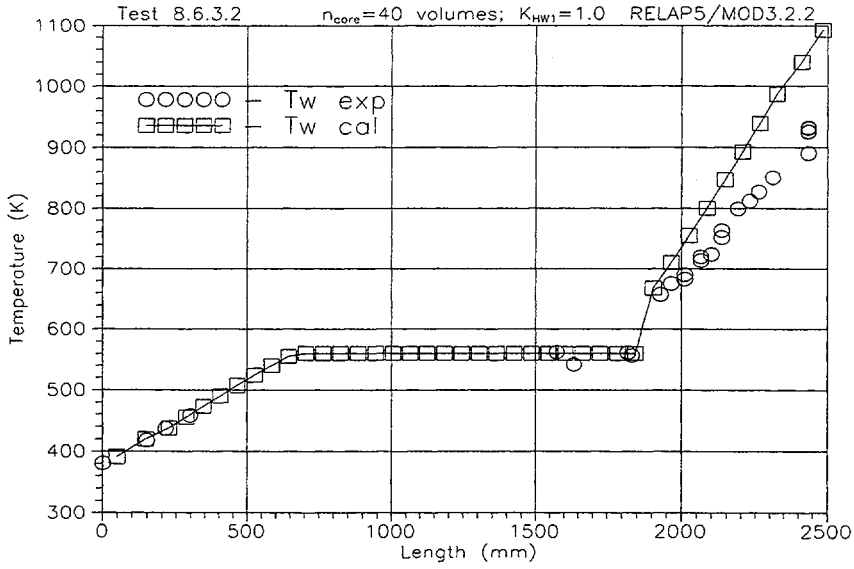

Fig.C-6. Comparison of the axial profile of calculated rod's wall temperature TW (t2cal) in the FA model and axial distribution of measured rod's cladding temperatures for test 8.6.3.2.

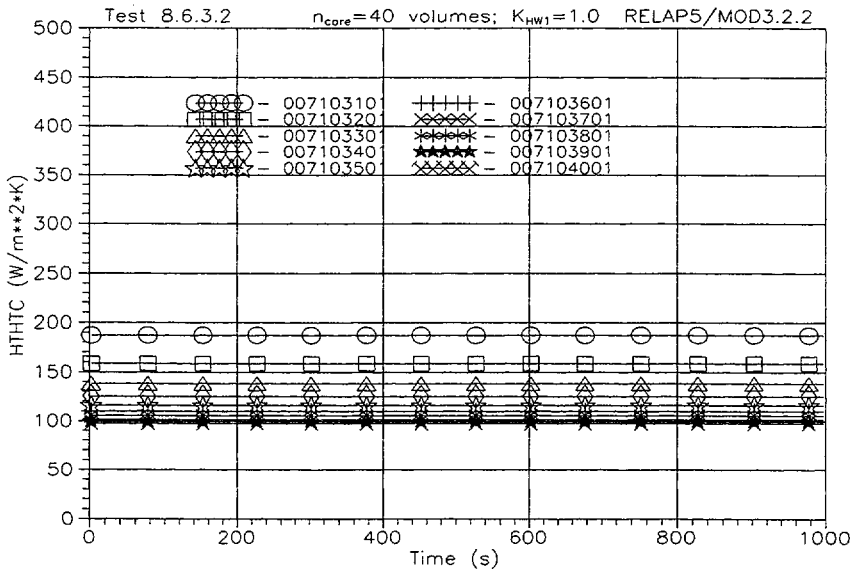

Fig.C-7. Histories of the calculated coefficients Hw1(tcal) of heat transfer from the rods to a vapor in the uncovered part of the FA model in experiment 8.6.3.2.

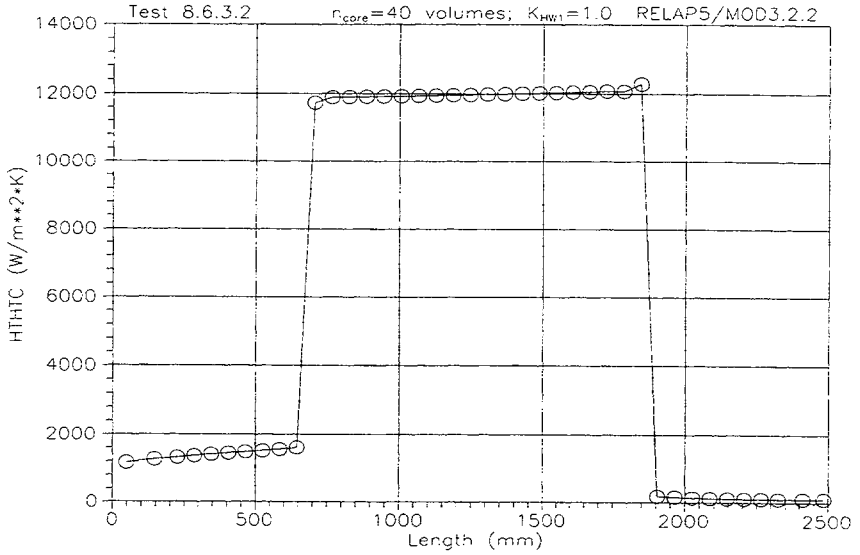

Fig.C-8. Core axial distribution of the calculated coefficients Hw1(t2cal) of heat transfer from the rods to a coolant for experiment 8.6.3.2.

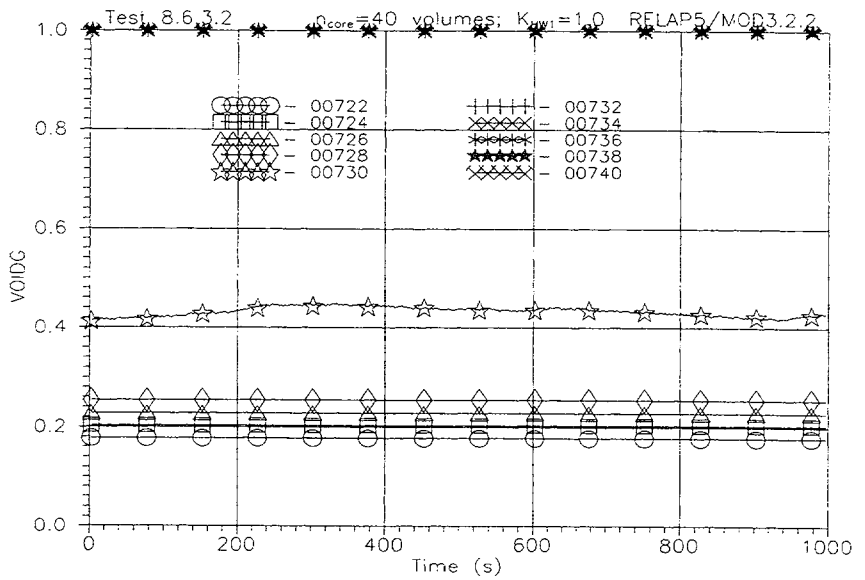

Fig.C-9. Calculated void fractions histories in the upper part of FA channel in experiment 8.6.3.2.

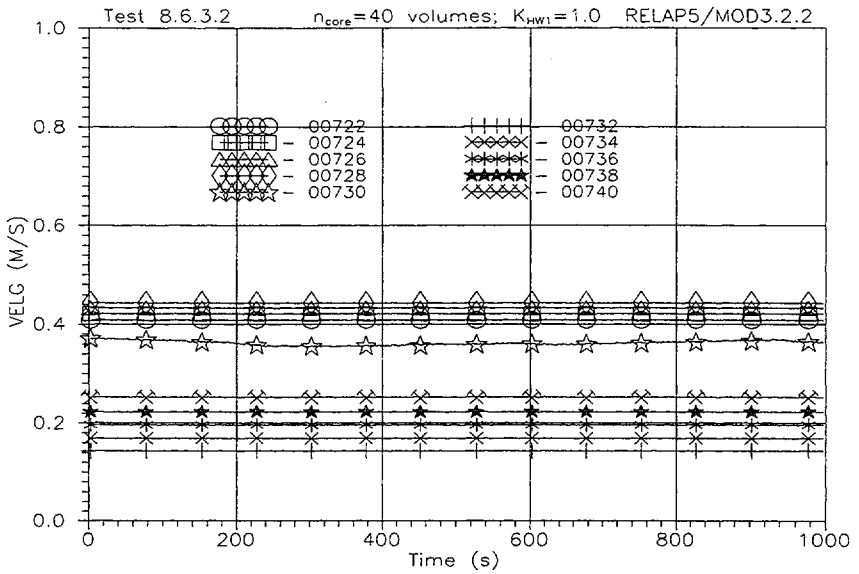

Fig.C-10. Calculated Vg (tcal) vapor velocities histories in the upper part of FA channel in experiment 8.6.3.2.

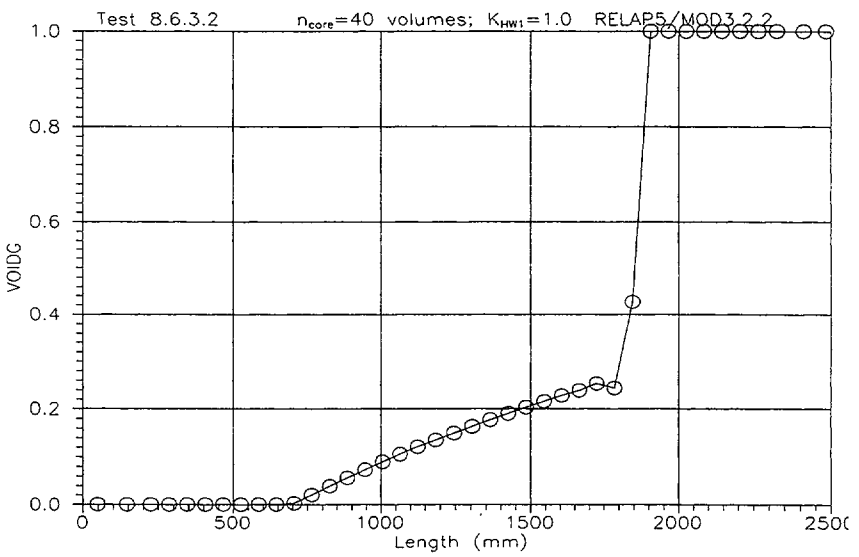

Fig.C-11. Calculated axial distribution of the void fractions in the FA channel in experiment 8.6.3.2.

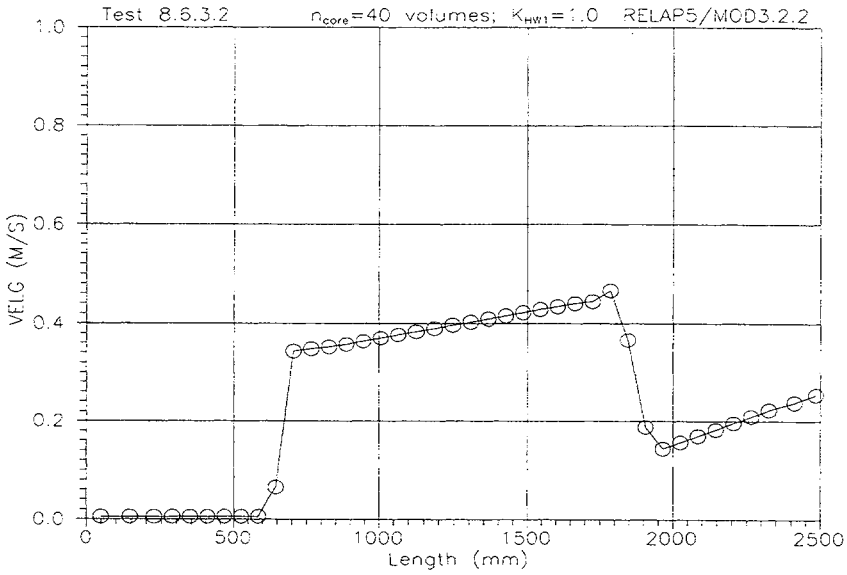

Fig.C-12. Calculated axial distribution of the vapor velocities in the FA channel at pressure Pup=27.3 bar and FA power W=16.8 kW in experiment 8.6.3.2.

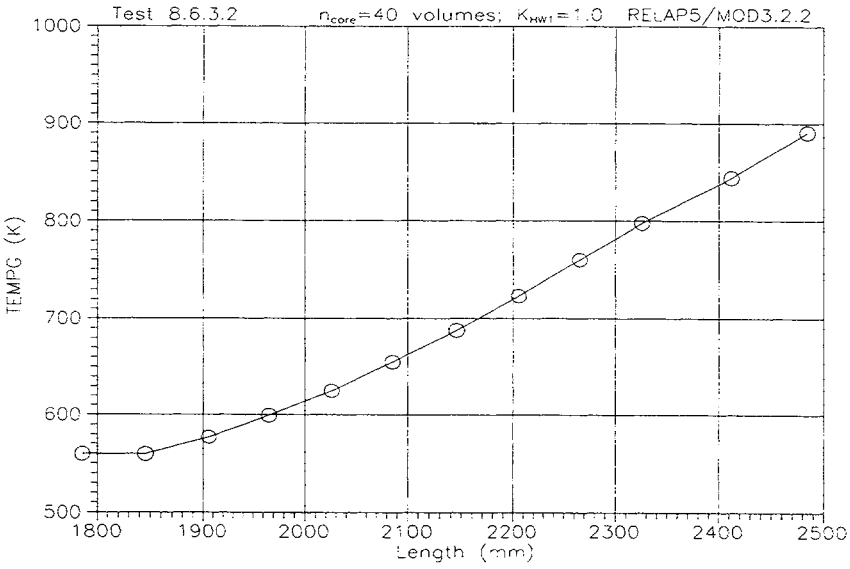

Fig.C-13. Axial distribution of the calculated vapor temperatures Tg (x) in the uncovered part of FA channel for the test 8.6.3.2.

Appendix D

Sensitivity Studies Results

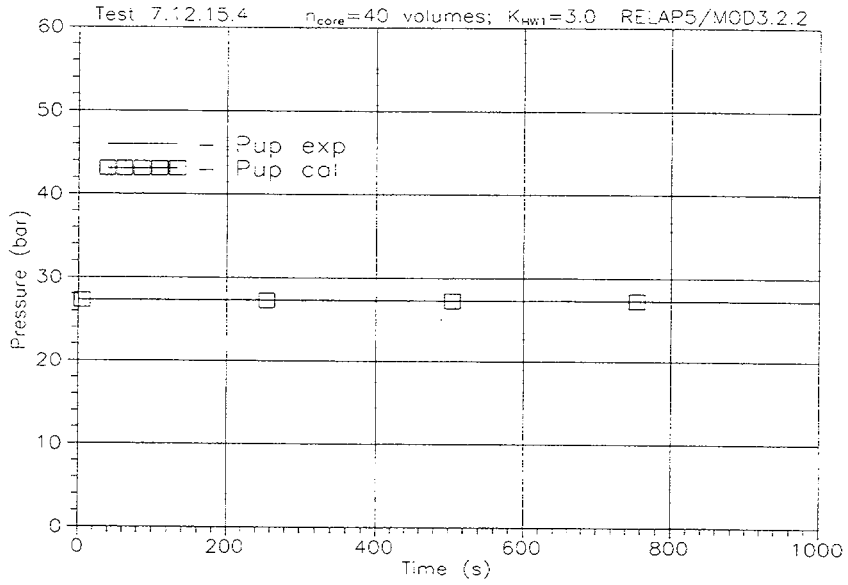

Fig.D-1. Comparison of the calculated P_{UP} (tcal) and measured P_{UP} (texp) pressure histories in the upper plenum model in experiment 7.12.15.4.

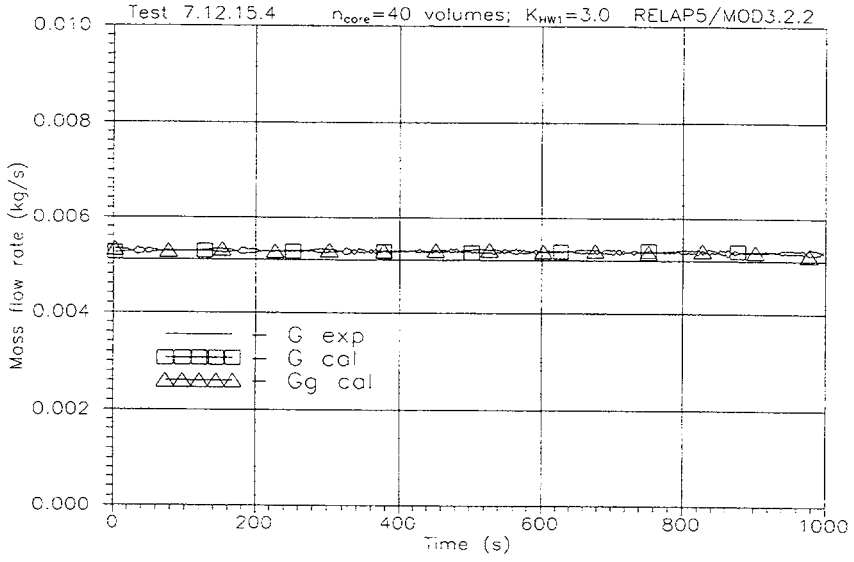

Fig.D-2. Comparison of the calculated G_L (tcal) , Gg (tcal) and measured G (texp) mass flow rate histories at the inlet of the FA channel in experiment 7.12.15.4.

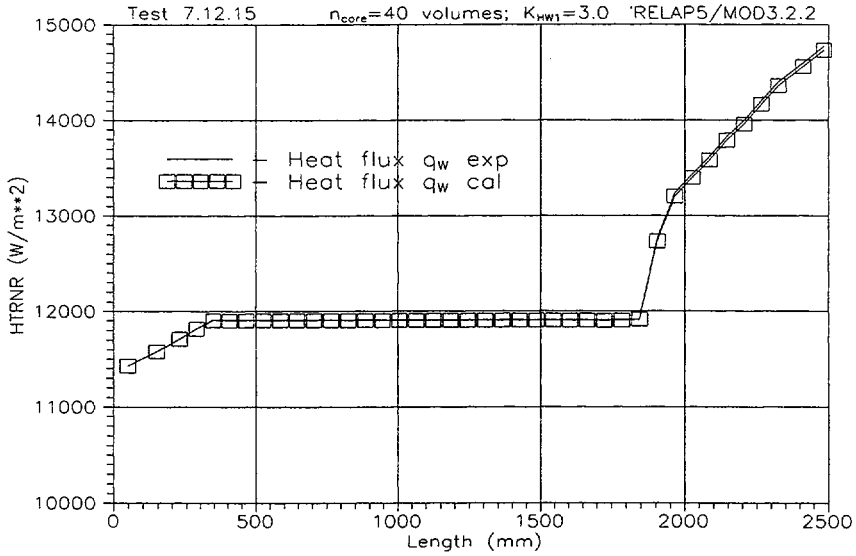

Fig.D-3. Comparison of the distributions of experimental qw (t0exp) and calculated qw (t1cal) specific heat fluxes from the outer surfaces of the rod simulators to a coolant on the FA height for the initial time moment in experiment 7.12.15.4.

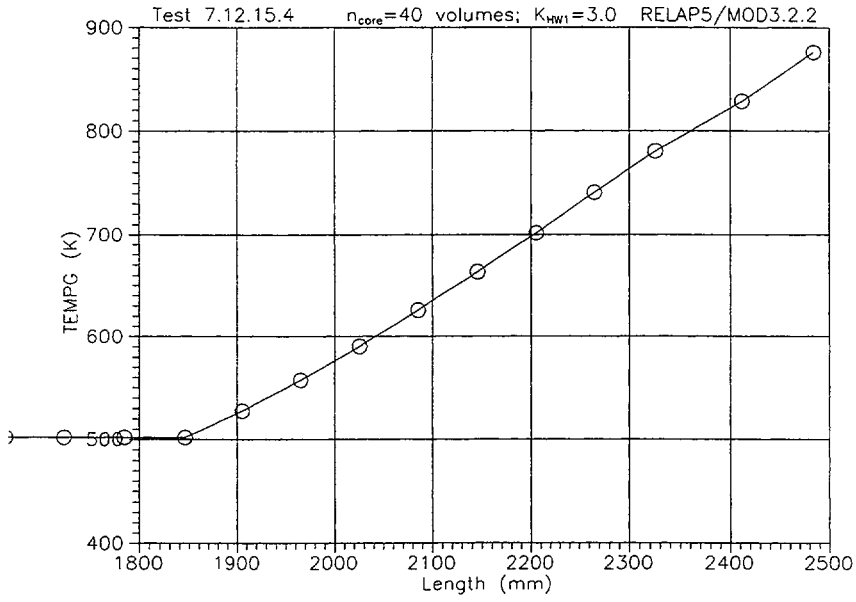

Fig.D-4. Axial distribution of the calculated vapor temperatures Tg (x) in the uncovered part of the FA channel at K_{HW1}=3.0 for the test 7.12.15.4.

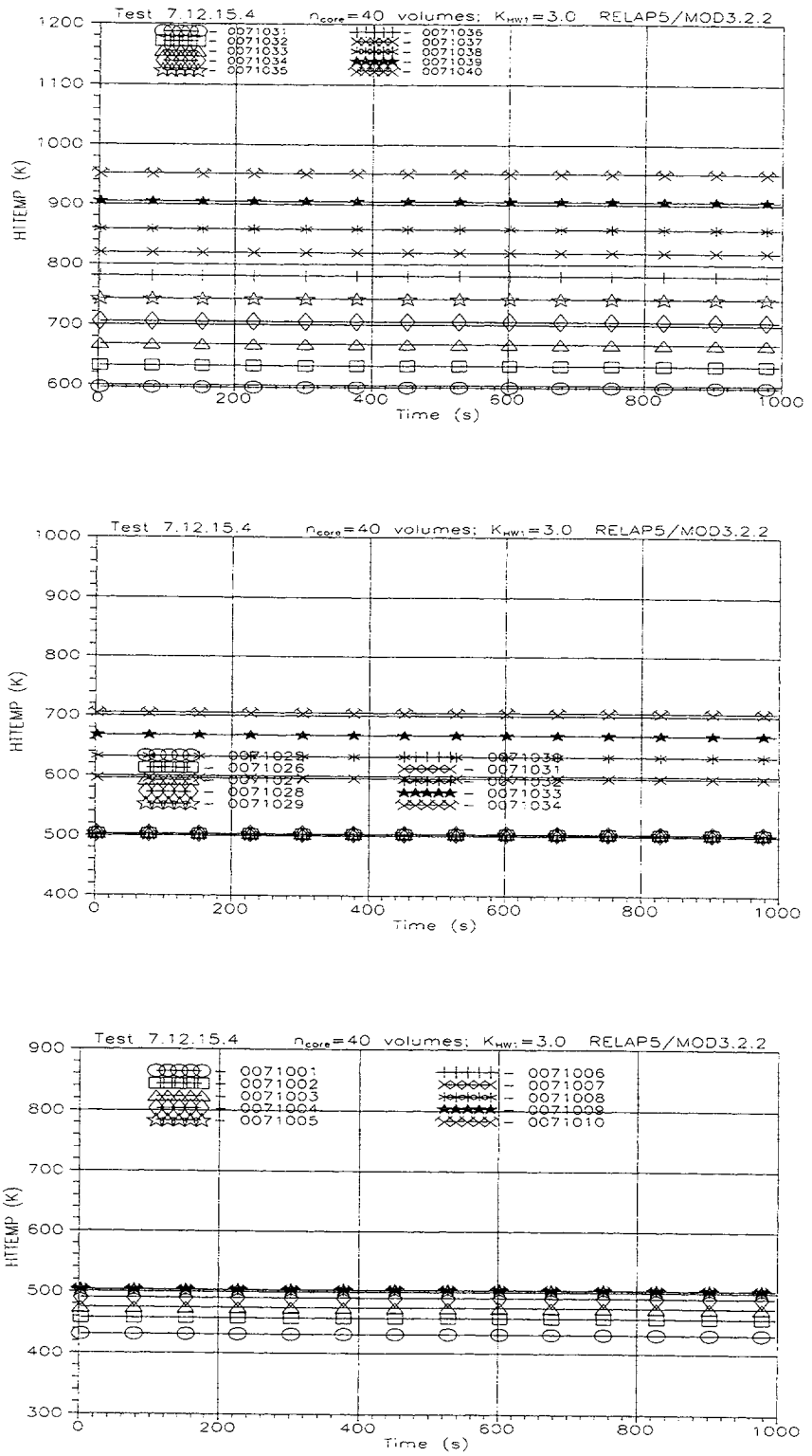

Fig.D-5. Calculated TW(tcal) rod's wall temperatures histories in the upper, middle and bottom parts of the FA model in experiment 7.12.15.4.

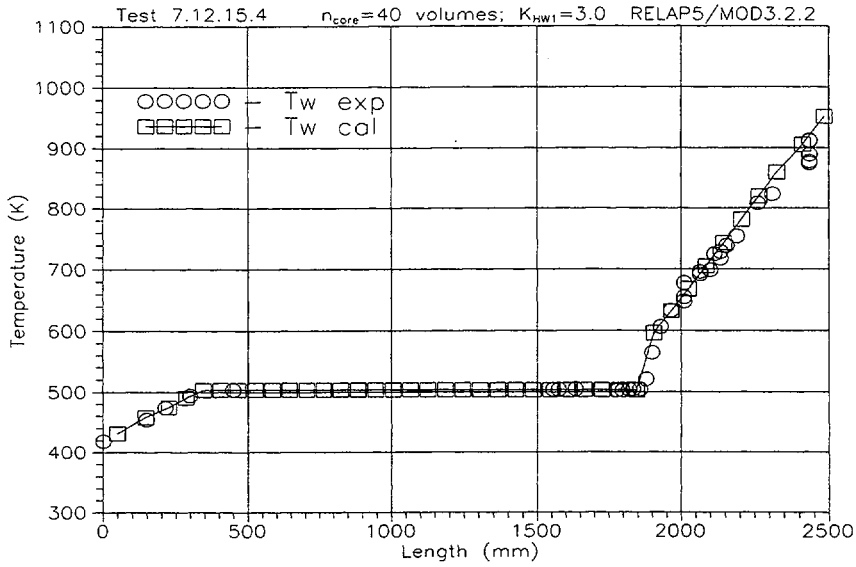

Fig.D-6. Comparison of the axial profile of calculated rod's wall temperature TW (t1cal) at K_{HW1}=3.0 in the FA model and axial distribution of measured rod's cladding temperatures for test 7.12.15.4.

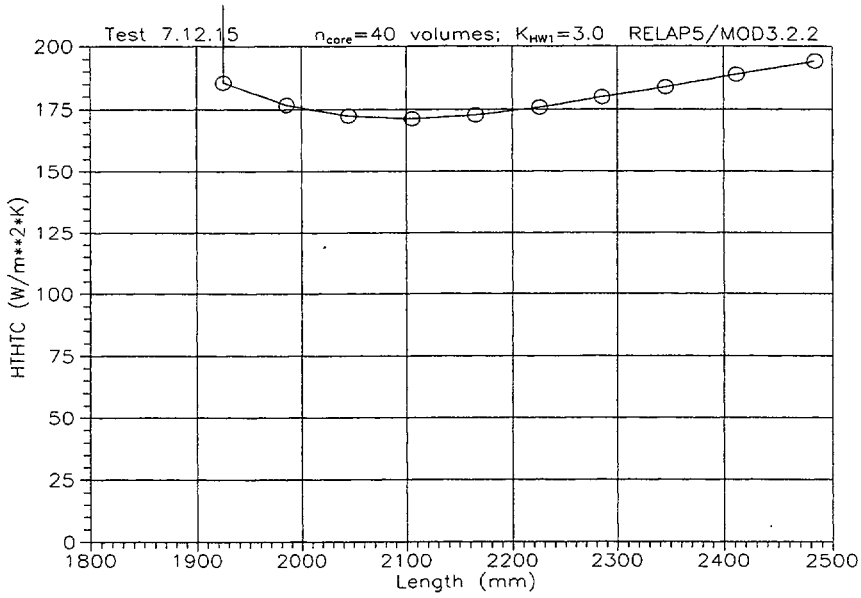

Fig.D-7. Axial distribution of the calculated coefficients Hw1(t2cal) of heat transfer from the rods to a coolant at K_{HW1}=3.0 in the upper part of the FA model for experiment 7.12.15.4.

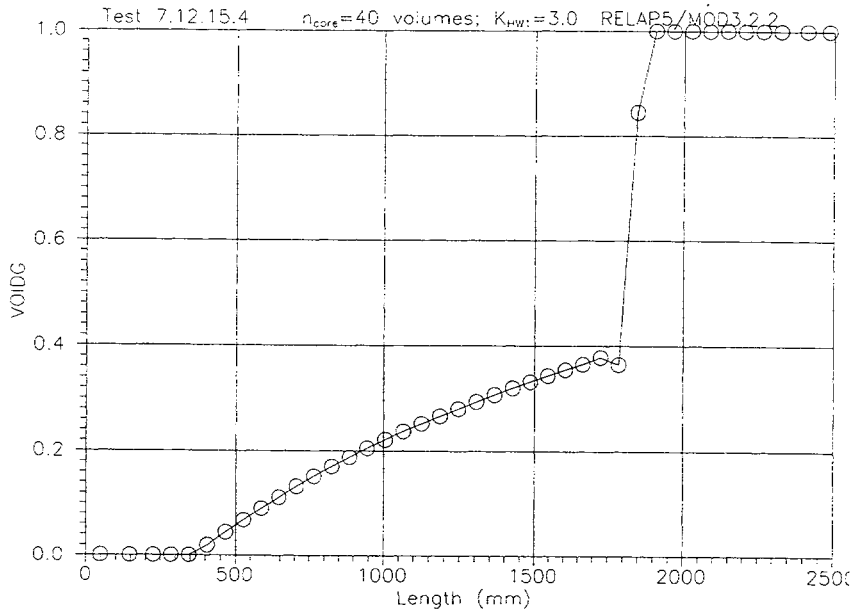

Fig.D-8. Calculated core axial distribution of the void fractions in the FA channel in experiment 7.12.15.4.

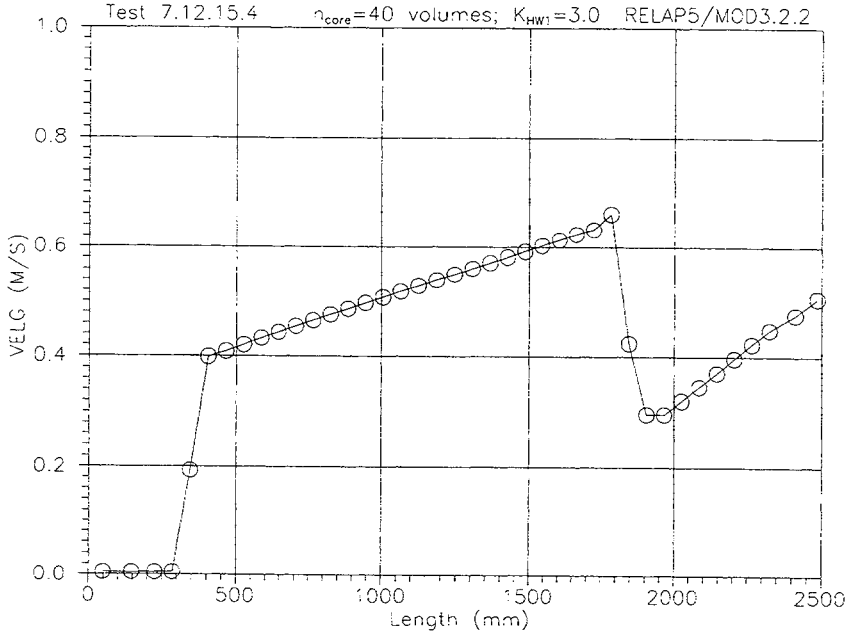

Fig.D-9. Calculated core axial distribution of the vapor velocities in the FA channel at pressure Pup=27.3 bar and FA power W=16.8 kW in experiment 7.12.15.4.

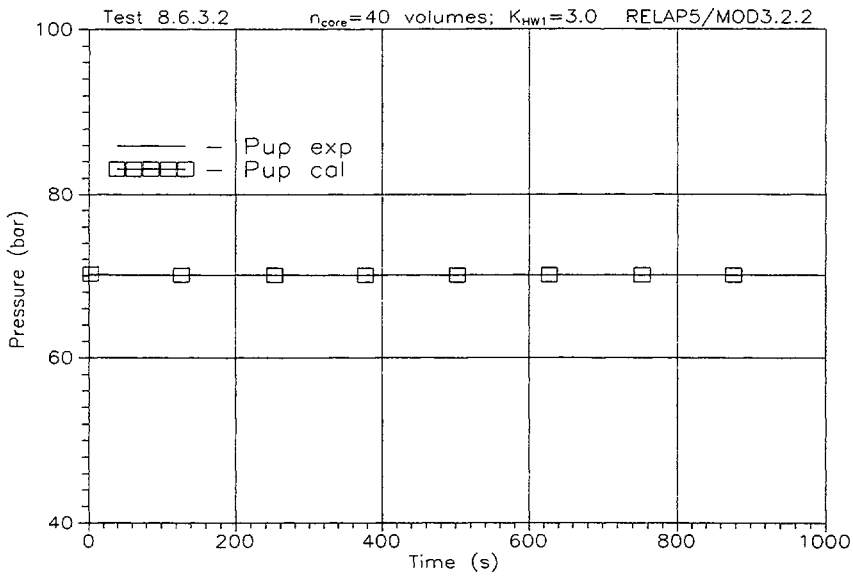

Fig.D-10. Comparison of the calculated P_{UP} (tcal) and measured P_{UP} (texp) pressure histories in the upper plenum model in experiment 8.6.3.2.

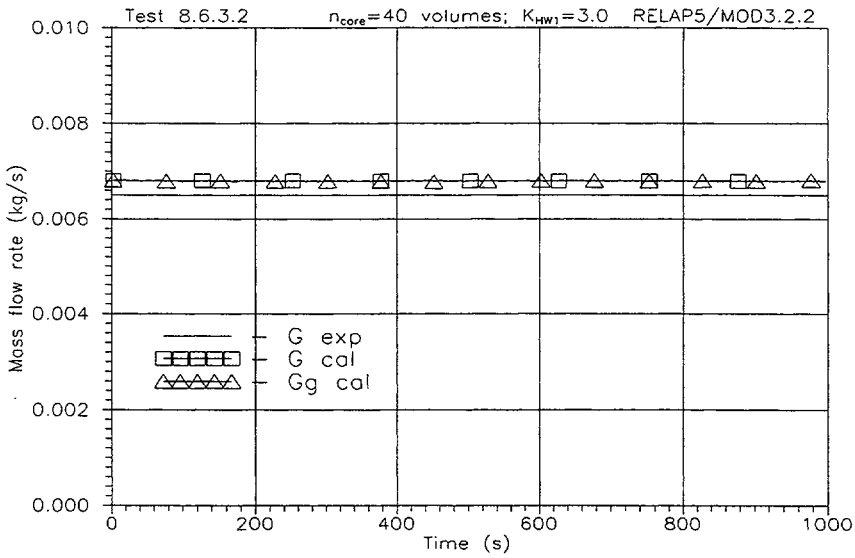

Fig.D-11. Comparison of the calculated G_L (tcal) , Gg (tcal) and measured G (texp) mass flow rate histories at the inlet of the FA channel in experiment 8.6.3.2.

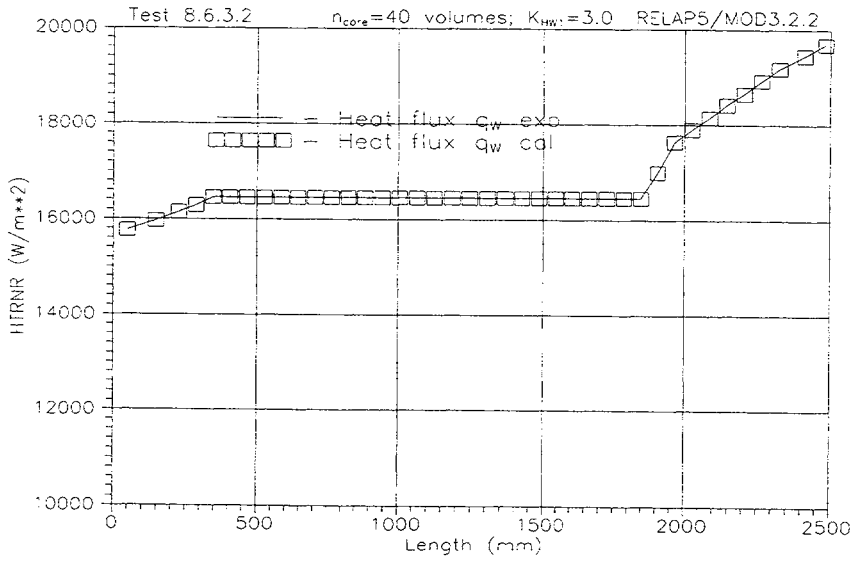

Fig.D-12. Comparison of the distributions of experimental qw (t0exp) and calculated qw (t1cal) specific heat fluxes from the outer surfaces of the rod simulators to a coolant on the FA height for the initial time moment in experiment 8.6.3.2.

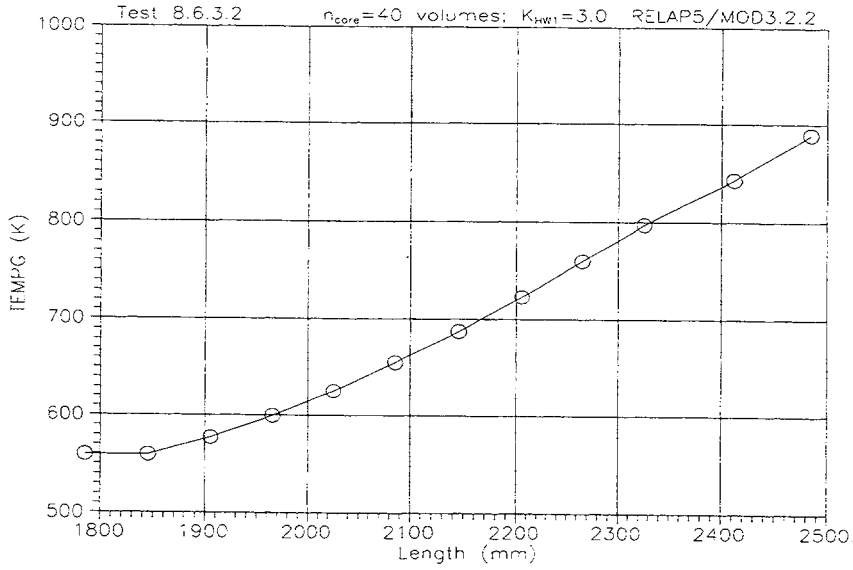

Fig.D-13. Axial distribution of the calculated vapor temperatures Tg (x) in the uncovered part of the FA channel at K_{HW1}=3.0 for the test 8.6.3.2.

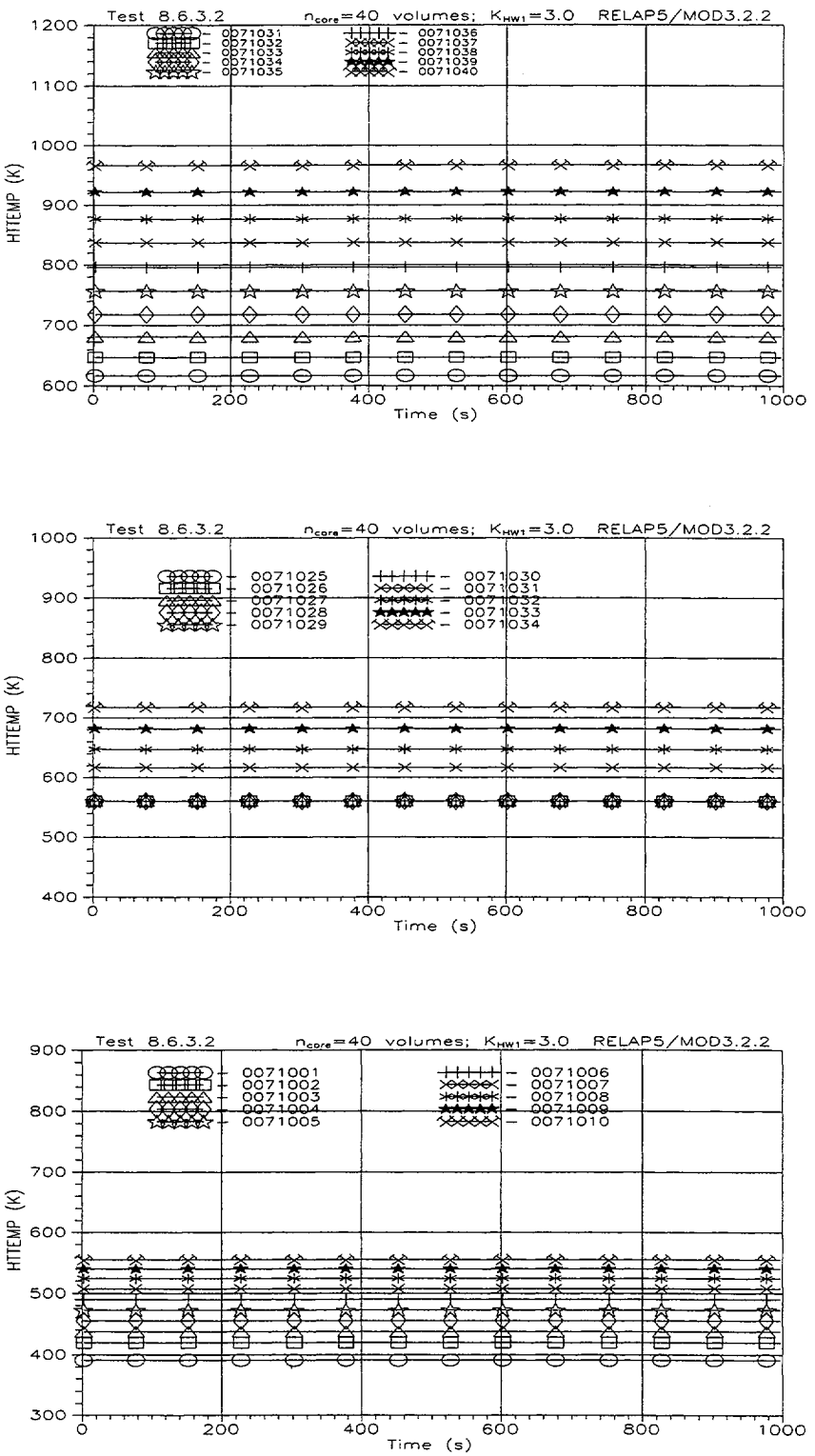

Fig.D-14. Histories of the calculated TW (tcal) rod's wall temperatures in the upper, middle and bottom of the FA model in experiment 8.6.3.2.

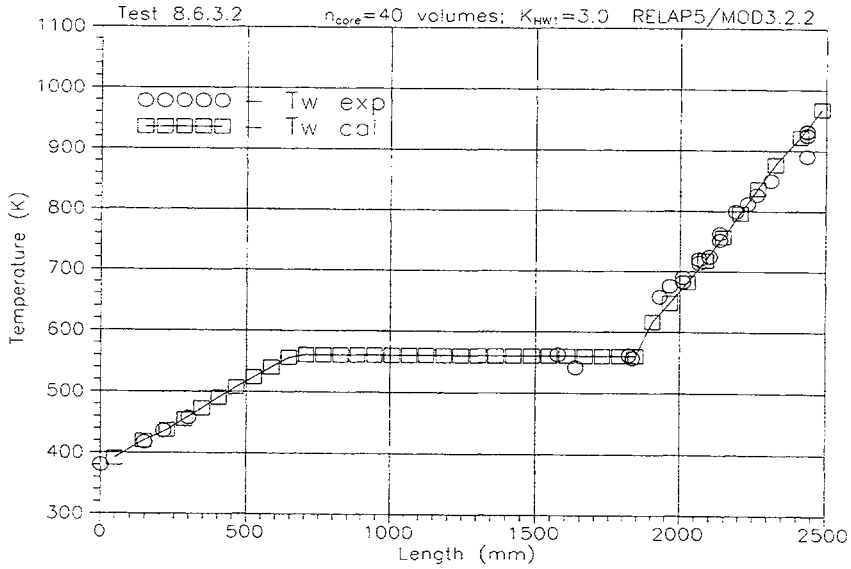

Fig.D-15. Comparison of the axial profile of calculated rod's wall temperature TW (t2cal) at K_{HW1}=3.0 in the FA model and axial distribution of measured rod's cladding temperatures for test 8.6.3.2.

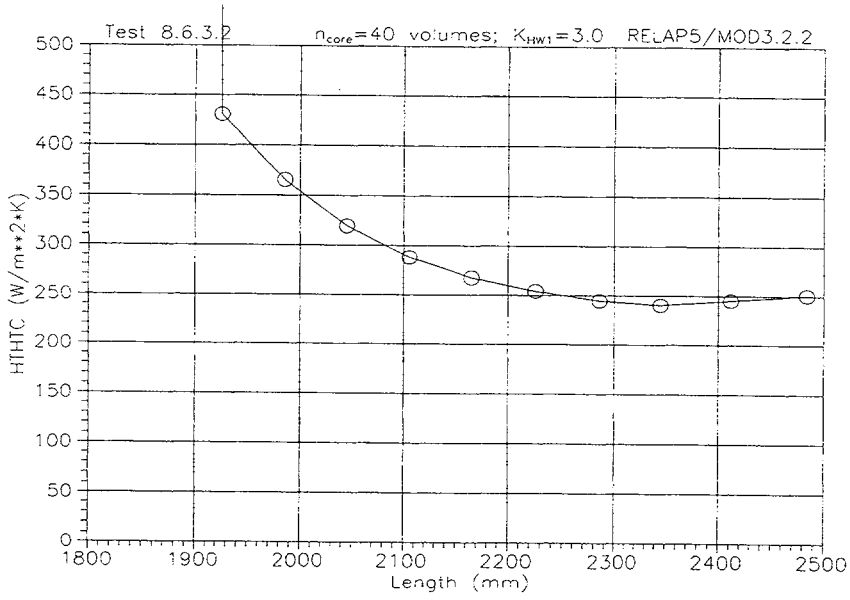

Fig.D-16. Axial distribution of the calculated coefficients Hw1(t2cal) of heat transfer from the rods to a coolant in the upper part of the FA model for experiment 8.6.3.2.

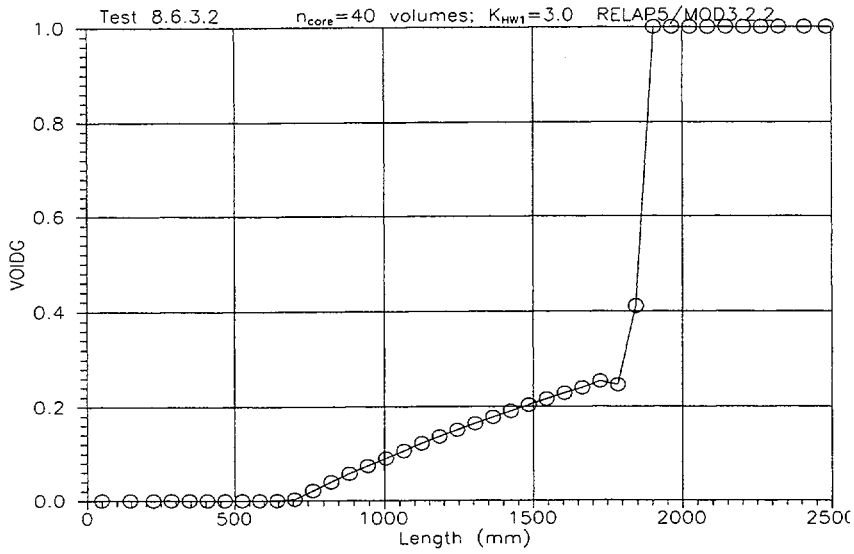

Fig.D-17. Calculated axial distribution of the void fractions in the FA channel in experiment 8.6.3.2.

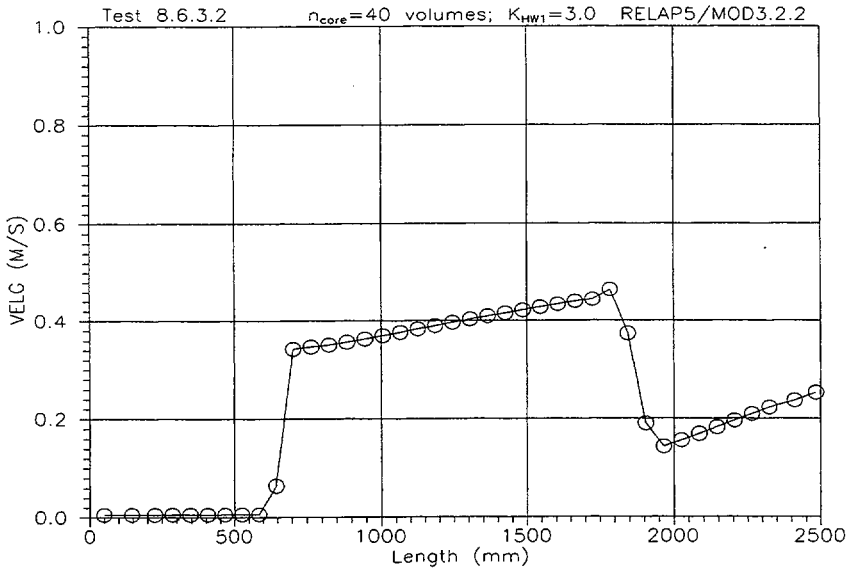

Fig.D-18. Calculated axial distribution of the vapor velocities in the FA channel at pressure Pup=27.3 bar and FA power W=16.8 kW in experiment 8.6.3.2.

Appendix E

Base Case input deck listing for Test 8.6.3.2

```
=vti test
*****************************************
* Assessment of RELAP5/MOD3.2.2GAMMA
* against VTI VVER 8.6.3.2 test
* Initial conditions
* FA model power = 22,97 kWt
* UP outlet pressure = 7.01 MPa
*****************************************
*0000100 new stdy-st
0000100 new transnt
*0000101 inp-chk
0000102 si si
0000104 *cmpress
110                 air
*****************************************
* TIME STEPS CONTROL CARDS
*****************************************
*0000201 10.  1.0-6  0.00025 14003  100  4000  40000
0000201 3000.  1.0-6  0.025 14003  100  4000  40000
*
*
* = ========================== ========
* PRIMARY CIRCUIT
* ----------------------------------------
* Lower Plenum
* ----------------------------------------
0050000 lowr pipe
0050001 2
0050101 21.1-3 2
0050301 0.272 2
0050601 90.0 2
0050801 5.0-5 0.164 2
0050901 0.0 0.0 1
0051001 000000 2
0051101 0000000 1
0051201 103 .702589e+07 344.996 0.0 0.0 0.0  1
0051202 103 .702328e+07 348.225 0.0 0.0 0.0  2
0051300 0
0051301 -3.89245e-08 -3.89245e-08 0.0 1
0051401 0.164 0.0 1.0 1.0  1
*
10052000  2 3 2 0 0.082
10052100  0 1
10052101  1 0.086 1 0.09
10052201  1 2
10052301  0.0 2
10052400  -1
10052401 345.00 345.00 345.00
10052402 348.22 348.22 348.22
*10052401  340.0 3
10052501  005010000 10000 1 1 0.272 2
10052601  0 0 0000 1 0.272  2
10052701  0 0.0 0.0 0.0 2
10052801  0.0 15.0 15.0 0.0 0.0 0.0 0.0 1.0 2
*
0060000 incore sngljun
0060101 005010000 007000000 0.0 0.0 0.0 0000000
0060201 0 4.70647e-03  4.70647e-03 0.0
*
*----------------------------------------------
* Core Model
*----------------------------------------------
0070000 core pipe
0070001 42
0070101 1.478-3 42
0070301 0.0975 2
0070302 0.06  38
0070303 0.0725 40
0070304 0.0625 42
0070601 90. 42
0070801 1.0-5 8.02-3 42
0070901 0.0  0.0 1
0070902 0.27 0.27  2
0070903 0.0  0.0 3
0070904 0.0  0.0 4
0070905 0.0  0.0 5
0070906 0.27 0.27  6
0070907 0.0  0.0 7
0070908 0.0  0.0 8
0070909 0.0  0.0 9
0070910 0.27 0.27 10
0070911 0.0  0.0  11
0070912 0.0  0.0  12
0070913 0.0  0.0  13
0070914 0.27 0.27 14
0070915 0.0  0.0  15
0070916 0.0  0.0  16
0070917 0.0  0.0  17
0070918 0.27 0.27 18
0070919 0.0  0.0  19
0070920 0.0  0.0  20
0070921 0.0  0.0  21
0070922 0.27 0.27 22
0070923 0.0  0.0  23
0070924 0.0  0.0  24
0070925 0.0  0.0  25
0070926 0.27 0.27 26
0070927 0.0  0.0  27
0070928 0.0  0.0  28
0070929 0.0  0.0  29
0070930 0.27 0.27 30
0070931 0.0  0.0  31
0070932 0.0  0.0  32
0070933 0.0  0.0  33
0070934 0.27 0.27 34
0070935 0.0  0.0  35
0070936 0.0  0.0  36
0070937 0.0  0.0  37
0070938 0.27 0.27 38
0070939 0.0  0.0  39
0070940 0.0  0.0  40
0070941 0.0  0.0  41
0071001 10100 42
0071101 0001000 41
0071201 103 .702152e+07 377.452 0.0 0.0 0.0  1
0071202 103 .702061e+07 406.842 0.0 0.0 0.0  2
0071203 103 .701989e+07 424.966 0.0 0.0 0.0  3
0071204 103 .701936e+07 443.082 0.0 0.0 0.0  4
0071205 103 .701883e+07 461.178 0.0 0.0 0.0  5
0071206 103 .701832e+07 478.962 0.0 0.0 0.0  6
0071207 103 .701782e+07 496.343 0.0 0.0 0.0  7
0071208 103 .701733e+07 513.325 0.0 0.0 0.0  8
0071209 103 .701686e+07 529.761 0.0 0.0 0.0  9
0071210 103 .701640e+07 545.477 0.0 0.0 0.0 10
0071211 100 .701596e+07  .125550e+07  .258170e+07  .260623e-02 0.0 11
0071212 100 .701552e+07  .125860e+07  .258170e+07  .207902e-01 0.0 12
0071213 100 .701510e+07  .125870e+07  .258170e+07  .391013e-01 0.0 13
0071214 100 .701469e+07  .125870e+07  .258170e+07  .567685e-01 0.0 14
0071215 100 .701428e+07  .125870e+07  .258170e+07  .736818e-01 0.0 15
0071216 100 .701388e+07  .125870e+07  .258170e+07  .900012e-01 0.0 16
0071217 100 .701348e+07  .125860e+07  .258170e+07  .105740  0.0 17
0071218 100 .701309e+07  .125860e+07  .258170e+07  .121060  0.0 18
0071219 100 .701271e+07  .125860e+07  .258170e+07  .135700  0.0 19
0071220 100 .701233e+07  .125860e+07  .258170e+07  .150000  0.0 20
0071221 100 .701196e+07  .125860e+07  .258170e+07  .163860  0.0 21
0071222 100 .701160e+07  .125850e+07  .258170e+07  .177520  0.0 22
0071223 100 .701124e+07  .125850e+07  .258170e+07  .190480  0.0 23
0071224 100 .701088e+07  .125850e+07  .258170e+07  .203260  0.0 24
0071225 100 .701053e+07  .125850e+07  .258170e+07  .215650  0.0 25
0071226 100 .701019e+07  .125850e+07  .258170e+07  .228080  0.0 26
0071227 100 .700985e+07  .125850e+07  .258170e+07  .239170  0.0 27
0071228 100 .700952e+07  .125840e+07  .258170e+07  .254270  0.0 28
0071229 100 .700918e+07  .125840e+07  .258180e+07  .240130  0.0 29
0071230 100 .700889e+07  .125840e+07  .258180e+07  .463610  0.0 30
0071231 100 .700876e+07  .125840e+07  .264490e+07  1.00000  0.0 31
0071232 100 .700874e+07  .125840e+07  .271020e+07  1.00000  0.0 32
0071233 100 .700873e+07  .125840e+07  .277590e+07  1.00000  0.0 33
0071234 100 .700871e+07  .125840e+07  .284190e+07  1.00000  0.0 34
0071235 100 .700870e+07  .125840e+07  .290850e+07  1.00000  0.0 35
0071236 100 .700868e+07  .125840e+07  .297540e+07  1.00000  0.0 36
0071237 100 .700867e+07  .125840e+07  .304330e+07  1.00000  0.0 37
0071238 100 .700866e+07  .125840e+07  .311220e+07  1.00000  0.0 38
0071239 100 .700864e+07  .125840e+07  .319640e+07  1.00000  0.0 39
0071240 100 .700863e+07  .125840e+07  .328140e+07  1.00000  0.0 40
0071241 100 .700862e+07  .125840e+07  .327760e+07  1.00000  0.0 41
0071242 100 .700861e+07  .125840e+07  .327370e+07  1.00000  0.0 42
0071300 0
0071301  4.80217e-03  4.80217e-03 0.0 01
0071302  4.92188e-03  4.92188e-03 0.0 02
0071303  5.00835e-03  5.00835e-03 0.0 03
0071304  5.10578e-03  5.10578e-03 0.0 04
0071305  5.21578e-03  5.21578e-03 0.0 05
0071306  5.33863e-03  5.33863e-03 0.0 06
0071307  5.47606e-03  5.47606e-03 0.0 07
0071308  5.63140e-03  5.63140e-03 0.0 08
0071309  5.80783e-03  5.80783e-03 0.0 09
0071310  6.00949e-03  0.12846  0.0 10
0071311  6.18187e-03  0.34266  0.0 11
0071312  5.98735e-03  0.34755  0.0 12
0071313  5.76625e-03  0.35301  0.0 13
```

```
0071314 5.53664e-03 0.35902 0.0 14
0071315 5.29519e-03 0.36587 0.0 15
0071316 5.04039e-03 0.37263 0.0 16
0071317 4.77064e-03 0.37942 0.0 17
0071318 4.48620e-03 0.38578 0.0 18
0071319 4.18582e-03 0.39270 0.0 19
0071320 3.87177e-03 0.39920 0.0 20
0071321 3.54425e-03 0.40566 0.0 21
0071322 3.20487e-03 0.41156 0.0 22
0071323 2.85219e-03 0.41816 0.0 23
0071324 2.48868e-03 0.42431 0.0 24
0071325 2.11390e-03 0.43049 0.0 25
0071326 1.72878e-03 0.43592 0.0 26
0071327 1.33018e-03 0.44325 0.0 27
0071328 9.23651e-04 0.44285 0.0 28
0071329 4.90328e-04 0.49636 0.0 29
0071330 0.27500 0.27139 0.0 30
0071331 0.13770 0.13770 0.0 31
0071332 0.15003 0.15003 0.0 32
0071333 0.16272 0.16272 0.0 33
0071334 0.17566 0.17566 0.0 34
0071335 0.18884 0.18884 0.0 35
0071336 0.20216 0.20216 0.0 36
0071337 0.21539 0.21539 0.0 37
0071338 0.22837 0.22837 0.0 38
0071339 0.24387 0.24387 0.0 39
0071340 0.25918 0.25918 0.0 40
0071341 0.25849 0.25849 0.0 41
0071401 8.02-3 0.0 1.000 1.00 41
*
10071000 40 5 2 0 0.0
10071100 0 1
10071101 1 0.00165 1 0.0028 1 0.00405 1 0.00455
10071201 1 1 3 3 1 4
10071301 1.0 1 0.0 4
10071400 -1
10071401 419.04 416.85 402.02 391.55 391.03
10071402 447.81 445.66 430.64 420.04 419.52
10071403 465.80 463.68 448.49 437.77 437.26
10071404 483.77 481.68 466.36 455.55 455.04
10071405 501.86 499.79 484.31 473.39 472.89
10071406 519.29 517.26 501.78 490.86 490.37
10071407 536.36 534.36 518.89 507.96 507.48
10071408 553.03 551.06 535.59 524.66 524.19
10071409 569.12 567.19 551.71 540.79 540.33
10071410 584.48 582.58 567.11 556.18 555.73
10071411 589.19 587.30 571.82 560.90 560.44
10071412 589.22 587.32 571.85 560.92 560.47
10071413 589.21 587.32 571.85 560.92 560.47
10071414 589.21 587.31 571.84 560.92 560.46
10071415 589.20 587.31 571.84 560.91 560.46
10071416 589.20 587.31 571.83 560.91 560.45
10071417 589.19 587.30 571.83 560.90 560.45
10071418 589.19 587.30 571.82 560.90 560.44
10071419 589.18 587.29 571.82 560.89 560.44
10071420 589.18 587.29 571.81 560.89 560.43
10071421 589.17 587.28 571.81 560.88 560.43
10071422 589.17 587.28 571.80 560.88 560.42
10071423 589.16 587.27 571.80 560.87 560.42
10071424 589.16 587.27 571.79 560.87 560.41
10071425 589.15 587.26 571.79 560.86 560.41
10071426 589.15 587.26 571.78 560.86 560.40
10071427 589.14 587.25 571.78 560.85 560.40
10071428 589.14 587.25 571.77 560.85 560.39
10071429 589.14 587.24 571.77 560.84 560.39
10071430 589.10 587.21 571.74 560.81 560.36
10071431 697.32 695.48 679.49 668.19 667.76
10071432 740.69 738.85 722.26 710.54 710.10
10071433 784.99 783.19 766.36 754.47 754.04
10071434 830.62 828.87 811.80 799.75 799.33
10071435 877.01 875.30 857.98 845.74 845.33
10071436 922.43 920.75 903.21 890.82 890.43
10071437 968.32 966.64 948.84 936.27 935.87
10071438 1015.0 1013.4 995.34 982.60 982.21
10071439 1067.1 1065.5 1047.2 1034.2 1033.9
10071440 1118.3 1116.8 1098.2 1085.2 1084.8
*10071401 559.0 5
10071501 0 0 0 1 1.8525 2
10071502 0 0 0 1 1.14 38
10071503 0 0 0 1 1.3775 40
10071601 007010000 10000 110 1 1.8525 2
10071602 007030000 10000 110 1 1.14 38
10071603 007390000 10000 110 1 1.3775 40
10071701 001 3.634569e-02 0.0 0.0 1
10071702 001 3.681150e-02 0.0 0.0 2
10071703 001 2.290184e-02 0.0 0.0 3
10071704 001 2.309970e-02 0.0 0.0 4
10071705 001 2.333816e-02 0.0 0.0 5
10071706 001 2.333816e-02 0.0 0.0 6
10071707 001 2.333816e-02 0.0 0.0 7
10071708 001 2.333816e-02 0.0 0.0 8
10071709 001 2.333816e-02 0.0 0.0 9
10071710 001 2.333816e-02 0.0 0.0 10
10071711 001 2.333816e-02 0.0 0.0 11
10071712 001 2.333816e-02 0.0 0.0 12
10071713 001 2.333816e-02 0.0 0.0 13
10071714 001 2.333816e-02 0.0 0.0 14
10071715 001 2.333816e-02 0.0 0.0 15
10071716 001 2.333816e-02 0.0 0.0 16
10071717 001 2.333816e-02 0.0 0.0 17
10071718 001 2.333816e-02 0.0 0.0 18
10071719 001 2.333816e-02 0.0 0.0 19
10071720 001 2.333816e-02 0.0 0.0 20
10071721 001 2.333816e-02 0.0 0.0 21
10071722 001 2.333816e-02 0.0 0.0 22
10071723 001 2.333816e-02 0.0 0.0 23
10071724 001 2.333816e-02 0.0 0.0 24
10071725 001 2.333816e-02 0.0 0.0 25
10071726 001 2.333816e-02 0.0 0.0 26
10071727 001 2.333816e-02 0.0 0.0 27
10071728 001 2.333816e-02 0.0 0.0 28
10071729 001 2.333816e-02 0.0 0.0 29
10071730 001 2.333816e-02 0.0 0.0 30
10071731 001 2.411948e-02 0.0 0.0 31
10071732 001 2.502257e-02 0.0 0.0 32
10071733 001 2.539293e-02 0.0 0.0 33
10071734 001 2.574808e-02 0.0 0.0 34
10071735 001 2.613620e-02 0.0 0.0 35
10071736 001 2.645837e-02 0.0 0.0 36
10071737 001 2.685410e-02 0.0 0.0 37
10071738 001 2.721940e-02 0.0 0.0 38
10071739 001 3.334989e-02 0.0 0.0 39
10071740 001 3.374837e-02 0.0 0.0 40
10071900 1
10071901 0.0109 0.04875 2.45125 0.04875 0.14625 0.27 0.27 1.0 0.125 1.34 1.0
1
10071902 0.0109 0.14625 2.35375 0.14625 0.04875 0.27 0.27 1.0 0.125 1.34 1.0
2
10071903 0.0109 0.2256 2.2744 0.03 0.21 0.27 0.27 1.0 0.125 1.34 1.0 3
10071904 0.0109 0.2856 2.2144 0.09 0.15 0.27 0.27 1.0 0.125 1.34 1.0 4
10071905 0.0109 0.3456 2.1544 0.15 0.09 0.27 0.27 1.0 0.125 1.34 1.0 5
10071906 0.0109 0.4056 2.0944 0.21 0.03 0.27 0.27 1.0 0.125 1.34 1.0 6
10071907 0.0109 0.4656 2.0344 0.03 0.21 0.27 0.27 1.0 0.125 1.34 1.0 7
10071908 0.0109 0.5256 1.9744 0.09 0.15 0.27 0.27 1.0 0.125 1.34 1.0 8
10071909 0.0109 0.5856 1.9144 0.15 0.09 0.27 0.27 1.0 0.125 1.34 1.0 9
10071910 0.0109 0.6456 1.8544 0.21 0.03 0.27 0.27 1.0 0.125 1.34 1.0 10
10071911 0.0109 0.7056 1.7944 0.03 0.21 0.27 0.27 1.0 0.125 1.34 1.0 11
10071912 0.0109 0.7656 1.7344 0.09 0.15 0.27 0.27 1.0 0.125 1.34 1.0 12
10071913 0.0109 0.8256 1.6744 0.15 0.09 0.27 0.27 1.0 0.125 1.34 1.0 13
10071914 0.0109 0.8856 1.6144 0.21 0.03 0.27 0.27 1.0 0.125 1.34 1.0 14
10071915 0.0109 0.9456 1.5544 0.03 0.21 0.27 0.27 1.0 0.125 1.34 1.0 15
10071916 0.0109 1.0056 1.4944 0.09 0.15 0.27 0.27 1.0 0.125 1.34 1.0 16
10071917 0.0109 1.0656 1.4344 0.15 0.09 0.27 0.27 1.0 0.125 1.34 1.0 17
10071918 0.0109 1.1256 1.3744 0.21 0.03 0.27 0.27 1.0 0.125 1.34 1.0 18
10071919 0.0109 1.1856 1.3144 0.03 0.21 0.27 0.27 1.0 0.125 1.34 1.0 19
10071920 0.0109 1.2456 1.2544 0.09 0.15 0.27 0.27 1.0 0.125 1.34 1.0 20
10071921 0.0109 1.3256 1.1944 0.15 0.09 0.27 0.27 1.0 0.125 1.34 1.0 21
10071922 0.0109 1.3856 1.1344 0.21 0.03 0.27 0.27 1.0 0.125 1.34 1.0 22
10071923 0.0109 1.4456 1.0744 0.03 0.21 0.27 0.27 1.0 0.125 1.34 1.0 23
10071924 0.0109 1.5056 1.0144 0.09 0.15 0.27 0.27 1.0 0.125 1.34 1.0 24
10071925 0.0109 1.5656 0.9544 0.15 0.09 0.27 0.27 1.0 0.125 1.34 1.0 25
10071926 0.0109 1.6256 0.8944 0.21 0.03 0.27 0.27 1.0 0.125 1.34 1.0 26
10071927 0.0109 1.6856 0.8344 0.03 0.21 0.27 0.27 1.0 0.125 1.34 1.0 27
10071928 0.0109 1.7456 0.7744 0.09 0.15 0.27 0.27 1.0 0.125 1.34 1.0 28
10071929 0.0109 1.8056 0.7144 0.15 0.09 0.27 0.27 1.0 0.125 1.34 1.0 29
10071930 0.0109 1.8656 0.6544 0.21 0.03 0.27 0.27 1.0 0.125 1.34 1.0 30
10071931 0.0109 1.9256 0.5944 0.03 0.21 0.27 0.27 1.0 0.125 1.34 1.0 31
10071932 0.0109 1.9856 0.5344 0.09 0.15 0.27 0.27 1.0 0.125 1.34 1.0 32
10071933 0.0109 2.0456 0.4744 0.15 0.09 0.27 0.27 1.0 0.125 1.34 1.0 33
10071934 0.0109 2.1056 0.4144 0.21 0.03 0.27 0.27 1.0 0.125 1.34 1.0 34
10071935 0.0109 2.1656 0.3544 0.03 0.21 0.27 0.27 1.0 0.125 1.34 1.0 35
10071936 0.0109 2.2256 0.2944 0.09 0.15 0.27 0.27 1.0 0.125 1.34 1.0 36
10071937 0.0109 2.2856 0.2344 0.15 0.09 0.27 0.27 1.0 0.125 1.34 1.0 37
10071938 0.0109 2.3456 0.1744 0.21 0.03 0.27 0.27 1.0 0.125 1.34 1.0 38
10071939 0.0109 2.41185 0.08815 0.01565 0.08815 0.27 0.27 1.0 0.125 1.34 1.0
39
10071940 0.0109 2.48435 0.01565 0.08815 0.01565 0.27 0.27 1.0 0.125 1.34 1.0
40
*
10072000 42 4 2 0 0.028
```

```
10072100  0 1
10072101  1 0.040 1 0.0535
10072102  1 0.0635
10072201  2 1 2 2 1 3
10072301  0.0 3
10072400  -1
10072401 377.24 376.59 376.18 376.17
10072402 406.89 407.00 407.08 407.08
10072403 425.15 425.85 426.31 426.32
10072404 443.40 444.81 445.74 445.75
10072405 461.62 463.89 465.36 465.38
10072406 479.37 481.54 482.95 482.96
10072407 496.71 498.65 499.91 499.93
10072408 513.63 515.25 516.31 516.32
10072409 530.00 531.22 532.02 532.03
10072410 545.63 546.37 546.88 546.88
10072411 558.51 558.59 558.65 558.65
10072412 559.08 559.13 559.16 559.16
10072413 559.10 559.14 559.17 559.17
10072414 559.09 559.14 559.17 559.17
10072415 559.09 559.14 559.17 559.17
10072416 559.09 559.13 559.17 559.17
10072417 559.08 559.13 559.17 559.17
10072418 559.08 559.13 559.17 559.17
10072419 559.08 559.13 559.16 559.16
10072420 559.07 559.12 559.16 559.16
10072421 559.07 559.12 559.16 559.16
10072422 559.07 559.12 559.15 559.16
10072423 559.06 559.11 559.15 559.15
10072424 559.06 559.11 559.15 559.15
10072425 559.06 559.11 559.15 559.15
10072426 559.05 559.10 559.14 559.14
10072427 559.05 559.10 559.14 559.14
10072428 559.05 559.10 559.14 559.14
10072429 559.04 559.09 559.13 559.13
10072430 559.04 559.12 559.17 559.17
10072431 575.06 573.95 573.28 573.28
10072432 594.55 591.82 590.18 590.17
10072433 617.20 612.37 609.49 609.46
10072434 642.66 635.24 630.83 630.79
10072435 670.66 660.11 653.89 653.83
10072436 700.80 686.60 678.27 678.19
10072437 732.14 713.83 703.16 703.07
10072438 763.72 740.88 727.66 727.55
10072439 802.87 773.85 757.23 757.10
10072440 842.36 806.87 786.46 786.31
10072441 840.02 804.29 783.81 783.66
10072442 837.68 801.71 781.16 781.01
10072501  007010000 10000 1 1 0.0975  2
10072502  007030000 10000 1 1 0.06 38
10072503  007390000 10000 1 1 0.0725 40
10072504  007410000 10000 1 1 0.0625 42
10072601  0 0 0000 1 0.0975  2
10072602  0 0 0000 1 0.06 38
10072603  0 0 0000 1 0.0725 40
10072604  0 0 0000 1 0.0625 42
10072701  0 0.0 0.0 0.0 42
10072801  0.0305 15.0 15.0 0.0 0.0 0.0 0.0 1.0 42
*
0080000 outcore sngljun
*0080101 007010000 009000000 0.0 0.5 0.5 0100100
0080101 007010000 009000000 0.9-3 0.0 0.0 0000000
0080110 8.0-3 0.0 1.0 1.0
0080201 0 0.42336 0.42336  0.0
*
* ----------------------------------------
* Upper plenum
* ----------------------------------------
0090000 upplenum  pipe
0090001 15
0090101 6.65-3 15
0090301 0.1 1, 0.11 2, 0.21 4, 0.20 13, 0.14 15
0090601 90.0 15
0090801 5.0-5 0.092 15
0090901 0.0 0.0 14
0091001 000000 15
0091101 0000000 14
0091201 100 .700859e+07  .125840e+07  .327330e+07  1.00000  0.0  1
0091202 100 .700857e+07  .125840e+07  .327280e+07  1.00000  0.0  2
0091203 100 .700855e+07  .125840e+07  .327190e+07  1.00000  0.0  3
0091204 100 .700851e+07  .125840e+07  .327090e+07  1.00000  0.0  4
0091205 100 .700847e+07  .125840e+07  .326990e+07  1.00000  0.0  5
0091206 100 .700844e+07  .125840e+07  .326880e+07  1.00000  0.0  6
0091207 100 .700840e+07  .125840e+07  .326780e+07  1.00000  0.0  7
0091208 100 .700837e+07  .125840e+07  .326660e+07  1.00000  0.0  8
0091209 100 .700833e+07  .125840e+07  .326540e+07  1.00000  0.0  9
0091210 100 .700830e+07  .125840e+07  .326410e+07  1.00000  0.0 10
0091211 100 .700826e+07  .125840e+07  .326280e+07  1.00000  0.0 11
0091212 100 .700823e+07  .125840e+07  .326140e+07  1.00000  0.0 12
0091213 100 .700819e+07  .125840e+07  .325990e+07  1.00000  0.0 13
0091214 100 .700816e+07  .125840e+07  .325890e+07  1.00000  0.0 14
0091215 100 .700814e+07  .125840e+07  .316290e+07  1.00000  0.0 15
0091300 0
0091301 5.72766e-02  5.72766e-02  0.0  01
0091302 5.72542e-02  5.72542e-02  0.0  02
0091303 5.72098e-02  5.72098e-02  0.0  03
0091304 5.71637e-02  5.71637e-02  0.0  04
0091305 5.71181e-02  5.71181e-02  0.0  05
0091306 5.70705e-02  5.70705e-02  0.0  06
0091307 5.70208e-02  5.70208e-02  0.0  07
0091308 5.69690e-02  5.69690e-02  0.0  08
0091309 5.69147e-02  5.69147e-02  0.0  09
0091310 5.68580e-02  5.68580e-02  0.0  10
0091311 5.67986e-02  5.67986e-02  0.0  11
0091312 5.67365e-02  5.67365e-02  0.0  12
0091313 5.66715e-02  5.66715e-02  0.0  13
0091314 5.43874e-06  5.43874e-06  0.0  14
0091401 0.092 0.0 1.0 1.0  14
*
10092000  15 3 2 0 0.046
10092100  0 1
10092101  1 0.050 1 0.054
10092201  1 2
10092301  0.0 2
10092400  -1
10092401 875.64 875.63 875.62
10092402 875.32 875.31 875.30
10092403 874.68 874.66 874.66
10092404 874.00 873.98 873.98
10092405 873.32 873.30 873.29
10092406 872.60 872.58 872.57
10092407 871.84 871.82 871.82
10092408 871.05 871.03 871.02
10092409 870.21 870.19 870.18
10092410 869.33 869.31 869.30
10092411 868.41 868.39 868.38
10092412 867.45 867.43 867.42
10092413 866.44 866.42 866.41
10092414 865.72 865.69 865.69
10092415 821.03 821.03 821.03
*10092401  821.5 3
10092501  009010000 10000 1 1 0.1 1
10092502  009020000 10000 1 1 0.11  2
10092503  009030000 10000 1 1 0.21  4
10092504  009050000 10000 1 1 0.2 13
10092505  009140000 10000 1 1 0.14  15
10092601  000 0 0000 1 0.1 1
10092602  000 0 0000 1 0.11 2
10092603  000 0 0000 1 0.21 4
10092604  -12 0 3011 1 0.2 13
10092605  -12 0 3011 1 0.14 15
10092701  0 0.0 0.0 0.0 15
10092801  0.0 15.0 15.0 0.0 0.0 0.0 0.0 1.0 15
*
0100000 coreout sngljun
0100101 009140003 011000000 0.0 0.0 0.0 0000000
0100201 0 0.24771 0.24771  0.0
*
* ----------------------------------------
* Hot Leg
* ----------------------------------------
0110000 hotleg pipe
0110001 18
0110101 1.52-3 18
0110301 0.2 10, 0.15 17, 0.1052 18
0110601 -2.0 10, -90.0 18
0110801 5.0-5 0.044 18
0110901 0.0 0.0 17
0111001 000000 18
0111101 0000000 17
0111201 100 .700816e+07  .125840e+07  .325810e+07  1.00000  0.0  1
0111202 100 .700816e+07  .125840e+07  .325720e+07  1.00000  0.0  2
0111203 100 .700816e+07  .125840e+07  .325630e+07  1.00000  0.0  3
0111204 100 .700817e+07  .125840e+07  .325540e+07  1.00000  0.0  4
0111205 100 .700817e+07  .125840e+07  .325450e+07  1.00000  0.0  5
0111206 100 .700817e+07  .125840e+07  .325350e+07  1.00000  0.0  6
0111207 100 .700817e+07  .125840e+07  .325260e+07  1.00000  0.0  7
0111208 100 .700817e+07  .125840e+07  .325160e+07  1.00000  0.0  8
0111209 100 .700817e+07  .125840e+07  .325060e+07  1.00000  0.0  9
0111210 100 .700817e+07  .125840e+07  .324960e+07  1.00000  0.0 10
```

```
0111211 100 .700819e+07 .125840e+07 .324880e+07 1.00000 0.0 11
0111212 100 .700822e+07 .125840e+07 .324800e+07 1.00000 0.0 12
0111213 100 .700824e+07 .125840e+07 .324720e+07 1.00000 0.0 13
0111214 100 .700827e+07 .125840e+07 .324640e+07 1.00000 0.0 14
0111215 100 .700830e+07 .125840e+07 .324560e+07 1.00000 0.0 15
0111216 100 .700832e+07 .125840e+07 .324480e+07 1.00000 0.0 16
0111217 100 .700835e+07 .125840e+07 .324400e+07 1.00000 0.0 17
0111218 100 .700837e+07 .125840e+07 .324340e+07 1.00000 0.0 18
0111300 0
0111301 0.24755 0.24755 0.0 01
0111302 0.24740 0.24740 0.0 02
0111303 0.24723 0.24723 0.0 03
0111304 0.24707 0.24707 0.0 04
0111305 0.24690 0.24690 0.0 05
0111306 0.24672 0.24672 0.0 06
0111307 0.24654 0.24654 0.0 07
0111308 0.24636 0.24636 0.0 08
0111309 0.24617 0.24617 0.0 09
0111310 0.24597 0.24597 0.0 10
0111311 0.24583 0.24583 0.0 11
0111312 0.24568 0.24568 0.0 12
0111313 0.24553 0.24553 0.0 13
0111314 0.24538 0.24538 0.0 14
0111315 0.24522 0.24522 0.0 15
0111316 0.24507 0.24507 0.0 16
0111317 0.24491 0.24491 0.0 17
0111401 0.044 0.0 1.0 1.0 17
*
10112000 18 3 2 0 0.022
10112100 0 1
10112101 1 0.026 1 0.030
10112201 1 2
10112301 0.0 2
10112400 -1
10112401 865.81 865.78 865.77
10112402 865.21 865.18 865.17
10112403 864.59 864.56 864.55
10112404 863.96 863.93 863.92
10112405 863.33 863.29 863.28
10112406 862.68 862.65 862.64
10112407 862.03 861.99 861.98
10112408 861.36 861.33 861.32
10112409 860.69 860.65 860.64
10112410 860.01 859.97 859.96
10112411 859.61 859.57 859.56
10112412 859.11 859.07 859.06
10112413 858.60 858.56 858.55
10112414 858.09 858.05 858.04
10112415 857.57 857.53 857.52
10112416 857.05 857.01 857.00
10112417 856.53 856.49 856.48
10112418 856.16 856.12 856.11
*10112401 821.5 3
10112501 011010000 10000 1 1 0.2 10
10112502 011110000 10000 1 1 0.15 17
10112503 011180000 10000 1 1 0.1052 18
10112601 -12 0 3011 1 0.2 10
10112602 -12 0 3011 1 0.15 17
10112603 -12 0 3011 1 0.1052 18
10112701 0 0.0 0.0 0.0 18
10112801 0.0 15.0 15.0 0.0 0.0 0.0 0.0 1.0 18
*
*
0120000 oucore sngljun
0120101 011010000 014000000 0.0 0.0 0.0 0000000
0120201 0 0.25912 0.24480 0.0
*
* ----------------------------------------
* Steam Condenser and Water Cooler
* ----------------------------------------
0140000 heatexch pipe
0140001 20
0140101 7.20-3 6 9.8-3 14 7.20-3 20
0140301 0.14 20
0140601 -90.0 20
0140801 5.0-5 16.0-3 5
0140802 5.0-5 50.0-3 15
0140803 5.0-5 16.0-3 20
0140901 0.0 0.0 19
0141001 000000 20
0141101 0000000 19
0141201 100 .700840e+07 .124750e+07 .288240e+07 .995200 0.0 1
0141202 100 .700844e+07 .124780e+07 .271920e+07 .991480 0.0 2
0141203 100 .700848e+07 .124870e+07 .263110e+07 .990140 0.0 3
0141204 100 .700853e+07 .125000e+07 .259420e+07 .987840 0.0 4
0141205 100 .700858e+07 .125100e+07 .258190e+07 .989200 0.0 5
0141206 100 .700863e+07 .125130e+07 .258180e+07 .991680 0.0 6
0141207 100 .700868e+07 .125830e+07 .258180e+07 .997770 0.0 7
0141208 100 .700873e+07 .125840e+07 .258180e+07 .999850 0.0 8
0141209 100 .700878e+07 .125840e+07 .258180e+07 .998060 0.0 9
0141210 100 .700926e+07 .125840e+07 .258180e+07 .116080 0.0 10
0141211 103 .701022e+07 559.012 0.0 0.0 0.0 11
0141212 103 .701124e+07 559.012 0.0 0.0 0.0 12
0141213 103 .701225e+07 559.019 0.0 0.0 0.0 13
0141214 103 .701327e+07 559.029 0.0 0.0 0.0 14
0141215 103 .701443e+07 386.947 0.0 0.0 0.0 15
0141216 103 .701575e+07 356.921 0.0 0.0 0.0 16
0141217 103 .701709e+07 350.620 0.0 0.0 0.0 17
0141218 103 .701843e+07 348.948 0.0 0.0 0.0 18
0141219 103 .701977e+07 348.417 0.0 0.0 0.0 19
0141220 103 .702111e+07 348.224 0.0 0.0 0.0 20
0141300 0
0141301 3.65580e-02 3.27312e-02 0.0 01
0141302 4.98510e-02 2.09881e-02 0.0 02
0141303 6.85847e-02 1.31201e-02 0.0 03
0141304 7.64202e-02 7.48590e-03 0.0 04
0141305 0.11440 3.07829e-03 0.0 05
0141306 7.18394e-02 8.08266e-04 0.0 06
0141307 5.81765e-02 8.43391e-04 0.0 07
0141308 0.70891 8.48019e-04 0.0 08
0141309 0.33806 2.49391e-04 0.0 09
0141310 1.06252e-03 -0.40777 0.0 10
0141311 9.39059e-04 8.06602e-04 0.0 11
0141312 9.38895e-04 6.78740e-04 0.0 12
0141313 9.38735e-04 7.01262e-04 0.0 13
0141314 1.27751e-03 1.17414e-03 0.0 14
0141315 9.93676e-04 9.93676e-04 0.0 15
0141316 9.71927e-04 9.71927e-04 0.0 16
0141317 9.67956e-04 9.67956e-04 0.0 17
0141318 9.66902e-04 9.66902e-04 0.0 18
0141319 9.66536e-04 9.66536e-04 0.0 19
0141401 16.0-3 0.0 1.0 1.0 6
0141402 50.0-3 0.0 1.0 1.0 13
0141403 16.0-3 0.0 1.0 1.0 19
*
10143000 20 3 2 0 0.075
10143100 0 1
10143101 1 0.083 1 0.09
10143201 1 2
10143301 0.0 2
10143400 -1
10143401 665.54 665.49 665.48
10143402 558.88 558.88 558.88
10143403 558.87 558.87 558.87
10143404 558.88 558.88 558.88
10143405 558.90 558.89 558.89
10143406 558.87 558.86 558.86
10143407 559.02 559.02 559.02
10143408 559.02 559.02 559.02
10143409 559.06 559.06 559.06
10143410 559.01 559.01 559.01
10143411 559.01 559.01 559.01
10143412 559.02 559.02 559.02
10143413 559.03 559.03 559.03
10143414 559.04 559.04 559.04
10143415 386.97 386.97 386.97
10143416 356.93 356.93 356.93
10143417 350.63 350.63 350.63
10143418 348.95 348.95 348.95
10143419 348.42 348.42 348.42
10143420 348.23 348.23 348.23
*10143401 590.0 3
10143501 014010000 10000 1 1 0.14 20
10143601 -12 0 3011 1 0.14 20
10143701 0 0.0 0.0 0.0 20
10143801 0.0 15.0 15.0 0.0 0.0 0.0 0.0 1.0 20
*
0150000 outheat sngljun
0150101 014010000 016000000 0.0 0.0 0.0 0000000
0150201 0 8.86352e-02 8.86352e-02 0.0
*
* ----------------------------------------
* Lower Water Pipe
* ----------------------------------------
0160000 lowpipe pipe
0160001 18
0160101 7.85-5 18
0160201 7.85-5 11 2.4-6 12 7.85-5 17
0160301 0.15 1, 0.2 6 0.222 7, 0.11 18
0160601 -90.0 7, 0.0 18
```

```
0160801 5.0-5 0.01 18
0160901 0.0 0.0 17
0161001 000000 18
0161101 0000000 11
0161102 0000100 12
0161103 0000000 17
0161201 103 .702250e+07 348.224 0.0 0.0 0.0  1
0161202 103 .702417e+07 348.224 0.0 0.0 0.0  2
0161203 103 .702609e+07 348.225 0.0 0.0 0.0  3
0161204 103 .702800e+07 348.225 0.0 0.0 0.0  4
0161205 103 .702992e+07 348.225 0.0 0.0 0.0  5
0161206 103 .703183e+07 348.226 0.0 0.0 0.0  6
0161207 103 .703385e+07 348.226 0.0 0.0 0.0  7
0161208 103 .703492e+07 348.226 0.0 0.0 0.0  8
0161209 103 .703492e+07 348.226 0.0 0.0 0.0  9
0161210 103 .703491e+07 348.226 0.0 0.0 0.0 10
0161211 103 .703491e+07 348.226 0.0 0.0 0.0 11
0161212 103 .703491e+07 348.227 0.0 0.0 0.0 12
0161213 103 .702459e+07 348.226 0.0 0.0 0.0 13
0161214 103 .702458e+07 348.226 0.0 0.0 0.0 14
0161215 103 .702458e+07 348.226 0.0 0.0 0.0 15
0161216 103 .702458e+07 348.227 0.0 0.0 0.0 16
0161217 103 .702458e+07 348.227 0.0 0.0 0.0 17
0161218 103 .702458e+07 348.227 0.0 0.0 0.0 18
0161300 0
0161301 8.86351e-02  8.86351e-02 0.0  01
0161302 8.86350e-02  8.86350e-02 0.0  02
0161303 8.86349e-02  8.86349e-02 0.0  03
0161304 8.86348e-02  8.86348e-02 0.0  04
0161305 8.86346e-02  8.86346e-02 0.0  05
0161306 8.86345e-02  8.86345e-02 0.0  06
0161307 8.86344e-02  8.86344e-02 0.0  07
0161308 8.86343e-02  8.86343e-02 0.0  08
0161309 8.86343e-02  8.86343e-02 0.0  09
0161310 8.86343e-02  8.86343e-02 0.0  10
0161311 8.86342e-02  8.86342e-02 0.0  11
0161312 8.86342e-02  8.86342e-02 0.0  12
0161313 8.86346e-02  8.86346e-02 0.0  13
0161314 8.86346e-02  8.86346e-02 0.0  14
0161315 8.86346e-02  8.86346e-02 0.0  15
0161316 8.86345e-02  8.86345e-02 0.0  16
0161317 8.86345e-02  8.86345e-02 0.0  17
0161401 0.010 0.0 1.0 1.0  11
0161402 0.00175 0.0 1.0 1.0  12
0161403 0.010 0.0 1.0 1.0  17
*
10162000  18 3 2 0 0.005
10162100  0 1
10162101  1 0.010 1 0.016
10162201  1 2
10162301  0.0 2
10162400  -1
10162401 348.22 348.22 348.22
10162402 348.23 348.23 348.23
10162403 348.23 348.23 348.23
10162404 348.23 348.23 348.23
10162405 348.23 348.23 348.23
10162406 348.23 348.23 348.23
10162407 348.23 348.23 348.23
10162408 348.23 348.23 348.23
10162409 348.23 348.23 348.23
10162410 348.23 348.23 348.23
10162411 348.23 348.23 348.23
10162412 348.23 348.23 348.23
10162413 348.23 348.23 348.23
10162414 348.23 348.23 348.23
10162415 348.23 348.23 348.23
10162416 348.23 348.23 348.23
10162417 348.23 348.23 348.23
10162418 348.23 348.23 348.23
*10162401  325.0 3
10162501  016010000 10000 1 1 0.150 1
10162502  016020000 10000 1 1 0.200 6
10162503  016070000 10000 1 1 0.222 7
10162504  016080000 10000 1 1 0.11  18
10162601  0 0 0 1 0.150  1
10162602  0 0 0 1 0.200  6
10162603  0 0 0 1 0.222  7
10162604  0 0 0 1 0.11 18
10162701  0 0.0 0.0 0.0 18
10162801  0.0 15.0 15.0 0.0 0.0 0.0 0.0 1.0 18
*
0170000 inlow sngljun
0170101 016010000 005020001 0.0 0.0 0.0 0000000
0170201 0 8.86345e-02  8.86345e-02 0.0
**
*=============================================================
* SECOND CIRCUIT
*=============================================================
2010000 tdv201 tmdpvol
2010101 0.0 2.0 2.0 0.0 0.0 0.0 1.0-6 0.0 0
2010200 103
2010201 0.0 10.5+6 550.2
*
2020000 regul  tmdpjun
2020101 201000000 203000000 0.0
2020200 1
2020201 0.0 0.50 0.0 0.0
*
2030000 htexch pipe  * heat exchanger
2030001 6
2030101 1.327-4 6
2030301 0.14 6
2030601 90.0 6
2030801 2.0-6 0.0136 6
2030901 0.0 0.0 5
*
*crdno tlpvbfe
2031001 0000000  6
*crdno efvcahs
2031101 0001000 5
*
2031201 103 .100139e+08 551.936 0.0 0.0 0.0  1
2031202 103 .100113e+08 553.273 0.0 0.0 0.0  2
2031203 103 .100088e+08 554.287 0.0 0.0 0.0  3
2031204 103 .100063e+08 555.083 0.0 0.0 0.0  4
2031205 103 .100038e+08 555.723 0.0 0.0 0.0  5
2031206 103 .100013e+08 556.191 0.0 0.0 0.0  6
2031300 0
*2031301 0.0 0.0  0.0  5
2031301 4.9667  4.9667 0.0  1
2031302 4.9829  4.9829 0.0  2
2031303 4.9954  4.9954 0.0  3
2031304 5.0054  5.0054 0.0  4
2031305 5.0135  5.0135 0.0  5
*
2040000 sj204 sngljun
2040101 203010000 205000000 0.0 0.0  0.0  001100
2040201 0 5.0195  5.0195 0.0
*
2050000 tdv205 tmdpvol
2050101 0.0 2.0 2.0 0.0 0.0 0.0 1.0-6 0.0 0
2050200 103
2050201 0.0 10.0+6 550.1
*
12031000  6 2 2 0 0.0068
12031100  0 1
12031101  1 0.008
12031201  1 1
12031301  0. 1
12031400  -1
12031401 553.60 556.94
12031402 554.45 556.81
12031403 555.18 556.97
12031404 555.78 557.19
12031405 556.28 557.41
12031406 556.60 557.42
*12031401  550.1  2
12031501  203010000  10000 1  1 2.0 6
12031601  014010000  10000 110  1 2.0 6
12031701  0 0.0 0.0  0.0 6
12031801  0.0 20.0 20.0 0.0 0.0 0.0 0.0 1.0 6
12031901  0.0 20.0 20.0 0.0 0.0 0.0 0.0 1.0 6
*-------------------------------------------------
2110000 tdv211 tmdpvol
2110101 0.0 2.0 2.0 0.0 0.0 0.0 1.0-6 0.0 0
2110200 103
2110201 0.0 8.5+6 345.0
*
2120000 regul  tmdpjun
2120101 211000000 213000000 0.0
2120200 1
2120201 0.0 0.50 0.0 0.0
*
2130000 htexch pipe  * heat exchanger
2130001 6
2130101 1.327-4 6
2130301 0.14 6
2130601 90.0 6
2130801 2.0-6 0.0136 6
```

```
2130901 0.0 0.0 5
*
*crdno tlpvbfe
2131001 0000000  6
*crdno efvcahs
2131101 0001000 5
*
2131201 103 .801473e+07 347.537 0.0 0.0 0.0  1
2131202 103 .801204e+07 347.948 0.0 0.0 0.0  2
2131203 103 .800937e+07 348.035 0.0 0.0 0.0  3
2131204 103 .800670e+07 348.058 0.0 0.0 0.0  4
2131205 103 .800402e+07 348.065 0.0 0.0 0.0  5
2131206 103 .800135e+07 348.068 0.0 0.0 0.0  6
2131300 0
*2031301 0.0 0.0  0.0  5
2131301  3.8501  3.8501 0.0 1
2131302  3.8511  3.8511 0.0 2
2131303  3.8513  3.8513 0.0 3
2131304  3.8513  3.8513 0.0 4
2131305  3.8513  3.8513 0.0 5
*
2140000 sj204 sngljun
2140101 213010000 215000000 0.0 0.0  0.0  001100
2140201 0 3.8514  3.8514 0.0
*
2150000 tdv205 tmdpvol
2150101 0.0 2.0 2.0 0.0 0.0 0.0 1.0-6 0.0 0
2150200 103
2150201 0.0 8.0+6 345.0
*
12131000  6 2 2 0 0.0068
12131100  0 1
12131101  1 0.008
12131201  1 1
12131301  0. 1
12131400  -1
12131401 350.63 355.07
12131402 348.44 349.16
12131403 348.14 348.29
12131404 348.09 348.12
12131405 348.07 348.09
12131406 348.07 348.08
12131501  213010000  10000 1  1 2.0 6
12131601  014150000  10000 110  1 2.0 6
12131701  0 0.0 0.0  0.0 6
12131801  0.0 20.0 20.0 0.0 0.0 0.0 0.0 1.0 6
12131901  0.0 20.0 20.0 0.0 0.0 0.0 0.0 1.0 6
*----------------------------------------------
**general tables
*----------------------------------------------
*s-steel
20100100  tbl/fctn 1 1
20100101  295.0 15.
20100102  400.0 16.
20100103  500.0 18.
20100104  600.0 20.
20100105  700.0 21.
20100106  800.0 23.
20100107  900.0 25.
20100108 1000.0 26.
20100109 1100.0 28.
20100110 1200.0 29.
20100111 1400.0 29.
20100151  295.0 3.686+6
20100152  400.0 3.686+6
20100153  500.0 3.801+6
20100154  600.0 3.874+6
20100155  700.0 3.955+6
20100156  800.0 3.991+6
20100157  900.0 4.039+6
20100158 1000.0 4.043+6
20100159 1100.0 4.113+6
20100160 1200.0 4.115+6
20100161 1400.0 4.115+6
*talkohlorit
20100200  tbl/fctn 1 1
20100201  295.0 1.5
20100202  400.0 1.2
20100203  500.0 1.1
20100204  600.0 1.0
20100205  700.0 0.9
20100206  800.0 0.8
20100207  900.0 0.75
20100208 1400.0 0.75
20100251  295.0 2.128+6
20100252  400.0 2.408+6
20100253  500.0 2.604+6
20100254  600.0 2.772+6
20100255  700.0 2.940+6
20100256  800.0 3.080+6
20100257  900.0 3.220+6
20100258 1400.0 3.220+6
*
20100300  tbl/fctn 1 1
20100301  2.5
20100351  4.55+6
**heat source
20200100  power 0 1. 1000.
*20200101  0.00 0.0
*20200102 10.00 0.00
*20200103 20.00 22.97
20200103 00.00 22.97
**heat
20200200  temp 0
20200201  0.00 547.0
**heat
20200300  temp 0
20200301  0.00 325.0
*
20200400  temp 0
20200401  0.00 430.0
*
20200500  temp 0
20200501  0.00 520.0
*
20201100  htc-t 0
20201101  0.00 0.0
*
20201200  temp 0
20201201  0.00 295.0
.*end of data set
```

NRC FORM 335 (2-89) NRCM 1102, 3201, 3202

U.S. NUCLEAR REGULATORY COMMISSION

BIBLIOGRAPHIC DATA SHEET

(See instructions on the reverse)

1. REPORT NUMBER (Assigned by NRC, Add Vol., Supp., Rev., and Addendum Numbers, if any.)

NUREG/IA-0208

2. TITLE AND SUBTITLE

Analyses of the VTI Test Data on the Behavior of the Heated Rod Temperatures in the Partially Uncovered VVER-440 Core Model Using RELAP5/MOD3.2.2 GAMMA

3. DATE REPORT PUBLISHED

MONTH	YEAR
April	2002

4. FIN OR GRANT NUMBER

5. AUTHOR(S)

V.A.Vinogradov, A.Y.Balykin

6. TYPE OF REPORT

technical

7. PERIOD COVERED *(Inclusive Dates)*

8. PERFORMING ORGANIZATION - NAME AND ADDRESS *(If NRC, provide Division, Office or Region, U.S. Nuclear Regulatory Commission, and mailing address; if contractor, provide name and mailing address.)*

Russian Research Center "Kurchatov Institute"
Kurchatov Square 1
123182, Moscow Russia

9. SPONSORING ORGANIZATION - NAME AND ADDRESS *(If NRC, type "Same as above"; if contractor, provide NRC Division, Office or Region, U.S. Nuclear Regulatory Commission, and mailing address.)*

Division of System Analysis and Regulatory Effectiveness
Office of Nuclear Regulatory Research
U. S. Nuclear Regulatory Commission
Washington, DC 20555-0001

10. SUPPLEMENTARY NOTES

This is a Russian CAMP in-kind contribution

11. ABSTRACT *(200 words or less)*

This report has been prepared as a part of the Agreement on Research Participat ion and Technical Exchange under the International Code Application and Maintenance Program.
VTI test data on the behavior of the heated rod temperatures in the partially u ncovered VVER -440 core model were simulated with RELAP5/MOD3.2.2GAMMA to assess the code, especially its heat transfer mode ls for modeling phenomena in the partially uncovered core under Small Break LOCA conditions. This problem addres ses the phenomena of high importance to VVER-440 safety.
Series of the experiments have been carried out in the VVER-440 loop model at t he VTI Test Facility which are directly related to this issue. Two tests conducted in the stationary conditions with the transi tion mode of a steam flow in the core channel were chosen for the assessment calculations with the code.
Experimental VVER-440 loop model includes the models of all the main elements o f a reactor, loop's hot leg model and cold leg simulator, and also a steam generator simulator with an active heat removal . The fuel assembly model consists of 19 electrically heated rod simulators of 9.1 mm outer diameter and 2.5 m heated he ight. The rod simulators are composed in the rod bundle in a hexagonal array with a pitch equal 12.2 mm (P/D=1.34).
First a study of the effect of the hydraulic nodalization to the code results w as performed using different number of hydraulic volumes for the core model. After the choice of proper nodalization and maximum user-specified time step, the base case calculations were done for the tests. The differences between the code predicti ons for the behavior of rod's wall temperatures and test data are described and analyzed.
Sensitivity studies were carried out to investigate the influence of an increas e in the calculated coefficients of heat transfer from the heated rods to a steam flow on the axial distribution of rod's wall te mperatures in the uncovered part of core model.

12. KEY WORDS/DESCRIPTORS *(List words or phrases that will assist researchers in locating the report.)*

partially uncovered core, RELAP5, VVER-440

13. AVAILABILITY STATEMENT

unlimited

14. SECURITY CLASSIFICATION

(This Page)

unclassified

(This Report)

unclassified

15. NUMBER OF PAGES

16. PRICE

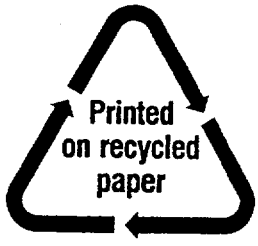

Federal Recycling Program